Characterizing the Drivers of Carbon Use in Post-Anoxic Denitrification

Kayla Bauhs

Thesis submitted to the faculty of the Virginia Polytechnic Institute and State University in partial fulfillment of the requirements for the degree of

Master of Science
In
Civil Engineering

Amy J. Pruden-Bagchi
Charles B. Bott
Zhiwu (Drew) Wang

July 6th, 2021
Blacksburg, VA

Keywords: denitrification, post-anoxic, methanol, internal carbon, endogenous

Characterizing the Drivers of Carbon Use in Post-Anoxic Denitrification

Kayla Bauhs

ACADEMIC ABSTRACT

Three of Hampton Roads Sanitation District's (HRSD's) conventional activated sludge Water Resource Recovery Facilities (WRRFs) add methanol for post-anoxic denitrification: the Virginia Initiative Plant (VIP), Nansemond Plant (NP), and Army Base (AB). From 2017-2020, VIP averaged 0.49 ± 0.03 lb COD/lb N removed, while NP and AB averaged 1.48 ± 0.06 and 2.11 ± 0.15 lb COD/lb N, respectively. Significant methanol savings at VIP may result from post-anoxic denitrification using internal carbon that was stored in the anaerobic zone. An investigation into the factors affecting internal carbon-driven (internal C) denitrification was done via a series of batch tests. The capacity for internal C denitrification was demonstrated with sludge from all three WRRFs, despite not necessarily being used full-scale. For each WRRF, an increase in these rates correlated to higher phosphorus uptake rates, suggesting a dependence on the PAO population. Shorter aerobic times and more acetate in the anaerobic stage were shown to increase internal C denitrification rates to varying degrees, and this type of denitrification was only observed for bio-P biomass that was also nitrifying. Beyond internal carbon, other denitrification factors explored include moving the methanol dose point further into the anoxic zone, longer post-anoxic residence times, plug-flow conditions, solids residence time (SRT), and anoxic conditions prior to methanol dosing. Contributions from slowly biodegradable COD were minimal. Understanding the conditions that promote denitrification with internal carbon or other carbon sources would be required for effective strategies to achieve methanol savings at NP and AB that would rival those at VIP.

Characterizing the Drivers of Carbon Use in Post-Anoxic Denitrification

Kayla Bauhs

GENERAL ABSTRACT

Three of Hampton Roads Sanitation District's (HRSD's) Water Resource Recovery Facilities (WRRFs) add methanol to facilitate denitrification in the post-anoxic zone: the Virginia Initiative Plant (VIP), Nansemond Plant (NP), and Army Base (AB). Significant methanol savings at VIP may result from denitrification using carbon that was stored in the biomass earlier in the treatment process. An investigation into the factors affecting this type of denitrification with internal carbon was done via a series of batch tests. All three WRRFs were able to use this internal carbon for denitrification in the batch tests, despite not necessarily using it full-scale. These denitrification rates were shown to relate to the performance of the biomass that is also responsible for phosphorus removal. Shorter aerobic times prior to the anoxic phase and more acetate in the stage where carbon is stored were shown to increase these denitrification rates, and this type of denitrification was only observed for biomass from WRRFs that implement nitrification. Beyond internal carbon, other denitrification factors explored include moving the methanol dose point further into the anoxic zone, longer post-anoxic residence times, plug-flow conditions, solids residence time (SRT), and anoxic conditions prior to methanol dosing. Contributions from carbon pushed downstream from overloading primary clarifiers was minimal. Understanding the conditions that promote denitrification with internal carbon or other carbon sources would be required for effective strategies to achieve methanol savings at NP and AB that would rival those at VIP.

Contents

List of Tables

List of Figures

1. Introduction

Nutrient removal at Water Resource Recovery Facilities (WRRFs) requires a combination of certain physical, chemical and/or biological treatment processes. For instance, biological phosphorus removal (bio-P) requires anaerobic conditions followed by aerobic conditions to select for poly-phosphate accumulating organisms (PAOs), a type of carbon-storing heterotroph. This biological attenuation of phosphorus (P) inside the biomass must be accompanied by physical removal of the biomass in order to eliminate the P from the system. As for nitrogen (N) removal, sufficient aerobic conditions and residences times as well as anoxic conditions are required in some combination in order to facilitate nitrification and denitrification, respectively, where N leaves the system as gaseous N_2.

Carbon requirements are an important consideration for N removal, and can dictate the configuration of the aerobic and anoxic zones at WRRFs. For instance, an anoxic zone preceding an aerobic zone is common practice, as in the Modified Ludzack-Ettinger (MLE) process, and is called "pre-anoxic" denitrification. The pre-anoxic zone takes advantage of the influent readily biodegradable chemical oxygen demand (rbCOD) in the system and uses it for denitrification, as opposed to it being oxidized aerobically, or essentially wasted. However, this configuration requires internal recycle of flow from the end of the aerobic zone, where nitrification must occur first, back to the anoxic zone to mix with the carbon-rich influent wastewater for subsequent denitrification. For that reason, extent of N removal is limited not only by the available carbon in the influent, but also the internal recycle capacity.

In order to meet total nitrogen (TN) concentrations less than approximately 5 mg/L, "post-anoxic" nitrate (NO_3) polishing is needed in addition to the pre-anoxic zone. Post-anoxic denitrification consists of an aerobic zone followed by the anoxic zone, and no recycles. At this point in the process, any rbCOD in the influent has been utilized in the pre-anoxic zone for denitrification or oxidized in the aerobic zone. Therefore, a supplemental carbon source is often added to facilitate denitrification in the post-anoxic zone, as in a 4- or 5-stage Bardenpho process. Denitrification via carbon from endogenous decay products will occur, but at rates that require residence times, and thus tank sizes, that are not reasonable for most WRRFs to provide. Adding an external carbon source will enable faster denitrification rates in smaller tanks, with more control over NO_x removal in meeting strict effluent TN limits. Methanol is a common selection for this purpose, and its use is well-documented.

1.1 Project Motivation and Objectives

Three of Hampton Roads Sanitation District's (HRSD's) conventional activated sludge WRRFs use a combination of pre-anoxic and post-anoxic zones with methanol addition as their biological N removal strategy. These include the Virginia Initiative Plant (VIP), Nansemond Plant (NP), and Army Base (AB). All three WRRFs rely on biological P and N removal, with means for chemical P removal as necessary. VIP is located in Norfolk, Virginia, and treats an average flow of 27

million gallons per day (MGD), with a design flow of 40 MGD, and a peak wet weather capacity of 100 MGD. A "VIP + 2" configuration is used here, consisting of the VIP process followed by a post-anoxic and reaeration zone. This general treatment schematic as well as the one for the 5-stage Bardenpho process is represented in ***Figure 1***. The annual average TN and Total Phosphorus (TP) limits permitted by the Virginia Pollutant Discharge Elimination System (VPDES) for VIP are 5 mg/L and 1 mg/L, respectively. NP is located in Suffolk, Virginia, and treats an average flow of 17 MGD, with a design flow of 30 MGD, and a peak wet weather capacity of 75 MGD. A 5-stage Bardenpho process is used here. The VPDES-permitted TN and TP limits for NP are 8 mg/L and 2 mg/L, respectively. AB is located in Norfolk, Virginia, and treats an average flow of 10 MGD, with a design flow of 18 MGD, and a peak wet weather capacity of 45 MGD. A 5-stage Bardenpho process is used here as well. The VPDES-permitted TN and TP limits for AB are 5 mg/L and 1 mg/L, respectively. As the effluent for each WRRF is discharged into water bodies that are part of the Chesapeake Bay Watershed, all WRRFs are also subject to TN and TP waste load allocations on a mass basis.

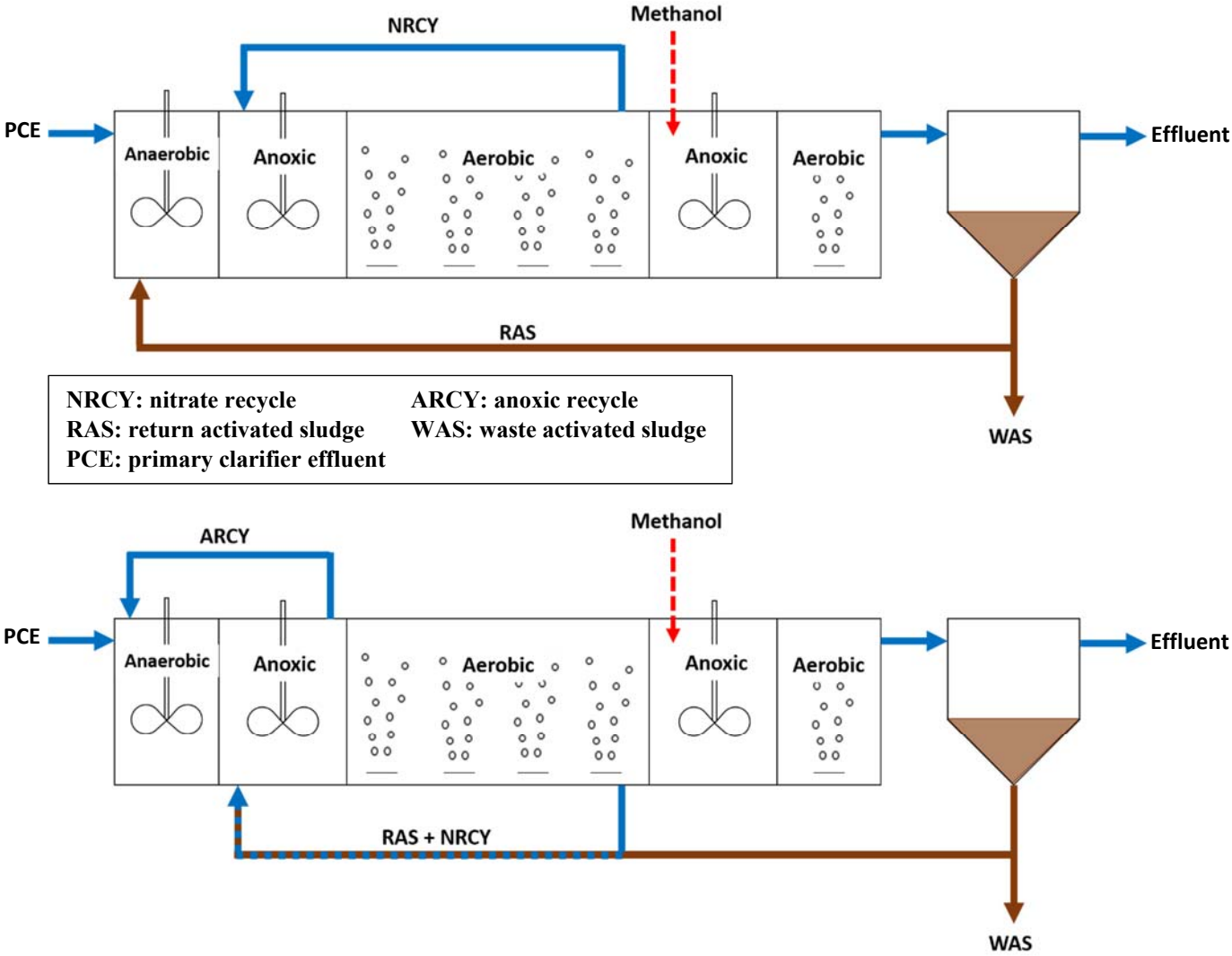

Figure 1. Schematics of the 5-stage Bardenpho process used at NP and AB (top) and the VIP+2 process used at VIP (bottom).

VIP, NP, and AB all add methanol in the post-anoxic zone to drive the TN concentrations well below the permitted levels. The comparative methanol doses for each WRRF were represented as the mass ratio of total methanol added to TN removed across the treatment process from the primary clarifier effluent (PCE) to final effluent. As shown in ***Figure 2***, the doses for VIP are consistently lower than at NP or AB. The averages from 2017-2020 for each methanol dose as well as for other key parameters are presented in ***Table 1***.

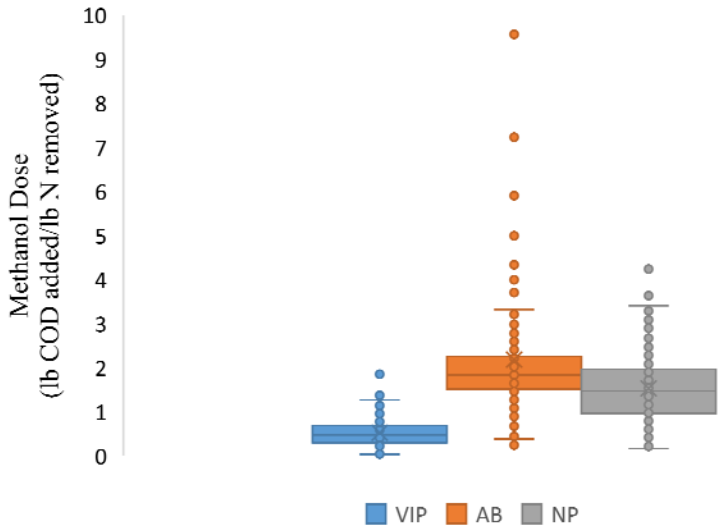

Figure 2. Distribution of methanol doses (lb COD added per lb N removed) from 2017-2020.

Table 1. Methanol addition and relevant parameters for each WRRF. Values are 2017-2020 averages.

WRRF	Methanol Dose (lb COD/lb N removed)	NRCY Flow (%)	Effluent TN (mg/L)	PCE rbCOD:TKN (lb/lb)	PCE rbCOD:TP (lb/lb)	F/M (mg rbCOD/mg MLVSS/d)
VIP	0.49 (± 0.03)	118 (± 2)	5.01 (± 0.16)	4.12 (± 0.65)	31.0 (± 4.3)	3.57 (± 0.57)
NP	1.48 (± 0.06)	342 (± 4)	4.73 (± 0.12)	2.00 (± 0.26)	10.4 (± 1.2)	0.66 (± 0.09)
AB	2.11 (± 0.15)	201 (± 3)	4.90 (± 0.18)	1.63 (± 0.32)	10.4 (± 1.7)	0.79 (± 0.14)

(± 95% confidence interval for the average)

The nitrate recycle (NRCY) capacity, or internal recycle, at VIP is restricted due to pumping limitations. Despite this low NRCY of only 118 ± 2% of influent flow, VIP is still able to meet an average TN of 5.01 ± 0.16 mg/L, similar to the other two facilities. So it stands to reason that superior post-anoxic denitrification at VIP compensates for the limitation in pre-anoxic denitrification capacity. Given that the methanol dose in the post-anoxic zone at VIP of 0.49 ± 0.03 lb COD/lb N removed is well below the other WRRFs, this superior post-anoxic denitrification is not due to excess methanol addition. Rather, some other mechanism of denitrification at VIP enables effluent TN limits to be met while simultaneously achieving significant methanol savings.

Data from nutrient profiles of the full-scale WRRF at VIP over the past few years, particularly the post-anoxic zone, further supports this idea of some sort of "mysterious" denitrification occurring here. The theoretical denitrification attributable to methanol was estimated using the known amount of methanol dosed and assuming 4.8 g COD/g NO_3-N removed. The endogenous decay contribution to denitrification was determined using this specific rate measured from batch tests and adjusted for full-scale temperature, MLSS concentrations, and flow rate. The leftover quantity of NO_x removal after subtracting these two contributions from the overall measured NO_x removal is considered "mysterious", and as shown in ***Figure 3*** and ***Figure 4***, constitutes a significant portion of the overall denitrification observed in train 1 and 2 (especially train 1). Of the average 3.8 mg N/L of NO_x removed across the zone, approximately 33% (or 1.26 mg N/L) is due to this mysterious carbon source. There are some periods, particularly recently, when methanol is simply turned off to the post-anoxic zone.

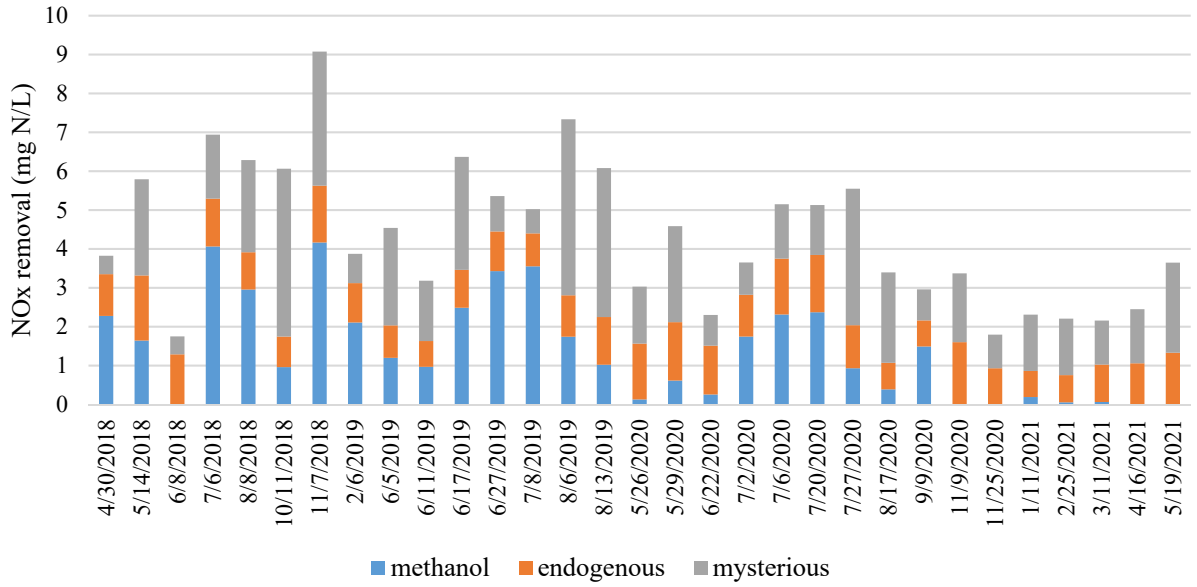

Figure 3. Quantification of various contributions to NO_x removal in post-anoxic train 1 from full-scale profiles at VIP from 2018-2021.

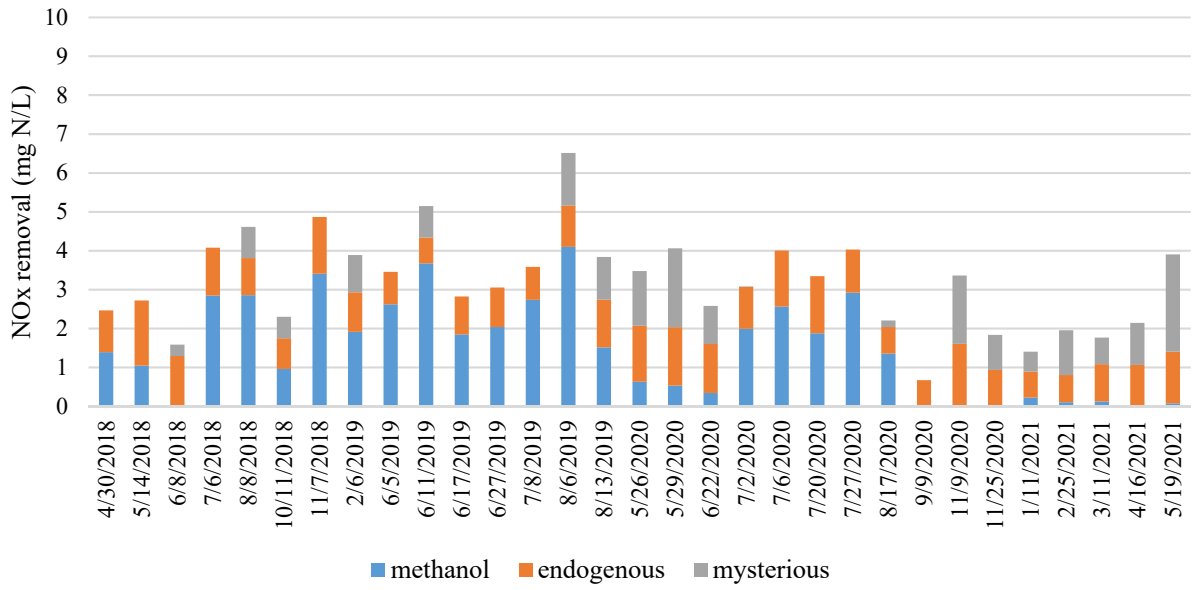

Figure 4. Quantification of various contributions to NO_x removal in post-anoxic train 2 from full-scale profiles at VIP from 2018-2021.

Also notable in ***Table 1*** is the PCE rbCOD:TKN and rbCOD:TP ratios for each WRRF. The rbCOD:TKN ratio at VIP is more than twice as much as the other two WRRFs, and the rbCOD:TP ratio is about three times as much. Furthermore, in the VIP process, RAS is returned to the pre-anoxic zone, requiring an extra anoxic recycle (ARCY) from the pre-anoxic to the anaerobic zone to maintain the mixed liquor there. In the Bardenpho process, RAS goes directly to the anaerobic zone. The slight difference in recycles causes the mixed liquor suspended solids (MLSS) and mixed liquor volatile suspended solids (MLVSS) concentrations in the anaerobic zone to be approximately half of that in the rest of the process at VIP, whereas the same concentration is maintained throughout the Bardenpho process at NP and AB. Thus, the excess of rbCOD at VIP is exacerbated when comparing on a biomass-specific basis, as shown by the F/M ratio of 3.57 ± 0.57 mg rbCOD/mg MLVSS/d at VIP compared to 0.66 ± 0.09 mg rbCOD/mg MLVSS/d and 0.79 ± 0.14 mg rbCOD/mg MLVSS/d at NP and AB. This all suggests an excess of carbon entering the anaerobic zone at VIP relative to nutrient and biomass concentrations, which could potentially facilitate superior carbon storage in that phase. It is possible that stored carbon from the anaerobic zone could be sustained until the post-anoxic zone, where it would then be used for denitrification. This was hypothesized to be the mechanism behind the mysterious denitrification observed full-scale that cannot be accounted for with methanol or endogenous decay carbon sources. It was this theory that initiated the analysis of post-anoxic internal-carbon driven (internal C) denitrification, specifically as it was thought to be the source of superior denitrification in VIP's post-anoxic zone that was driving methanol addition to low rates.

Besides internal C denitrification, other aspects of denitrification could be responsible for methanol savings. ***Figure 5*** shows an overview of the post-anoxic zone at each AB, NP, and VIP. One of the distinguishing features of the post-anoxic tanks at VIP is that they are relatively long and narrow compared to those at NP or AB. Operation of the trains can also be adjusted between

25%/75% aerobic/anoxic or 50%/50% aerobic/anoxic (***Figure 5*** shows 25%/75%). This zone is much closer to plug flow conditions than at the other WRRFs, which could factor into denitrification performance. Another difference is that VIP uses big bubble mixing in this zone, while mechanical top mixers are used at NP and AB. Although not tested during this study, the mixing type could play an important role in effective distribution of substrates throughout the tank for denitrification. Other factors, such as the location of the methanol addition or purposeful overloading of primary clarifiers to push on organic material, could also be of significance.

AB NP VIP

Figure 5. Overview of the post anoxic zone at each WRRF. The red boxes indicate the tanks/zones, and the yellow arrows indicate flow.

The differences in methanol demand at HRSD's WRRFs led to an investigation into the drivers of carbon use in post-anoxic denitrification. The overall objective was to determine how varying operational factors affect denitrification, whether based on methanol, endogenous decay products, or internal carbon. Chapter 2 includes a literature review of what has been found on the potential role of internal carbon as a source for denitrification, as well as other aspects of denitrification including methanol use and endogenous decay. Of particular focus was the role of internal carbon in post-anoxic denitrification, which is the subject of Chapter 3. The first objective was simply to determine if the biomass from each of HRSD's WRRFs even had the capacity for this type of denitrification, and how this changes over the span of several months. Meanwhile, other specific aspects were explored, such as aeration time prior to the post-anoxic phase, whether the biomass was from a nitrifying-denitrifying WRRF or not, how much carbon was available in the anaerobic phase, and correlation to bio-P performance. Comparison of batch test denitrification rates, including when methanol was added in the batch tests, to the full-scale methanol addition at the time also provided insight into the suspected dominant denitrifying population at each WRRF. Chapter 4 includes an evaluation of other operational factors influencing denitrification and methanol demand. Elements considered included the methanol dose point, tank performance and related residence times, relationship of SRT to endogenous decay denitrification, priming of the methylotrophs to use NO_2/NO_3 as electron acceptors at faster rates, and the role of slowly biodegradable COD (sbCOD) as a post-anoxic carbon source. The degree of plug flow was also considered, which involved the use of Sumo simulation software (Dynamita, France) to model the post-anoxic zone at VIP, as well as subsequent consideration of its potential use to model internal C denitrification.

Understanding the various drivers of denitrification are important with the ultimate goal of saving methanol costs, minimizing greenhouse gas production, and intensifying treatment processes that are capable of meeting stringent N and P requirements. Specifically, pinpointing the reason for methanol savings at VIP will be key in trying to implement changes at NP or AB to achieve similar savings. Regardless of whether the significant denitrification contributor at VIP is indeed internal carbon, identifying the conditions that promote the use of internal carbon for denitrification is essential to implementing this strategy full-scale. Maximizing the use of internal carbon will drive the necessity for externally added carbon even lower.

2. Literature Review

2.1 Post-Anoxic Denitrification

Denitrification is targeted in anoxic reactors either before ("pre-anoxic") or after ("post-anoxic") the aerobic zone. Pre-anoxic denitrification requires the recycle of mixed liquor from the end of the aeration zone back to the anoxic zone, such as occurs in the MLE process. Depending on the influent Total Kjeldahl Nitrogen (TKN), an MLE process can typically achieve 8-12 mg/L of TN in the effluent. To reduce the effluent TN to 3-5 mg/L, post-anoxic denitrification is targeted in addition to the pre-anoxic zone, such as in the 4-stage Bardenpho process. Unlike pre-anoxic denitrification, which takes advantage of the rbCOD and some of the sbCOD from the influent wastewater, post-anoxic denitrification usually requires addition of an external carbon source. At this phase in the treatment process, there is no available carbon substrate left in the wastewater, as it has been stored anaerobically, used for denitrification in the pre-anoxic phase, or oxidized aerobically. To facilitate denitrification beyond endogenous rates in the post-anoxic zone, an external carbon source is typically added, such as methanol.

2.2 Methanol for Denitrification

Methanol (MeOH) is a common external carbon source used in post-anoxic denitrification, as it is relatively inexpensive and leads to lower biomass production than other substrates (Onnis-Hayden & Gu, 2008). When biomass growth is included in the demand, the theoretical carbon dose required is 3.2 g MeOH/g NO_3-N removed (4.8 g COD/g NO_3-N). Typical doses in the field range from 3.3-3.8 g MeOH/g NO_3-N, which may incorporate other factors such as dissolved oxygen (DO) entering the anoxic zone that might consume methanol, as well as endogenous decay contributions to denitrification (Tchobanoglous et al., 2014). This dose rate also depends on the biomass and other reactor conditions. For instance a ratio as low as 2.5 mg MeOH/mg NO_3-N to achieve full denitrification with low nitrite (NO_2) accumulation was demonstrated by Foglar & Briški (2003). On the other hand, adding less methanol than stoichiometrically required for full denitrification can lead to NO_2 accumulation, which may or may not be intentional (Ginige et al., 2009). The methanol dose may also be adjusted up or down to achieve the necessary concentration in the tank for the desired denitrification rate. For instance, it may be dosed in excess of stoichiometric requirements if the anoxic volume is limited and requires a faster denitrification rate to achieve the target effluent TN concentration. However, there would then be methanol in the effluent that was "over-dosed" to achieve this concentration.

Methanol can also be consumed aerobically, so careful consideration must be given to the dose location, and whether there is the potential for DO there. If so, methanol may be oxidized aerobically before it can be used for denitrification.

Acetyl Co-A is the main compound in the glycolytic pathway and TCA cycle, which are used for processing organic compounds to obtain carbon and energy (Onnis-Hayden & Gu, 2008). Acetate

can be transformed to acetyl Co-A easily, and is commonly found in the WRRF influent already, so typically will lead to higher denitrification rates than methanol (Onnis-Hayden & Gu, 2008). Unlike ordinary heterotrophic organisms (OHOs) that can use a variety of carbon sources, only a specialized group of heterotrophs, called methylotrophs, are able to use methanol for denitrification. Methylotrophs are able to transform single carbon compounds such as methanol to acetyl Co-A via the serine cycle (Onnis-Hayden & Gu, 2008). The population of methylotrophs is relatively small compared to OHOs, and their population size depends on the amount of methanol fed to the system (Tchobanoglous et al., 2014).

Compared to acetate, propionate, or fermented primary solids, methanol led to the lowest sludge production, due to the relatively high amount of energy required for assimilation of the single-carbon compound, but also led to the lowest denitrification rate (Li et al., 2020). When using methanol as a carbon source, sufficient time for biomass adaptation must be provided in order to reach the target effluent TN. For instance, Nyberg et al. (1996) found that the acclimation period for ethanol was a single day, whereas with methanol was close to a month. Intermittent dosing of methanol to deal with peak loads in non-adapted biomass does not yield reliable denitrification (Ginige et al., 2009). Methylotrophs are relatively slow growers; Dold et al. (2008) measured a 1.3 d^{-1} specific growth rate for methylotrophs compared to 4 d^{-1} for heterotrophs using acetate. Thus, sufficient SRT must be provided in the system to avoid washout, particularly during winter.

2.3 Endogenous Decay

A commonly used and accepted model for decay is the lysis-regrowth model, as shown in ***Figure 6***. When biomass decays, part of it becomes debris, or material that is not biodegradable, at least within the relevant time scale at a WRRF. The other portion becomes particulate biodegradable substrate, which can be hydrolyzed to soluble biodegradable substrate. This substrate can then be used for growth of new biomass, hence the "regrowth" part of the model. As with any other type of rbCOD that is oxidized, this substrate from biomass can also be oxidized with the use of a terminal electron acceptor such as DO or NO_3/NO_2. Thus, the term "endogenous decay denitrification" is the result of NO_3/NO_2 reduction via the use of substrate generated from decay. The amount of new biomass created is less than the amount initially subjected to decay, so there is always a net loss of cell material. The accumulation of debris causes a reduction in viability of the population over time. Thus, as the solids residence time (SRT) increases, the biomass activity is lower. Activated Sludge Models use the lysis-regrowth model. Reduction factors are used to adjust decay rates under varying conditions: decay occurs slower under anoxic and anaerobic conditions than under aerobic conditions.

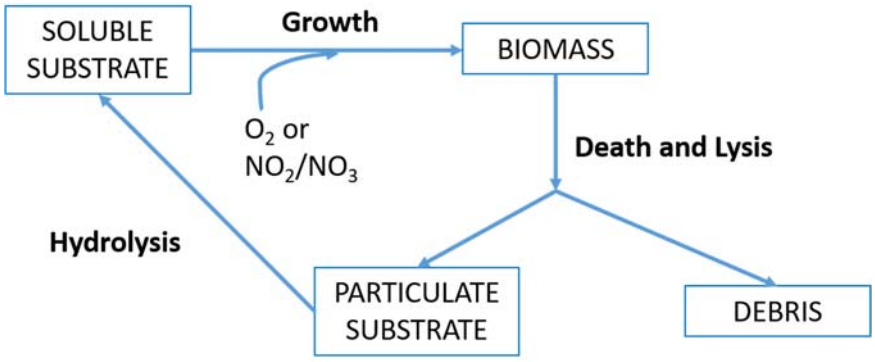

Figure 6. Schematic of lysis-regrowth processes (adapted from Grady et al., 2011).

Cells are subject to decay from predation and cell lysis, which can be called "external decay", and leads to the subsequent hydrolysis and regrowth steps as discussed above (Van Loosdrecht & Henze, 1999). On the other hand, under famine conditions, cells may also undergo "internal decay", which does not reduce the number of cells, but rather their size and activity as internal storage compounds are consumed and the cells become dormant (Kaprelyants & Kell, 1996). When endogenous decay is discussed in this paper in relation to denitrification, it is the external decay, where hydrolysis and regrowth of biomass uses NO_x as an electron acceptor, that is being referenced. The use of internal carbon for denitrification is a separate mechanism as investigated in this paper. This could be considered a form of internal decay, but is considered a distinct process from the external endogenous decay because it is suspected to occur via a select (yet unidentified) group of microorganisms that are likely similar to carbon-storing heterotrophs such as polyphosphate accumulating organisms (PAOs) and glycogen accumulating organisms (GAOs), and only under specific (yet unknown) conditions.

Denitrification using endogenous decay products as a carbon source will occur regardless of whether an external carbon source, such as methanol, is present or not. However, the rates of endogenous decay denitrification for various processes with post-anoxic stages vary quite a bit. ***Table 2*** lists some of these specific denitrification rates (SDNRs) reported in literature.

Table 2. Literature reported endogenous decay denitrification rates.

Source	Process type	Endogenous SDNR (mg N/g MLVSS/hr)
Henze, 1991	Full-scale WRRFs	0.2-0.5
Kujawa & Klapwijk, 1999	Anoxic batch reactor	0.2-0.6
Vocks et al., 2005	Pilot-scale AOA with membrane	0-0.6
Tchobanoglous et al., 2014	[*not specified*]	0.42-1.25
Shi et al., 2019	AOA SBR	0.35

Shi et al. (2019) were able to reach an effluent TN as low as 3.5 mg N/L with no external carbon source, but with a long hydraulic residence time (HRT) in the range of 12-15 hours. This would require reactors of very large volumes and is not practical for full-scale WRRFs. Post-anoxic denitrification rates without external carbon have been shown to be over 1.5 times faster with NO_2 than NO_3, which could reduce the post-anoxic HRT required to reach the desired effluent TN limits

(Shi et al., 2019). However, NO_2 accumulation in the preceding aerobic phase is not always feasible, and is not currently an operational focus at HRSD's 5-stage WRRFs. An anaerobic zone bypass to the post-anoxic zone provides external carbon from the influent, and RAS partial-redirection to this zone increases MLSS, both of which could be beneficial to endogenous decay denitrification (Basturk et al., 2020). This is also not always feasible given pre-existing configurations at WRRFs. An operational parameter that can be manipulated more readily in existing WRRFs is the SRT. Operating at a lower SRT can contribute to higher endogenous SDNRs, presumably due to a younger and more active biomass population (Vocks et al., 2005).

2.4 Internal Carbon Denitrification

Even without an external carbon source, denitrification rates exceeding endogenous decay rates have been observed (Coats et al., 2011; Vocks et al., 2005; Winkler et al., 2011). It is hypothesized that this is due to some internal carbon source, rather than external. Such a theory was validated by Vocks et al. (2005) when batch test denitrification rates using washed vs. unwashed sludge of the same source appeared to be identical, and still above expected endogenous decay denitrification rates. In addition, the COD concentrations were unchanging in these batch tests, further supporting a lack of an external carbon source. PAOs and GAOs are two types of carbon-storing heterotrophs that could play a role in this type of internal carbon-driven (internal C) denitrification.

2.4.1 PAOs and GAOs

PAOs are key organisms for the bio-P process. They store phosphorus intracellularly, so when they are removed from the system through solids wasting, phosphorus is also removed from the system. These are carbon-storing heterotrophs, which utilize internal carbon in the form of polyhydroxyalkanoate (PHA) and glycogen. ***Figure 7*** shows the modified Mino PAO model, with the key components and processes under anaerobic and aerobic conditions.

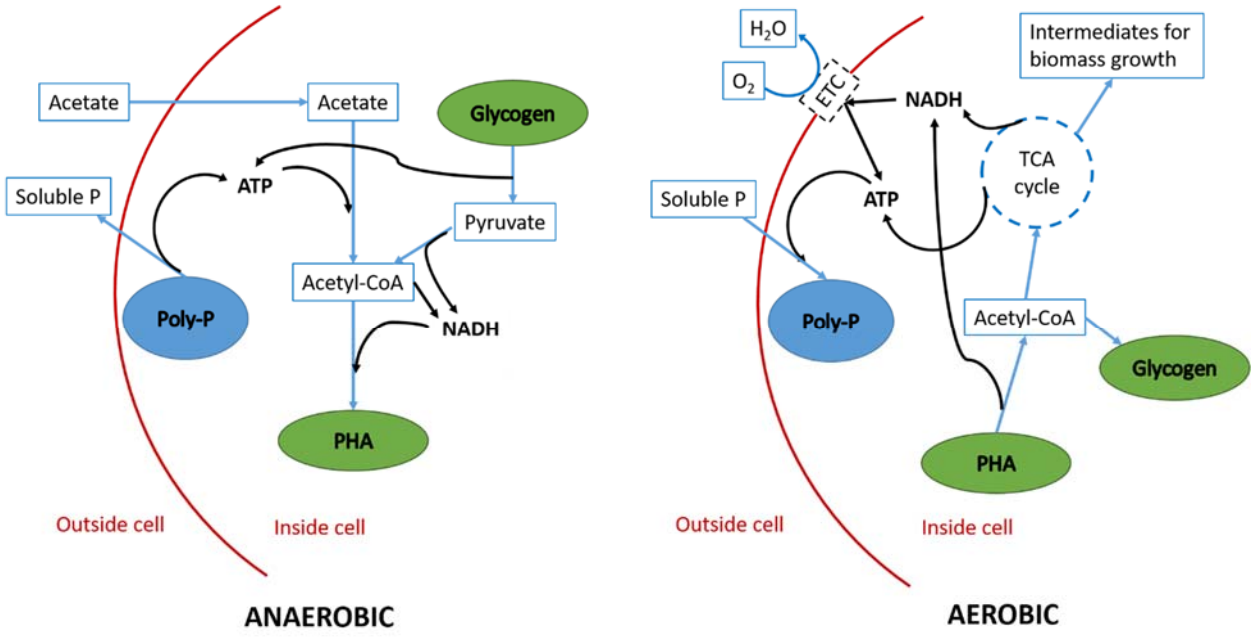

Figure 7. Modified Mino PAO model with both anaerobic and aerobic phases (adapted from Grady et al., 2011).

Under anaerobic conditions, acetate (or other VFA) is taken into the cell via the proton motive force (PMF). The acetate is converted to acetyl-CoA using ATP generated from polyphosphate (poly-P) hydrolysis, which releases soluble orthophosphate (OP) into the bulk liquid. Some of the ATP may also come from glycolysis. Acetyl-CoA is then transformed into PHA via reducing power, which is provided by glycolysis (as shown in ***Figure 7***) and/or the TCA cycle. The glycogen degradation pathway being either the Embden-Meyerhof Parnas (EMP) pathway or Entner-Doudoroff (ED) pathway, as well as the source of reducing power being either glycolysis or the TCA cycle, are both sources of discrepancy between different bio-P models (Oehmen et al., 2007).

PHA is degraded to acetyl-CoA in the aerobic phase, which then enters the TCA cycle. Oxygen is used as the terminal electron acceptor in the electron transport phosphorylation process to generate ATP. During the aerobic phase, PHA serves as a carbon or energy source for biomass growth, glycogen replenishment, and poly-P production, and must be optimally distributed to each (Mino et al., 1995). OP is taken up from solution and poly-P is regenerated in the cell, while glycogen is also regenerated through gluconeogenesis. The energy provided by PHA metabolism also allows growth of the PAO population, which increases the OP uptake capacity to take up more of the soluble OP in the bulk liquid than what was released during the anaerobic phase, so a net removal of OP occurs.

The GAO metabolism is very similar to that of PAOs, as shown in the Filipe-Zeng model represented in ***Figure 8***. However, these cells have no poly-P storage. Therefore, under anaerobic conditions, glycolysis is used not only for reducing power, but is the main source of ATP as well. Extra reducing power (NADH) is generated from this excess glycolysis for energy, and is

consumed by forming different types of PHA; PAOs mostly store carbon as polyhydroxybutyrate (PHB), while GAOs may contain up to 25% polyhydroxyvalerate (PHV) and only 75% PHB (Grady et al., 2011). GAOs have the same aerobic metabolism as PAOs, minus the OP uptake and regeneration of poly-P.

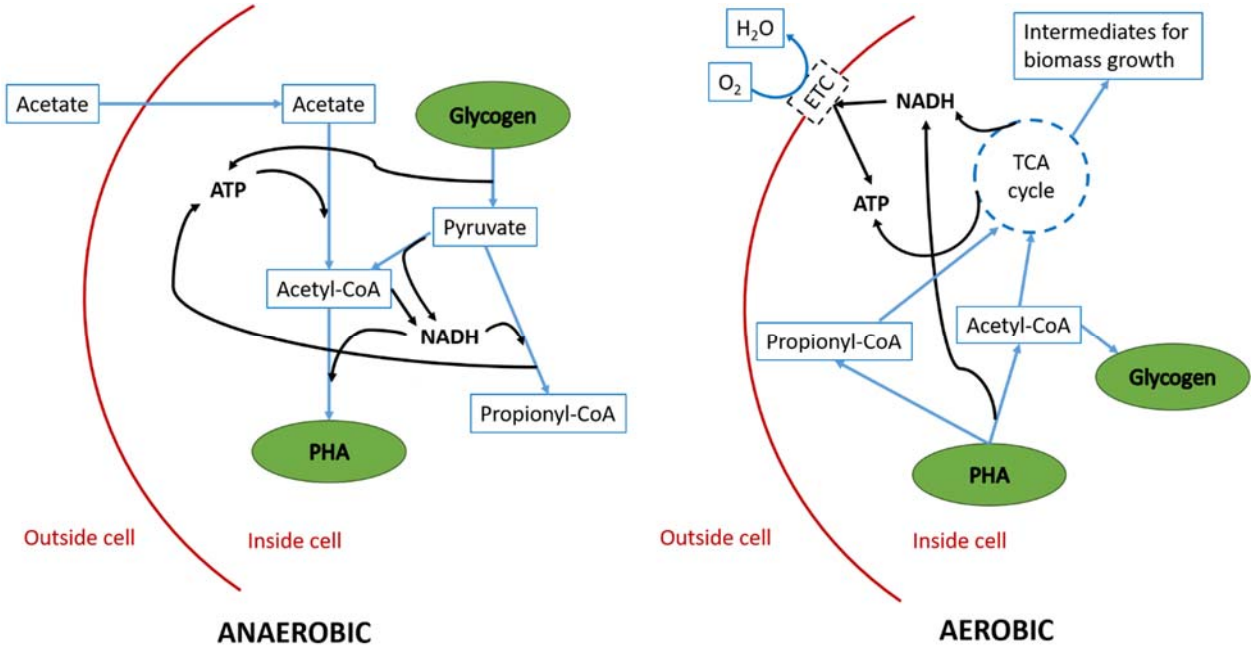

Figure 8. Filipe-Zeng GAO model with both anaerobic and aerobic phases (adapted from Grady et al., 2011).

2.4.2 Conditions for Carbon Storage

A feast/famine regime is used to select for carbon storing biomass. VFAs are provided and stored during the feast phase, and this stored carbon provides these organisms a competitive advantage in the famine phase (Dircks et al., 2001). Storage of carbon can occur aerobically, provided there is enough VFA, even though use of that carbon can also occur aerobically; an aerobic/anoxic SBR configuration was used as a feast/famine regime to facilitate PHA-storing biomass that was used for denitrification in the post-anoxic phase in multiple studies (Basset et al., 2016; Chen et al., 2015). An important component noted by Basset et al. (2016) was to minimize the non-VFA portion of COD that is only used for growth, as it competes for oxygen with the nitrifiers during the aerobic phase and reduces the PHA storage capacity of the biomass by being consumed during the famine phase for growth rather than storage. This limits the denitrification capacity of the reactor in the anoxic phase if not enough PHA is stored. While specific PAO or GAO species were not identified in these studies, the anaerobic/aerobic configuration used for biological phosphorus removal would also provide the feast/famine conditions for promoting carbon-storing biomass with the upfront anaerobic phase taking advantage of the influent VFA.

2.4.3 Internal Carbon Denitrification and Bio-P

A direct crossover between denitrification and bio-P is a denitrifying PAO (dPAO). These dPAOs are a subset of all PAOs that are able to take up OP anoxically while using NO_3/NO_2 as an electron acceptor instead of oxygen (Meinhold et al., 1999). Similar to dPAOs, denitrifying GAOs (dGAOs) can also be present in bio-P systems with anaerobic zones, which could contribute to the internal C denitrification in post-anoxic zones (Zeng et al., 2003). Winkler et al. (2011) explicitly observed GAOs in an internal C denitrification reactor, which were assumed to be responsible for the denitrification, and did not interfere with bio-P performance and/or PAO population.

Regardless of the specific metabolic process that may or may not be used by such carbon-storing heterotrophs, bio-P biomass has been directly identified as a prerequisite for internal C denitrification (Vocks et al., 2005). Post-anoxic denitrification rates for non-bio-P biomass with *no* upfront anaerobic reactor were shown to be 45% lower than those for bio-P biomass including an anaerobic reactor, but an otherwise identical process configuration.

2.4.4 Anoxic Glycogen and PHA degradation

Multiple studies have measured glycogen consumption explicitly in the post-anoxic phase and related it to the observed denitrification. Shi et al., 2019 found that the measured glycogen depletion would account for approximately 90% of the COD required for the measured NO_x removal during a 14-hour anoxic phase, and there was no other substantial drop in COD. Similarly, Vocks et al. (2005) measured a glycogen consumption rate of 2.2 mg COD/g MLVSS/hr that was very similar to the theoretical COD requirement of 2.34 mg COD/g MLVSS/hr for NO_x removal. This theoretical COD requirement, r_s (mg COD/g MLVSS/hr), was calculated as follows (from Kujawa & Klapwijk, 1999):

$$r_s = \frac{2.86(r_{D1} - r_{D2})}{1 - Y_H}$$

Where 2.86 mg COD/mg N is the theoretical COD demand for denitrification, r_{D1} is the overall denitrification rate (1.26 mg N/g MLVSS/hr), r_{D2} is the denitrification rate not associated with glycogen (0.81 mg N/g MLVSS/hr), and Y_H is the biomass yield (0.45 mg biomass/mg COD) on glycogen. Vocks et al. (2005) also observed a distinct 36% decrease in a batch test denitrification rate with no external carbon after 6 hours, which they attributed to depletion of the glycogen pool. This drop was similar to the 45% difference in denitrification rates between bio-P and non-bio-P biomass as mentioned previously from the same study.

It is generally assumed that PHA is no longer available by the anoxic phase, as it is consumed in the preceding aerobic phase while glycogen is being replenished (Smolders et al., 1995). Indeed, PHA was depleted by the end of the aerobic phase in the anaerobic/aerobic/anoxic SBR reactors run by Coats et al. (2011), so anoxic glycogen depletion was observed. When the aerobic period was shortened, there was some PHA carryover to the anoxic phase, and glycogen utilization didn't

begin until PHA was depleted, so it appears they are not used simultaneously for denitrification. Furthermore, extending the anoxic phase did not yield much more glycogen usage, so the biomass was not able to deplete the entire glycogen pool. Changing the carbon feed to the anaerobic reactor was also shown to affect the internal C denitrification rate. Augmenting the reactor with VFA (acetic and propionic acid) led to higher aerobic glycogen replenishment that ultimately increased the subsequent post-anoxic denitrification rate. Results from a combination of studies confirms this observation: as the initial post-anoxic glycogen concentration increases, the denitrification rates increase as well (Coats et al., 2011; Winkler et al., 2011). In the study by Winkler et al. (2011), changing the carbon source from a 90:10 mixture of wastewater to fermenter liquor to a synthetic acetate feed was shown to reduce glycogen accumulation in the aerobic phase and the amount used in the post-anoxic phase, yet denitrification rates were relatively unaffected.

On the other hand, multiple studies have demonstrated that PHA was left at the end of the aerobic phase, and was thus degraded for denitrification during the anoxic phase while glycogen was replenished (Krasnits et al., 2013; Liu et al., 2013). Some OP uptake occurred anoxically in the study by Liu et al. (2013) but relatively lower than expected for dPAOs for the observed N removal, so a combination of dPAOs and dGAOs were assumed to be responsible. Shortening the aerobic time increased the PHA available in the subsequent stage, increasing the denitrification rate. Another study with an aerobic/anoxic SBR showed both PHA and glycogen depletion during the anoxic phase, but attributed denitrification primarily to PHA, the highest rate for which was when acetate was used as the carbon source (Chen et al., 2015).

For the most part, while both PHA and glycogen seem to be interchangeable for use in post-anoxic denitrification, that is not the case for bio-P. For instance, Brdjanovic et al. (1998) showed that when PHA was depleted, extra OP was not taken up, even when poly-P was below saturation in the cell, and there was still glycogen present. Thus, glycogen cannot replace PHA for OP uptake during the aerobic phase.

Given the key roles of PHA and glycogen for PAO metabolism, the effect on bio-P performance from the consumption of these carbon sources instead in post-anoxic denitrification must be considered. Under "typical" steady state operating conditions, glycogen would start and end at the same concentration for each anaerobic/aerobic operating cycle. Brdjanovic et al. (1998) showed that by extending the aerobic phase from 2.25 to 26.25 hours, glycogen was further decreased beyond the typical end concentration in the 2.25-hour aerobic phase, but was never fully depleted by the end of the 26.25-hour phase. Similar to the Coats et al. (2011) study, this suggests that glycogen will never get fully depleted, even when the anoxic phase is extended to try to further improve N removal. This did result in diminished bio-P performance in subsequent operating cycles. However, Coats et al. (2011) was also able to maintain stable bio-P performance while post-anoxic denitrification via glycogen consumption was occurring in SBR reactors, at much more realistic aerobic HRTs. Phosphorus removal was near complete (96%) by the end of the aerobic phase, and glycogen oxidation during the anaerobic phase was actually above expected levels.

As previously discussed, glycogen is assumed to be the main source of reducing power for the transformation of acetyl-CoA to PHA in anaerobic PAO metabolism. However, the use of acetate through the TCA cycle to generate reducing power for this process has also been proven; feeding of 13-labeled acetate in an anaerobic phase following an aerobic starvation phase where glycogen was depleted led to generation of near-completely 13-C labeled CO_2, indicating TCA cycle dominance (rather glycolysis) for reducing power (Zhou et al., 2009). Furthermore, Zhou et al., (2009) combined data and predictions from multiple studies, which collectively showed that the amount of reducing power generated via the TCA cycle was shown to decrease as the amount of glycogen available increases. It seems that the situational TCA cycle contribution to reducing power could support stable bio-P conditions in spite of this "extra" glycogen depletion for denitrification in the post-anoxic zone; in other words, loss of glycogen to anoxic denitrification would be compensated for in the subsequent anaerobic phase by use of acetate in the TCA cycle for reducing power instead. Some PAOs may contain only pathways for a select method of generating reducing power, whereas others could be capable of both the glycolysis and TCA cycle route for reducing power (Oehmen et al., 2007).

2.5 Denitrification Enzymes

Apart from using NO_3 or NO_2 as the terminal electron acceptor instead of oxygen, denitrifying OHOs use the same biochemical pathway as aerobic respiration on organic carbon; these organisms are actually often facultative, or capable of both aerobic and anoxic respiration (Halling-Sorensen & Jorgensen, 2008). This involves the combination of electron transport (oxidative) phosphorylation and the PMF to generate ATP for a cell. The key for denitrification is the use of the four reductase enzymes that transfer the electron to the final electron acceptor: nitrate reductase (nar), nitrite reductase (nir), nitric oxide reductase (nor), and nitrous oxide reductase (nos), as shown in ***Figure 9***. Not all denitrifiers have all four reductase enzyme genes, and so are not capable of full denitrification (Song et al., 2015). Compared to other carbon sources such as acetate and propionate, methanol was shown to select for the highest proportion of incomplete denitrifiers, which could lead to accumulation of the intermediate nitrogenous oxide species (Li et al., 2020). A mixture of VFAs as the carbon source led to the highest diversity in the denitrifier population (Li et al., 2020). This diversity would increase the likelihood of having access to a more complete denitrification pathway than for a pure substance carbon source like methanol.

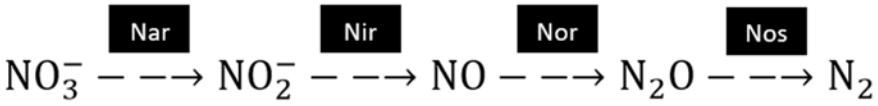

Figure 9. Species involved in complete denitrification and enzymes for each step.

The reductase enzymes can be located within the cytoplasm or periplasm (Ferguson, 1994). The route of electrons is more direct from the ubiquinone pool (one of the last stages in the electron transport chain) to the nar enzyme, whereas they must be directed to the nir, nor, and nos enzymes from the ubiquinone pool via the cytochrome bc1 complex (Ferguson, 1994). NO_2 accumulation

can often occur in anoxic zones, and a contributing factor could be this more direct route to the nar enzyme leading to more efficient NO_3 reduction.

Under aerobic conditions, the reductase enzyme activities are not inhibited directly, but rather outcompeted by oxygen, the more favorable electron acceptor (Ferguson, 1994). The expression of reductase genes, on the other hand, is directly inhibited by the presence of oxygen (Korner & Zumft, 1989). Rather than acting as a cohesive unit, each reductase is affected to a different extent by varying concentrations of oxygen, as well as by different concentrations of electron acceptors (Korner & Zumft, 1989). For instance, NO_3 initiated expression of all reductases, whereas NO_2 tended to favor nir (Korner & Zumft, 1989). This lack of coordination in reductase expression could be another contributing factor to accumulation of the nitrogenous oxide species, such as NO_2, during the denitrification process. A simple lack of oxygen was not enough for expression of these reductases, though, as a nitrogenous oxide compound had to be present (Korner & Zumft, 1989). So, while reductase *activities* are not completely inhibited under aerobic conditions, ensuring *expression* of these enzymes long-term requires minimization of DO concentrations as well as nitrogenous oxide species present to act as electron acceptors.

2.6 Slowly Biodegradable COD Conversion

At facilities with primary clarifiers and nutrient removal, an operating strategy is to overload the clarifiers in warm summer conditions to send more organic material downstream to the treatment process. The intent is that this material would contain and be converted to a usable form of carbon to enhance storage for bio-P or consumption for denitrification. The biodegradable particulate and colloidal material, considered sbCOD, gets hydrolyzed to soluble rbCOD that is more accessible to the biomass. ***Figure 10*** shows the classification of COD and this particular hydrolysis conversion. Zhang et al. (2016) showed that the sbCOD dropped throughout each stage of the treatment process at a full-scale anaerobic/anoxic/aerobic WRRF, by 20%, 12%, and 30%, respectively. Batch testing confirmed that sbCOD was reduced by 65% under 8 hours of anaerobic or aerobic conditions. An 8-hour anoxic test also showed that after an initial hour-long lag period for hydrolysis, particulate COD served as a feasible carbon source for NO_x removal, although to a lesser extent than acetate or rbCOD as used in other reactors (Zhang et al., 2016). Further support of sbCOD contributions was from a study by Krasnits et al. (2013), where in biofilm reactors operated with either synthetic acetate feed or real wastewater, a greater portion of the COD required for denitrification was credited to stored PHA for the acetate reactor than the real wastewater reactor (Krasnits et al., 2013). This was because some of the particulate COD from the real wastewater was adsorbed/entrapped during the feed stage, and therefore could have served as an external carbon source during the subsequent anoxic phase.

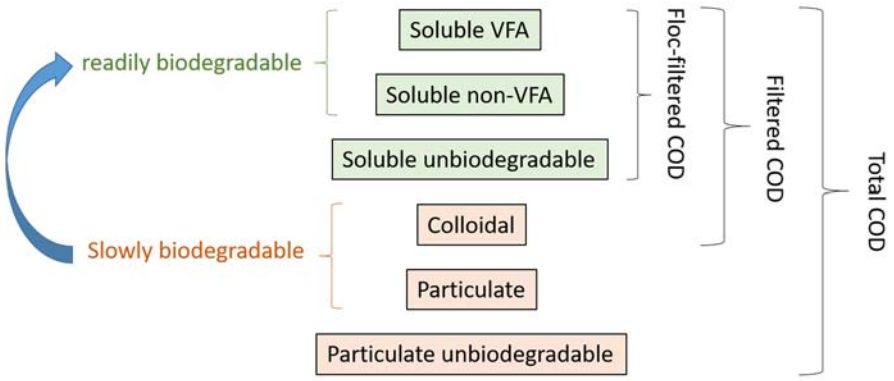

Figure 10. Components of wastewater COD. The arrow indicates production of rbCOD through hydrolysis.

However, while many papers support the role of sbCOD in denitrification, Winkler et al. (2011) showed that switching from a 90:10 mixture of wastewater:fermenter liquor (with some potential sbCOD) to synthetic acetate feed (no sbCOD) did not change the denitrification rate in the post-anoxic zone. The sbCOD was therefore assumed not to be a significant contributor to post-anoxic denitrification.

In another study by Li et al. (2020), chemically enhanced primary treatment (CEPT) was shown to remove 70% of influent organics, and these solids were subsequently fermented through the hydrolysis and acidogenesis steps to produce soluble COD, including VFAs that could be used for denitrification. Therefore, given that only 10-20% of influent carbon is rbCOD, simply overloading the primaries (without fermentation of primary solids) may not necessarily provide much usable carbon downstream (Peng et al., 2007). That is, unless the carbon is converted to rbCOD during the treatment process, but not completely utilized before it gets to the anoxic zone. The role of sbCOD in post-anoxic denitrification, at least for HRSD's WRRFs, is not known and will be reviewed.

3. Manuscript 1 – Investigating the Use of Stored Carbon in Post-Anoxic Denitrification

3.1 Abstract

Significant methanol savings at HRSD's Virginia Initiative Plant (VIP) are hypothesized to result from storage of internal carbon in the anaerobic zone that is used for denitrification in the post-anoxic zone. An investigation into the factors affecting internal carbon-driven (internal C) denitrification was done via a series of batch tests. The capacity for internal C denitrification was demonstrated with sludge from VIP, Nansemond Plant (NP), and Army Base (AB) in the batch tests, despite not necessarily being used full-scale at each WRRF. Internal C denitrification rates increased during winter, by as much as 1 mg N/g MLVSS/hr for VIP sludge. When the aeration time was increased from 0.5 to 2.5 hours or 4.5 hours, the form and/or amount of internal carbon used for denitrification is likely changing, and the SDNR decreased by an average of 0.21 mg N/g MLVSS/hr or 0.35 mg N/g MLVSS/hr, respectively. No denitrification beyond endogenous was observed for sludge from HRSD's non-nitrifying/denitrifying, bio-P WRRFs, so internal carbon denitrifiers need prior exposure to NO_2/NO_3. The increase in internal C denitrification rates when the acetate dose during the storage phase went from 20 mg COD/L to 100 mg COD/L was minor, ranging from 0.06 to 0.28 mg N/g MLVSS/hr. Internal C denitrification also seemed to inhibit the methylotrophic denitrification for some of these tests. For each WRRF, an increase in OP uptake rates was found to correlate to an increase in internal C denitrification rate, which suggests that internal C denitrification is tied to the PAO population.

3.2 Introduction and Background

Three of HRSD's conventional activated sludge WRRFs use a combination of pre-anoxic and post-anoxic zones with methanol addition as their biological N removal strategy. These include VIP, NP, and AB.

Unlike pre-anoxic denitrification, which takes advantage of the rbCOD from the influent wastewater, post-anoxic denitrification usually requires addition of an external carbon source. Shi et al. (2019) were able to reach an effluent TN as low as 3.5 mg N/L with no external carbon source, but with a long HRT in the range of 12-15 hours. This requires reactors of very large volumes and is not practical for full-scale WRRFs. VIP, NP, and AB all add methanol in the post-anoxic zone to drive the TN concentrations well below the permitted levels. The comparative methanol doses for each WRRF were represented as the mass ratio of total methanol added to TN removed across the treatment process from the PCE to final effluent. The rate of methanol addition at VIP is significantly lower than at the other two WRRFs; from 2017-2020, VIP averaged 0.49 ± 0.03 lb COD/lb N removed, while NP averaged 1.48 ± 0.06 lb COD/lb N removed and AB averaged 2.11 ± 0.15 lb COD/lb N removed.

It is hypothesized that internal C denitrification in the post-anoxic zone is a major driver of the methanol savings at VIP. Storage of carbon would occur in the anaerobic phase, and be used in

the post-anoxic zone to facilitate denitrification. The excess of carbon in the anaerobic zone at VIP supports this theory: the rbCOD:TKN ratio at VIP is 4.12 ± 0.65 mg COD/mg N, much higher than the ratios of 2.00 ± 0.26 mg COD/mg N at NP and 1.63 ± 0.32 mg COD/mg N at AB. The results from full-scale WRRF nutrient profiles at VIP indicate a large portion of NO_x removal occurring in the post-anoxic zone that cannot be attributed to methanol addition or endogenous decay denitrification. This likewise provides evidence for an additional carbon source being used for denitrification.

Even without an external carbon source, denitrification rates exceeding endogenous rates have been observed (Coats et al., 2011; Vocks et al., 2005; Winkler et al., 2011). It is hypothesized that this is due to some internal carbon source, rather than external. Such a theory was validated by Vocks et al. (2005) when batch test denitrification rates using washed vs. unwashed sludge of the same source appeared to be identical, and still above expected endogenous decay denitrification rates. In addition, the COD concentrations were unchanging in these batch tests, further supporting a lack of an external carbon source.

PAOs and GAOs are two types of carbon-storing heterotrophs that could play a role in this type of internal C denitrification. The two forms of internal carbon used by these organisms are PHA and glycogen. A relationship to bio-P performance is suggested by the correlation of methanol dose and final effluent OP concentrations at VIP. As shown in ***Figure 11***, when effluent OP concentrations increase in the warmer months (indicating deteriorating bio-P performance), so too does the methanol addition rate. This is not necessarily the case at AB or NP (***Figure 13*** and ***Figure 15***), where this internal C denitrification is not assumed to play much of a role, and relatedly where methanol savings are not nearly as significant. **Figure 12**, **Figure *14***, and **Figure *16*** show the direct correlation of effluent OP concentration and methanol dose for VIP, AB, and NP; at VIP the rough correlation of these factors is distinct from the lack of relationship in the graphs for NP and AB. Bio-P is expected to be less stable in summer, considering advantages of GAOs over PAOs at higher temperatures. As for methanol addition, it would be expected to drop during summer, as methylotrophic denitrification rates increase with the warmer temperatures (as with any reaction). However, this is not the case at VIP. The observed deterioration of bio-P at VIP seems to also inhibit denitrification performance, requiring higher methanol addition rates. Methanol dose is more or less consistent from early 2018 onwards at AB (***Figure 13***), and tends to increase slightly in summer-fall as expected at NP (***Figure 15***).

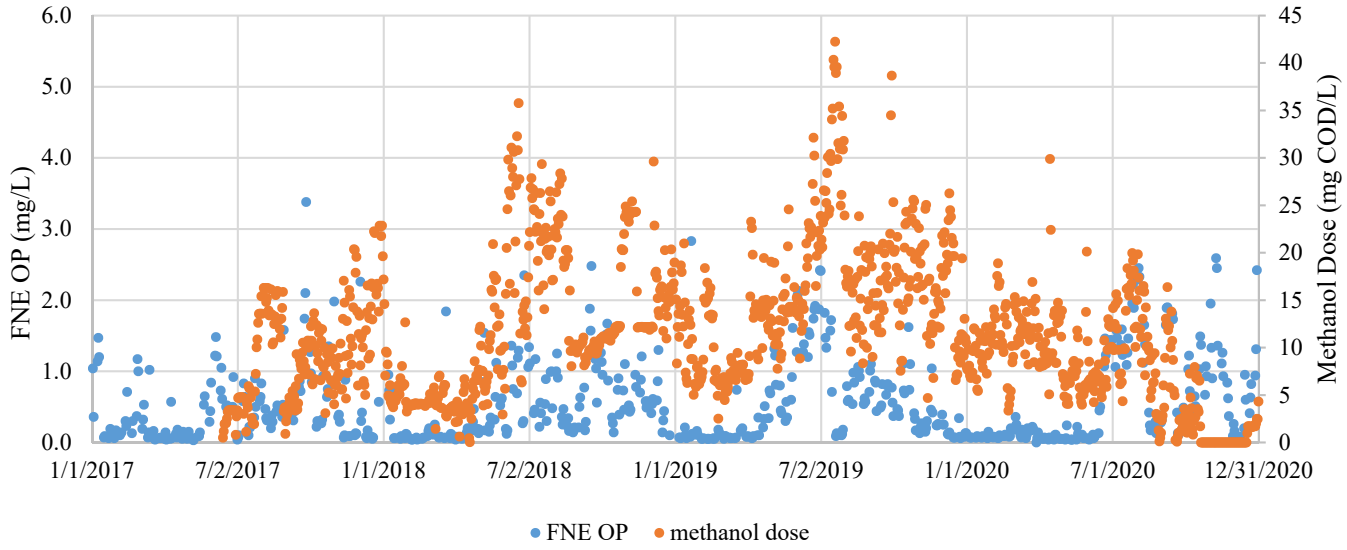

Figure 11. Seasonal variation of final effluent OP concentrations (FNE OP) and methanol dose at VIP.

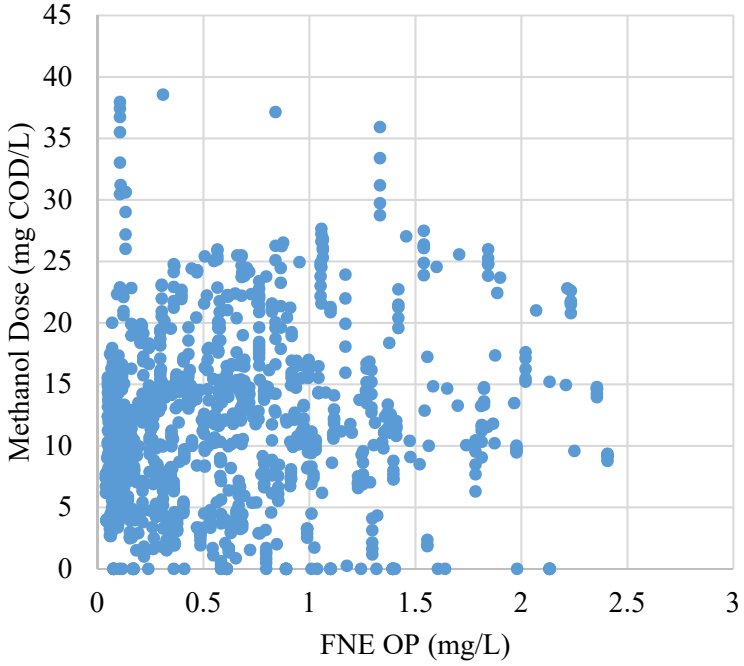

Figure 12. Direct correlation of final effluent OP concentrations (FNE OP) and methanol dose at VIP (7-day moving average for each).

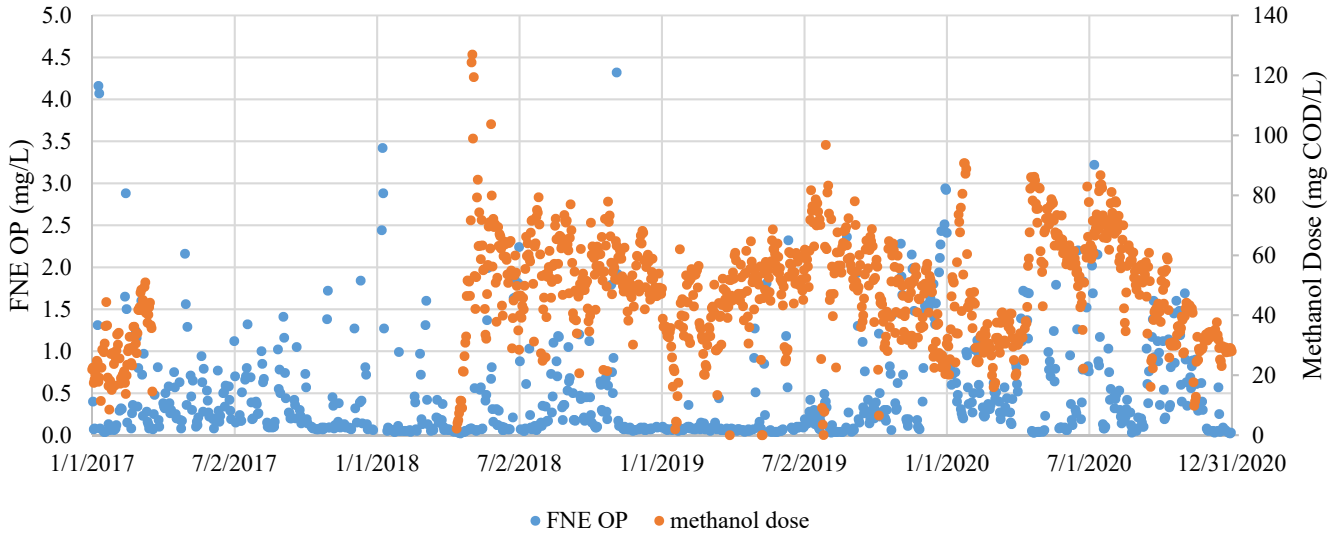

Figure 13. Seasonal variation of final effluent OP concentrations (FNE OP) and methanol dose at AB.

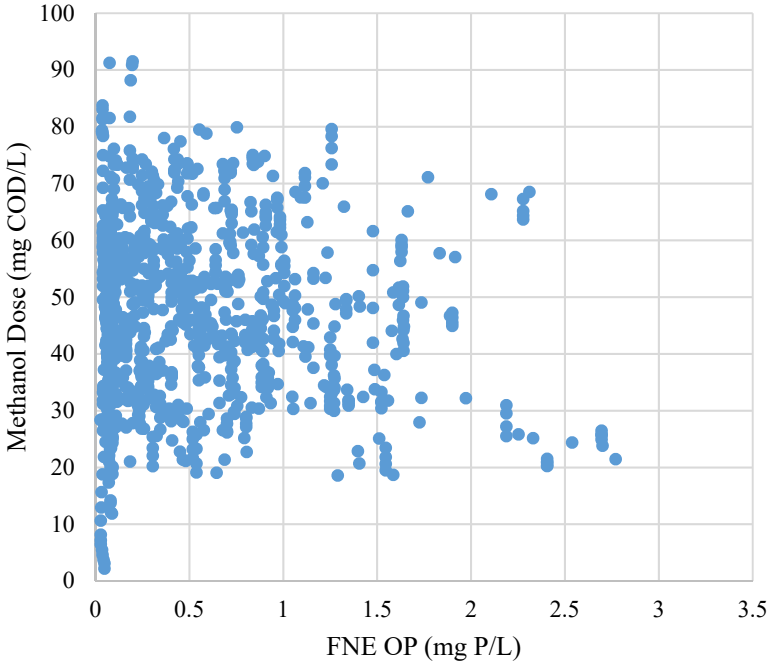

Figure 14. Direct correlation of final effluent OP concentrations (FNE OP) and methanol dose at AB (7-day moving average for each).

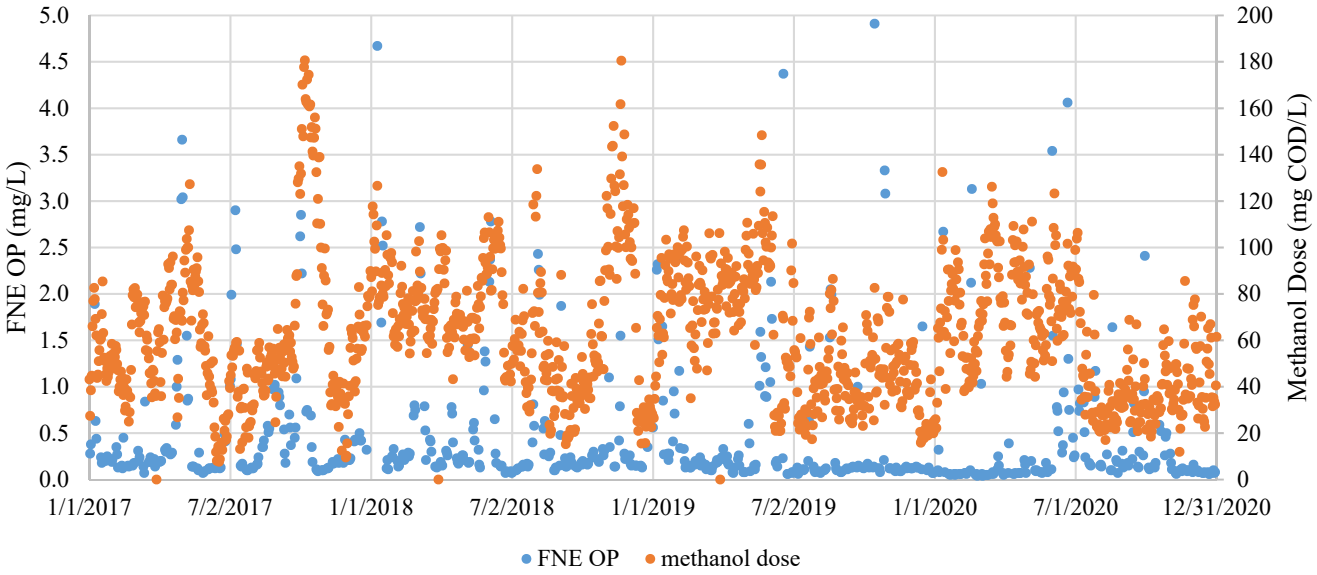

Figure 15. Seasonal variation of final effluent OP concentrations (FNE OP) and methanol dose at NP.

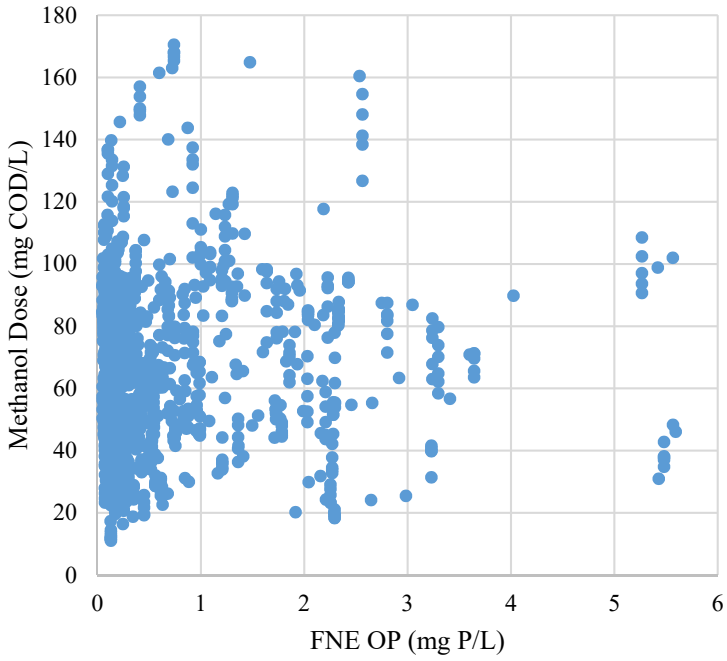

Figure 16. Direct correlation of final effluent OP concentrations (FNE OP) and methanol dose at NP (7-day moving average for each).

Internal C denitrification has been directly linked to bio-P processes in the literature. Post-anoxic denitrification rates for non-bio-P biomass with no upfront anaerobic reactor were shown to be 45% lower than those for bio-P biomass including an anaerobic reactor, and an otherwise identical process configuration (Vocks et al., 2005). Vocks et al. (2005) also observed a distinct 36% decrease in batch test denitrification rates with no external carbon after 6 hours, which they

attributed to depletion of the glycogen pool. This drop was similar to the 45% difference in denitrification rates between bio-P and non-bio-P biomass from this study.

It is generally assumed that PHA is no longer available by the anoxic phase, as it is consumed in the preceding aerobic phase while glycogen is being replenished (Smolders et al., 1995). Indeed, PHA was depleted by the end of the aerobic phase in the anaerobic/aerobic/anoxic SBR reactors run by Coats et al. (2011), so anoxic glycogen depletion was observed. When the aerobic period was shortened, there was some PHA carryover to the anoxic phase, and glycogen utilization didn't begin until PHA was depleted, so it appears they are not used simultaneously for denitrification. Furthermore, extending the anoxic phase did not yield much more glycogen usage, so the biomass was not able to deplete the entire glycogen pool. Beyond the aerobic time, changing the carbon feed to the anaerobic reactor has also been shown to affect internal C denitrification. Augmenting the reactor with VFA (acetic and propionic acid) led to higher aerobic glycogen replenishment that ultimately increased the subsequent post-anoxic denitrification rate (Coats et al., 2011).

Multiple studies have, however, demonstrated that PHA was left at the end of the aerobic phase, and was thus degraded for denitrification during the anoxic phase while glycogen was replenished (Krasnits et al., 2013; Liu et al., 2013). Some OP uptake occurred anoxically in the study by Liu et al. (2013) but relatively lower than expected for dPAOs for the observed N removal, so a combination of dPAOs and dGAOs was assumed to be responsible. Shortening the aerobic time increased the PHA available in the subsequent stage, increasing the denitrification rate.

It is evident that both post-anoxic glycogen and PHA depletion have been measured and linked to denitrification. Factors that appear to affect the type and amount of internal carbon source appear to be aerobic time and the amount of VFA available during the storage phase. Also demonstrated was the tie of internal C denitrification to bio-P biomass. Exploration of these factors and more were considered pertinent to the understanding of this type of denitrification in this study, and how it could be implemented full-scale, particularly for methanol savings at AB and NP. A series of batch tests were conducted, with several variations and types of sludge used to evaluate these factors. Mixed liquor was collected from the three HRSD WRRFs previously mentioned, and which are the focus of this study (VIP, NP, and AB), as well as from some other HRSD WRRFs. In particular for the internal C denitrification batch tests, sludge from HRSD's James River (JR) WRRF was included due to suspected use of internal carbon full-scale. JR has a design flow of 20 MGD, and utilizes an anaerobic/anoxic/aerobic (A2O) process with integrated fixed-film activated sludge (IFAS). Following the IFAS tank is a deaeration zone where no methanol is added, but some denitrification still occurs. The purpose of the deaeration zone is to allow the DO to drop prior to internal recycle back to the pre-anoxic zone. There is also a small reaeration zone at the very end.

The first objective was simply to determine if the biomass from each of HRSD's WRRFs even had the capacity for this type of denitrification in batch tests, and how this changes over the span of several months. Meanwhile, other specific aspects were explored, such as aeration time prior to the post-anoxic phase, whether the sludge was from a nitrifying-denitrifying WRRF or not, how

much carbon was available in the anaerobic phase, and correlation to bio-P performance. Comparison of overall denitrification performance, including when methanol was added in the batch tests, to the methanol addition at the full-scale also provided insight into the suspected dominant denitrifying population at each WRRF.

3.3 Materials and Methods

3.3.1 Sludge Sources

Mixed liquor from six of HRSD's WRRFs was used for some or all of the tests conducted. ***Table 3*** gives an overview of the relevant treatment process details at each WRRF and sample collection locations. Samples were generally collected at the end of the biological treatment process, prior to secondary clarification.

Table 3. Description of the HRSD WRRFs and location where sludge was collected for batch tests.

WRRF	Primary clarification ?	Secondary treatment	Nitrification + Denitrification ?	Post-anoxic methanol addition?	Sample collection location
VIP	Yes	VIP process + 2 (ANA/ANX/AER/ANX/AER)	Yes	Yes	Reaeration
NP	Yes	5-stage Bardenpho (ANA/ANX/AER/ANX/AER)	Yes	Yes	Reaeration
AB	Yes	5-stage Bardenpho (ANA/ANX/AER/ANX/AER)	Yes	Yes	Secondary clarifier influent
JR	Yes	A2O with IFAS in the aerobic zone and a small deaeration zone	Yes	No	Deaeration zone
AT	Yes	High rate ANA/AER	No	N/A	Secondary clarifier influent
CE	No	High rate ANA/AER	No	N/A	End of aeration tank

3.3.2 Batch Test Setup

All bench-scale batch tests were conducted in 4 L or 8 L reactors. Top entry paddle mixers were used. Temperature was controlled to 20°C ± 1°C using a water bath. A submersible heater and recirculation of water through copper tubing submersed in a cooler filled with ice water were used to adjust the temperature of the water bath. DO concentration was maintained at less than 0.1 mg/L for anoxic and anaerobic conditions, and greater than 2 mg/L for aerobic conditions via an air pump and aeration stone. DO control was managed via an InsiteIG dual channel controller and DO sensors. N_2 gas was used for sparging DO from the reactor to reach anaerobic/anoxic conditions, and a Styrofoam cover was applied to minimize surface oxygen transfer into the

system. Solutions of 22 g/L of $NaHCO_3$ and 0.6% sulfuric acid were used to automatically adjust the pH and maintain it between 6.9 and 7.2.

3.3.3 Batch Test Operation

After mixed liquor collection, the sample was adjusted from the full-scale WRRF temperature to the standard batch test temperature of 20°C. The sample was aerated during this time, which was usually for 1-2 hours prior to starting the test. This would prevent the sludge from going anaerobic, which could cause phosphorus release.

3.3.3.1 Endogenous Test

The reactors were kept under anoxic conditions for at least 24 hours prior to measuring the endogenous decay denitrification rate. There was no anaerobic carbon storage phase and no methanol was added, so the only carbon source was endogenous decay products. Additional NO_3 was added as necessary to prevent depletion of NO_x and resulting anaerobic conditions. Samples were collected hourly or so, typically over the course of 4-5 hours, and analyzed for NO_2 and NO_3. COD was also measured at the start and end of the period of sampling from which the rate was calculated to ensure there were no major changes.

3.3.3.2 Standard Anaerobic/Aerobic/Anoxic Test

The standard batch test consisted of anaerobic, aerobic, and anoxic (ANA/AER/ANX) phases at 45 min, 60 min, and 100 min, respectively. ***Figure 17*** shows the test schematic. 60 mg COD/L of acetate was added at the start of the anaerobic phase. The anoxic phase was split into two parallel reactors: one with methanol added, and one without. NO_3 was added to each at the start of the anoxic phase to reach a concentration of approximately 12 mg NO_3-N/L in the reactor. This test was conducted for all six of HRSD's WRRFs listed in ***Table 3***, including the non-nitrifying/denitrifying WRRFs Atlantic (AT) and Chesapeake-Elizabeth (CE). Tests were repeated over the course of August 2020 to April 2021, primarily for VIP, NP, and AB. There was no split of the reactor into two parallel reactors with and without methanol for the anoxic phase for this test when using sludge from CE, AT, and JR as these WRRFs do not add methanol as a C source for denitrification, and thus do not have an established methylotrophic population capable of using it.

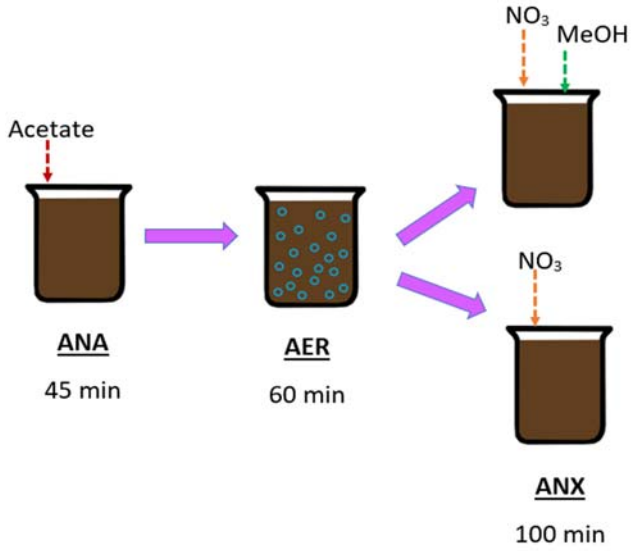

Figure 17. Schematic for the standard ANA/AER/ANX batch test with methanol addition.

3.3.3.3 Long vs. Short Aeration Test

The long vs. short aeration test was used to determine the effect of aeration time on post-anoxic SDNR. The same operating sequence as the standard ANA/AER/ANX test was used, with a couple modifications. ***Figure 18*** shows the schematic for the test. After 30 min of the aerobic phase, the reactor was split into two reactors. In one reactor, the anoxic phase was immediately started by sparging N_2 gas and spiking NO_3 ("short AER" reactor). The aerobic phase was continued for an additional 120 min in the other reactor ("long AER" reactor) prior to starting the anoxic phase. No methanol was added during the anoxic phase. This was conducted with sludge from VIP, NP, and JR. Initial tests were conducted with a 25 min anaerobic and 150 min (2.5 hour) long aerobic phase. Subsequent tests used a 45 min anaerobic and 390 min (4.5 hour) long aerobic phase to be closer to full-scale HRTs.

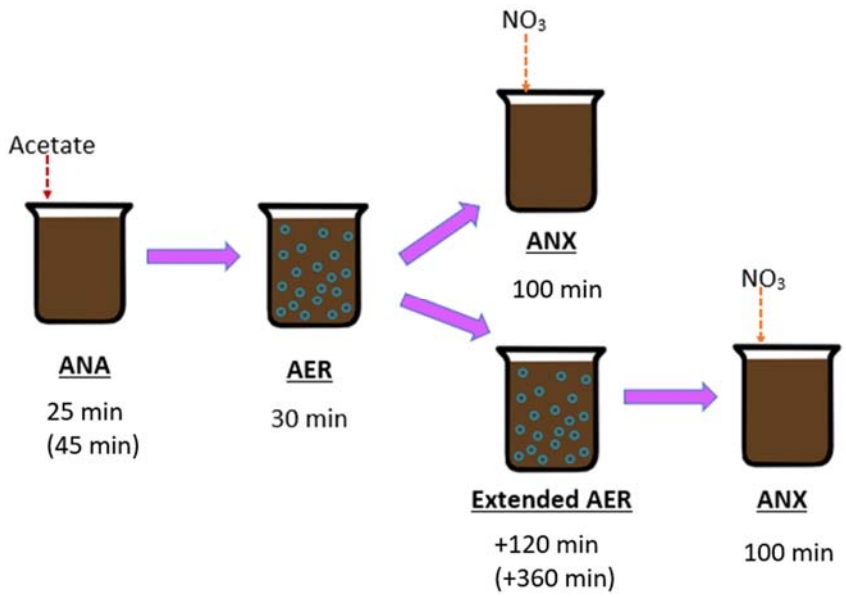

Figure 18. Schematic for the long vs. short aeration batch test.

3.3.3.4 High vs. Low Acetate Addition Test

The effect of acetate addition on post-anoxic denitrification was examined by adding either 20 mg COD/L ("low") of acetate or 100 mg COD/L ("high") at the start of the anaerobic phase. Two tests were conducted with the same sludge in parallel: one with the low acetate addition and one with the high acetate addition. Each followed the same procedure as the standard ANA/AER/ANX test (refer to ***Figure 17***). This test was done with sludge from VIP, NP, and AB.

A variation of this test was done with NP sludge. The reactor was aerated overnight prior to the test in order to eliminate the effect of residual internal carbon from full-scale on the results. The endogenous decay SDNR was measured after the overnight depletion period, once NO_3 was added and anoxic conditions were met. Residual NO_x was removed via methanol addition after the endogenous measurement, in order to establish anaerobic conditions at the start of the main part of the test. In addition, instead of 20 mg COD/L in the low acetate reactor, no acetate was added at all.

3.3.4 Sample Analysis and Rate Determination

Bio-P and denitrification were monitored by taking samples in each phase of the batch tests. Mixed liquor samples were collected with a 20 mL syringe from the 4 or 8 L reactor and passed through 0.45 µm filters. Filtered samples were analyzed for OP and COD in the anaerobic phase to determine the OP release and COD uptake rates. Initial samples were also analyzed for NO_3 and NO_2 until these concentrations were below 1 mg N/L. The COD consumption attributed to bio-P was determined by taking the total COD consumption measured and subtracting the COD required to denitrify the intial NO_x concentration that was measured in the reactor, which was primarily

NO_3. This was done by calculating the consumptive ratio (C_R) of 6.62 g COD/g NO_3-N, as follows (Tchobanoglous et al., 2014):

$$C_R = \frac{2.86}{1 - 1.42Y_H}$$

where 2.86 g COD/g NO_3-N is the stoichiometric requirement for NO_3 reduction, 1.42 g COD/g VSS is the COD value of biomass, and Y_H is the anoxic synthesis yield, which was assumed to be 0.40 g VSS/g COD removed. Samples were analyzed for OP in the aerobic phase to determine the OP uptake rates. In the anoxic phase, samples were analyzed for NO_3 and NO_2 to determine denitrification rates, COD to determine methanol consumption rates or monitor COD changes when no methanol was present, OP to monitor any potential additional OP uptake (due to dPAOs), and NH_4 to monitor accumulation from decay. The analytical methods for each parameter are listed in ***Table 4***.

Table 4. Methods used for the batch test sample analysis.

Parameter	Method	Method Name	Product Name, range
PO_4-P	Hach 10209	Ascorbic Acid, EPA 365.1	• Reactive Phosphorus TNTplus LR, 0.05-1.5 mg/L PO_4-P • Reactive Phosphorus TNTplus HR, 0.5-5.0 mg/L PO_4-P
	Hach 10214	Molybdovanadate	• Reactive Phosphorus TNTplus 1.6-30 PO_4-P
COD	Hach 8000	Reactor Digestion	• COD TNTplus LR, 3-150 mg/L COD • COD TNTplus HR, 20-1500 mg/L COD
NO_3-N	Hach 10206	Dimethylphenol	• Nitrate TNTplus LR, 0.23-13.50 mg/L NO_3-N • Nitrate TNTplus HR, 5-35 mg/L NO_3-N
NO_2-N	Hach 10207 Hach 10237	Diazotization	• Nitrite TNTplus LR, 0.015-0.600 mg/L NO_2-N • Nitrite TNTplus HR, 0.6-6.0 mg/L NO_2-N
NH_4-N	Hach 10205	EPA 350.1, 351.1, 351.2 Salicylate	• Ammonia TNTplus ULR, 0.015-2.00 mg/L NH_3-N • Ammonia TNTplus LR, 1-12 mg/L NH_3-N

MLSS was measured using a handheld InsiteIG Model 3150 suspended solids sensor at the beginning of each test. MLVSS was estimated by assuming an 80% volatile fraction of the MLSS, based on the average volatile fraction reported for the full-scale WRRFs. Specific rates, such as the SDNR, were determined by dividing the measured rates by the MLVSS concentration. These normalized rates allow a better comparison between tests from different times and for different WRRFs as the MLVSS concentration, which is representative of the biomass concentration, varies from test to test.

For the standard ANA/AER/ANX test, the methanol-only SDNR was determined by taking the difference between the SDNR in the reactor where methanol was added and subtracting the SDNR in the reactor without methanol. Internal C denitrification would occur in each reactor, so the difference between the two would be the denitrification attributable to methanol, or the "methanol-only" SDNR.

3.4 Results and Discussion

3.4.1 Endogenous Decay Denitrification

The endogenous decay denitrification tests were performed to determine the rate of denitrification observed using only carbon made available through endogenous decay. These rates served as a baseline against which all other denitrification rates (when no external carbon was added) were compared to in order to determine whether there was any extra denitrification observed. This extra denitrification would be attributable to internal carbon.

Accumulation of NH_4 could be used to estimate the decay occurring in the mixed liquor, and estimate an approximate amount of denitrification that could be associated with the carbon becoming available from the decay products based on the biomass composition. However, NH_4 accumulation was often insignificant and it was better to just measure the denitrification rate associated with this carbon source directly. An example of the results from one of the endogenous decay denitrification batch tests is shown in ***Figure 19***. A significant change in denitrification rate was observed (distinguished as NO_x - 1 and NO_x - 2), which was assumed to be due to the depletion of internal carbon in the biomass, as there was no external carbon source added to the mixed liquor. Despite the mixed liquor being collected from the reaeration zone at each WRRF, this higher initial denitrification rate was typically observed, suggested that the total usable internal carbon was not depleted by the end of the full-scale treatment process. As is the case for the test in ***Figure 19***, the reactor was often run for a total of 48 hours. However, the 24-hour and 48-hour rates were always very similar, so the 24-hour rate was used for all tests, regardless of the total reactor run time.

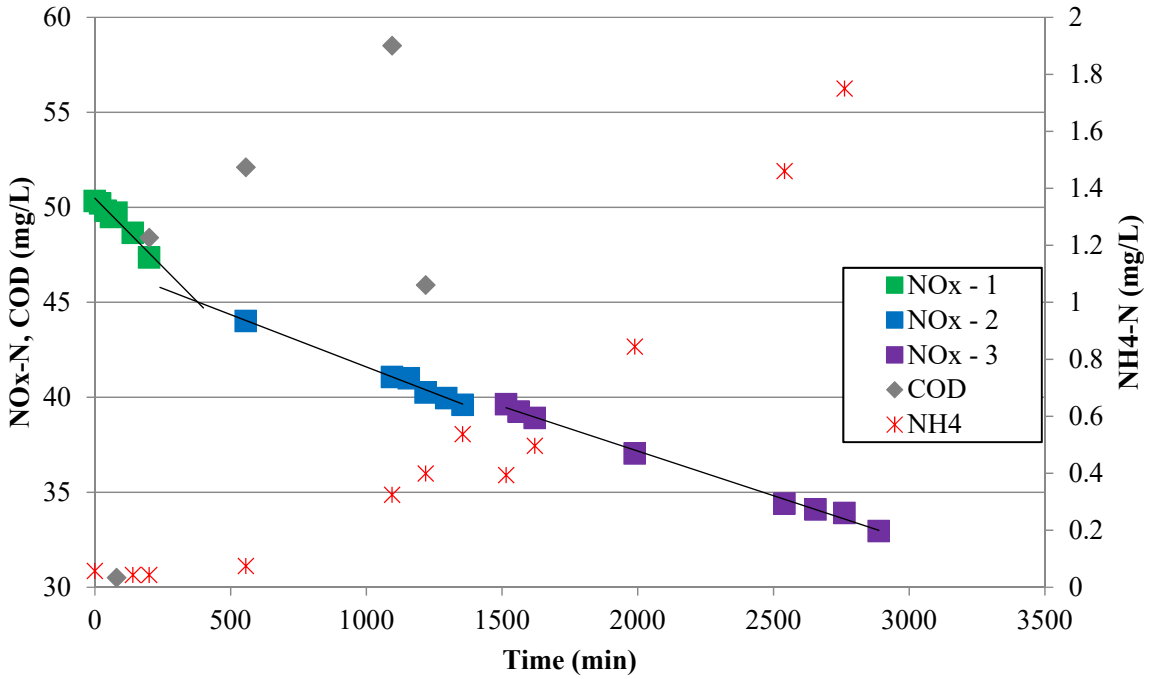

Figure 19. Example of the NO_x concentration over time in an endogenous decay denitrification batch test using VIP sludge.

These endogenous decay denitrification rate determination tests were performed for each WRRF where sludge was batch tested, and multiple times for some of the WRRFs, as the rates are subject to change over time as operational parameters, including SRT, change. ***Table 5*** shows the endogenous decay denitrification rates for each WRRF. The rates were higher for AT and CE, the high-rate WRRFs.

Table 5. Endogenous decay SDNR for each WRRF determined from batch tests. n = number of tests.

	Specific **NO_3** Denit Rate (mg NO_3-N/ g MLVSS/hr)	Specific **NO_x** Denit Rate (mg NO_x-N /g MLVSS/hr)
VIP (n=5)	0.29 (± 0.10)	0.32 (± 0.09)
AB (n=3)	0.37 (± 0.11)	0.37 (± 0.11)
NP (n=3)	0.42 (± 0.09)	0.40 (± 0.07)
CE (n=1)	0.80*	0.80*
AT (n=1)	0.68*	0.68*
JR (n=1)	0.41*	0.41*

(± 95% confidence interval for the average)
*only 1 test done, so no confidence interval

When endogenous SDNR determinations were done for the same mixed liquor as was used for another batch test (such as the standard ANA/AER/ANX test), the adjustments for determining internal C SDNRs were done using that rate. For batch tests when no endogenous decay SDNR was determined for that specific mixed liquor, factors such as time since a previous endogenous decay SDNR determination and/or similarity in SRTs between those days were considered when selecting an endogenous decay SDNR to use for adjustment.

3.4.2 Internal Carbon-Driven Denitrification Capacity

Appendix A has all results from internal carbon batch tests discussed in Section 3.4. The standard ANA/AER/ANX batch tests were performed periodically over the course of 9 months to evaluate the capacity of each of the 5-stage WRRFs for internal C denitrification, and monitor how that capacity changes over time. The internal C denitrification rates were obtained by taking the measured denitrification rate in the reactor with no methanol feed and subtracting the endogenous decay denitrification rate for that WRRF's biomass. ***Figure 20*** shows the resulting internal C SDNRs for each of the standard batch tests.

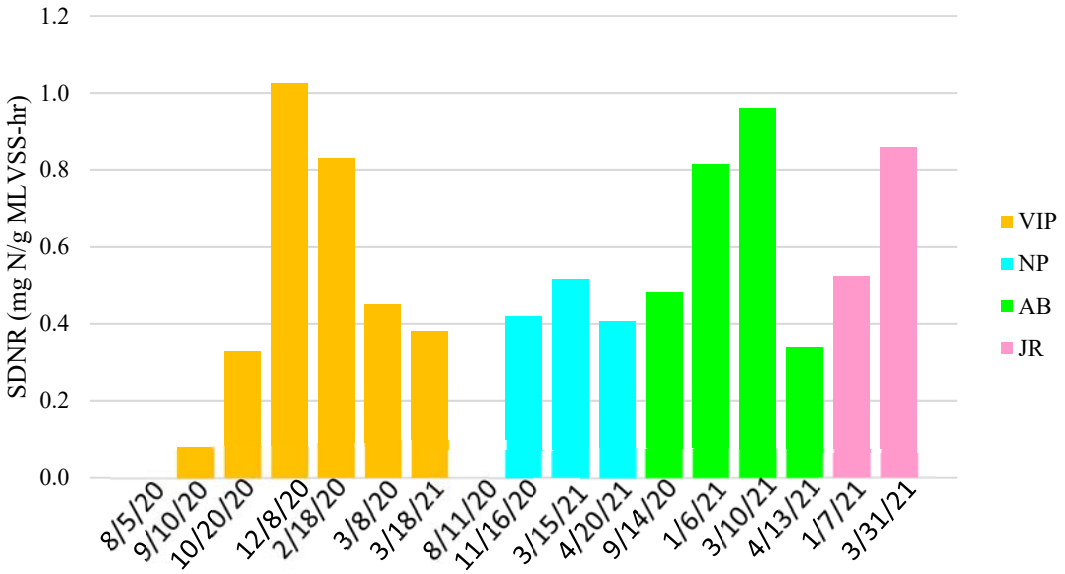

Figure 20. Standard ANA/AER/ANX batch test internal C denitrification rates.

All of the WRRFs show capacity for internal C denitrification in the batch test setting. Therefore, it is not a biomass limitation, but rather an operational factor that affects the initiation of internal C denitrification at full-scale. These rates are similar to those in literature: Coats et al. (2011) observed SDNRs of 0.69-0.90 mg N/g MLVSS/hr against an expected endogenous rate of 0.2-0.6 mg N/g MLVSS/hr, thus resulting in a corrected internal C SDNR that would fall into the range of 0.09-0.70 mg N/g MLVSS/hr.

These SDNRs increased during the winter months, when bio-P performance at the WRRFs is typically better due to repression of GAO competition at lower temperatures. For instance, the internal C denitrification was negligible for the initial test with VIP sludge in August 2020, but increased to over 1 mg N/g MLVSS/hr for the test in December 2020. This supports the dependence of internal C denitrification on the bio-P population or performance, as initially suggested by the full-scale effluent OP concentrations vs. methanol addition rates at VIP (see Section 3.2).

The internal C SDNRs were expected to be highest at VIP or JR. At VIP the full-scale denitrification from profiles and the rate of methanol addition per N removed is most indicative of this type of denitrification at this WRRF. At JR, no methanol is added in the zone following IFAS, but there is still significant denitrification that is suspected to occur from internal carbon. However, the VIP and JR internal C SDNRs were comparable to the SDNRs for the other WRRFs, particularly AB. The maximum rate for NP was significantly lower than the maximum rates observed at the other WRRFs, but these tests were only performed a select number of times during the 9-month period, and so there was no guarantee the maximum SDNR obtainable for each WRRF's sludge was observed. There seems to be something about the bench scale batch test operation that favors the use of internal carbon for denitrification in that setting regardless of what is happening full-scale at each WRRF, such as a non-limiting supply of VFA in the anaerobic

phase, or a relatively short aerobic period. The batch test setting also offers perfect plug flow conditions. This could encourage internal C denitrification, considering this phenomenon occurs at VIP where the post-anoxic zone is much closer to plug flow than at AB or NP. Some of these factors will be discussed in the following sections.

3.4.3 Long vs. Short Aeration Tests

The duration of the aerobic phase had an effect on the internal C SDNRs observed in the post-anoxic phase during the long vs. short aeration batch tests. When the aerobic time was increased from 0.5 to either 2.5 or 4.5 hours, the SDNRs decreased. ***Figure 21*** shows the overall SDNRs from each test performed with sludge from VIP, NP, and JR, as well as the estimated endogenous decay SDNRs. The short aerobic phase SDNRs ranged from 0.51 mg N/g MLVSS/hr (NP 9/8/2020) to 1.92 mg N/g MLVSS/hr (JR 2/22/2021). The long aerobic phase SDNRs ranged from 0.18 mg N/g MLVSS/hr (VIP 8/26/2020) to 1.50 mg N/g MLVSS/hr (JR 2/22/2021). The difference between the short and long aerobic phase reactors was generally larger when the long aerobic time was increased from 2.5 hours in the early tests to 4.5 hours in the later tests. The average difference between long and short aerobic SDNRs was 0.21 mg N/g MLVSS/hr for 2.5 hours and 0.35 mg N/g MLVSS/hr for 4.5 hours.

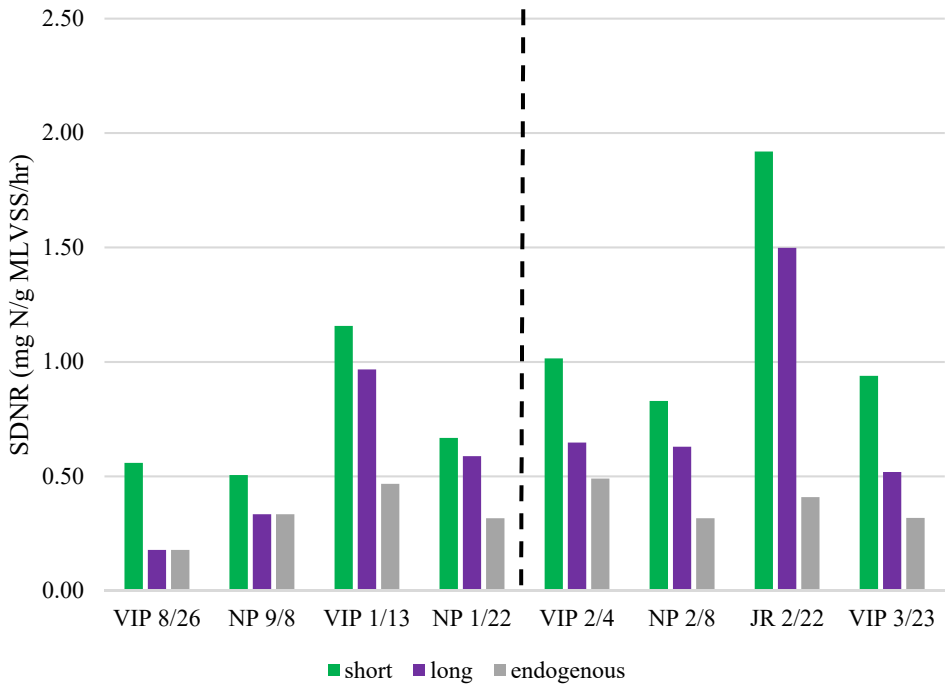

Figure 21. SDNRs from the long vs. short aeration batch tests, including endogenous decay SDNRs for comparison. To the right of dashed line are tests where the long AER was increased to 4.5 hours (instead of 2.5 hours).

The long aerobic time SDNRs did not exceed the estimated endogenous decay SDNR in the initial tests at VIP and NP (8/26/2020 and 9/8/2020, respectively), and so no internal carbon was assumed to be remaining in the biomass that could be used for denitrification in these reactors. These tests

were completed during the summer when temperatures were high at the WRRF and bio-P performance typically deteriorates. The relationship to bio-P will be discussed further in Section 3.4.6. For all of the following tests where rates exceeded endogenous decay SDNRs, it is possible that a change in carbon source is occurring between short and long aeration. As the aerobic phase progresses, PHA is depleted and glycogen is replenished. Thus, a short aerobic phase would favor higher PHA concentrations, and a longer aerobic phase would favor glycogen concentrations. Generally denitrification on glycogen has been shown to be lower than that with PHA, where literature values have been in the range of 1.12-10.8 mg N/g MLVSS/hr (Carvalho et al., 2007; Qin et al., 2005). For the long aeration reactors, either PHA has been partially depleted during the extended aerobic phase and less is available for denitrification in the anoxic phase, or PHA has been fully depleted and glycogen is used for denitrification instead, which could be less favorable. In either case, the drop in SDNR could be explained.

On the other hand, if glycogen is being used as a carbon source in both reactors, the extended aerobic phase may have gotten to the point of glycogen depletion instead of replenishment, as has been shown to occur from over-aeration by Brdjanovic et al., 1998. The point when it switched from replenishment to depletion in the tests by Brdjanovic et al., 1998 occurred sometime between 4 and 10 hours of aeration. Thus, less would be available for denitrification in the anoxic phase and would explain the lower SDNRs. However, given the long aeration time in the tests from this study was similar to full-scale aerobic HRTs (which range from 3.3 hours on average for AB to 7.5 hours for NP), glycogen depletion seems possible but unlikely.

While the internal carbon source has not explicitly been identified, the results from the long vs. short aeration test support the hypothesis that the aeration time changes the amount/form of the carbon source used for denitrification when no external carbon source is provided. This is a factor that should be considered during full-scale operation if this type of denitrification is being targeted.

3.4.4 Nitrifying vs. non-nitrifying biomass

The importance of bio-P biomass for internal C denitrification has been demonstrated (Vocks et al., 2005). As discussed in Section 3.4.2, sludge from the VIP, NP, AB, and JR WRRFs all showed capacity for internal C denitrification in the batch test setting, and these WRRFs all nitrify/denitrify as part of their full-scale processes. On the other hand, the standard ANA/AER/ANX batch test performed with sludge from the non-nitrifying/denitrifying WRRFs (CE and AT) showed no denitrification beyond the endogenous decay SDNRs, as shown in ***Table 6***. The only time when some internal C denitrification was observed was when unintentional nitrification was occurring at AT full-scale for the 11/10/20 test. As indicated by the OP release and uptake rates, each of these WRRFs had biomass performing sufficient bio-P. Thus, it can be concluded that the capacity for internal C denitrification is dependent on the process of nitrification/denitrification in addition to bio-P. Both CE and AT sludge showed endogenous decay denitrification, so even though no denitrification was occurring full-scale, there was still the capacity for denitrification in the batch test with the existing biomass. Exposure to NO_3/NO_2 must then be critical for the establishment of a population that can use internal C for denitrification. For instance, if either PAOs and/or

GAOs are the responsible organisms for internal C denitrification, they would be present in bio-P biomass, but seemingly also require exposure to the NO_3/NO_2 species in order to be able to use their internal carbon stores for denitrification. This exposure might induce gene expression for the enzymes required for this denitrification process in these organisms. Much more advanced analysis would be required to verify this theory. For example, metatranscriptomics could be used to identify when expression of these denitrification genes occurred, and which conditions change this expression. The specific organisms responsible for this internal C denitrification would also have to be identified first.

Table 6. SDNRs for each standard ANA/AER/ANX batch test performed with non-nitrifying/denitrifying sludge from AT and CE.

Test	Endogenous SDNR (mg N/g MLVSS/hr)	Total SDNR (mg N/g MLVSS/hr)	Specific OP release rate (mg P/g MLVSS/hr)	Specific OP uptake rate (mg P/g MLVSS/hr)
AT 11/10/20*	0.68	1.28	25.0	12.8
CE 11/23/20	0.80	0.81	10.8	5.5
AT 12/3/20	0.68	0.70	18.2	13.2
AT 12/15/20	0.68	0.72	21.6	13.7

*unintentional nitrification was occurring full-scale at the time this test was performed.

3.4.5 High vs. Low Acetate Test

As can be found from the data in **Appendix B**, the average VFA concentration from special year-long sampling at VIP and NP was just above 45 mg COD/L, and the values ranged from approximately 12-85 mg COD/L. Thus, a "low" value of 20 mg COD/L and "high" value of 100 mg COD/L was loosely based off of this range, making sure the low value was realistic for what was typically observed full-scale, and that the high value was actually well above the maximum to ensure these VFA-overload conditions were met.

Despite the relatively high rbCOD:TKN and rbCOD:TP ratios at VIP compared to NP or AB, and the resulting hypothesis that this extra carbon could be stored anaerobically and contribute to the internal C denitrification suspected at VIP, increasing the amount of acetate added anaerobically in the batch tests did not lead to a major increase in post-anoxic SDNRs. This increase between low and high acetate reactors was less than expected, ranging from 0.06 to 0.28 mg N/g MLVSS/hr. The resulting SDNRs from the high/low acetate tests (corrected for endogenous decay denitrification) are shown in ***Figure 22***.

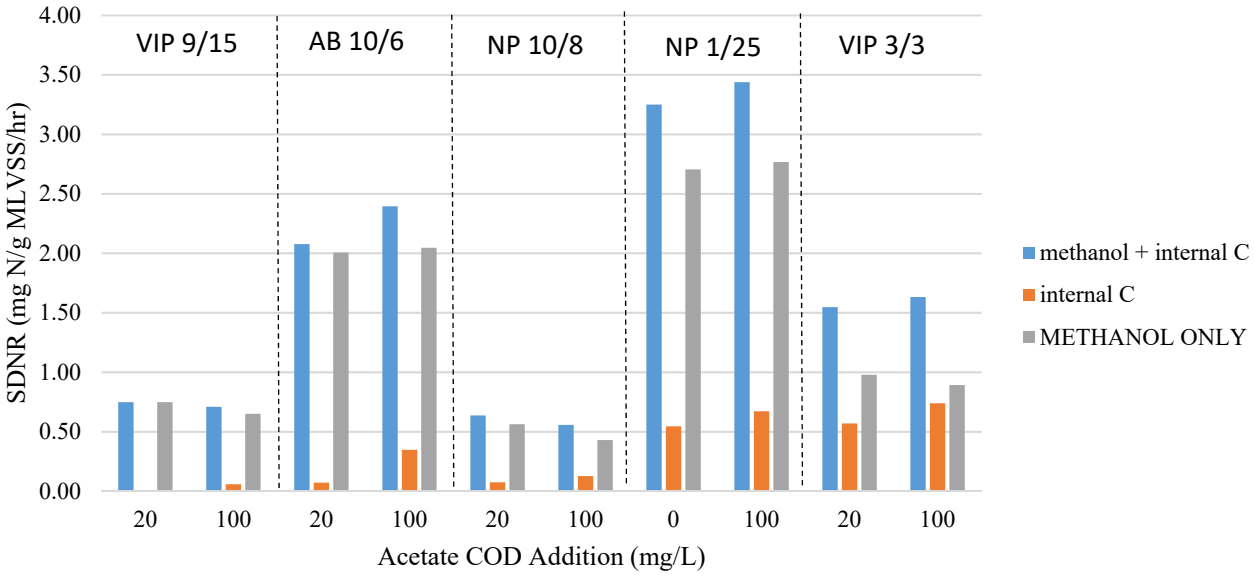

Figure 22. SDNRs from the high vs. low acetate batch tests.

For the initial test at each WRRF, the internal C SDNRs were generally low: all 0.35 mg N/g MLVSS/hr or lower. The low acetate reactor SDNRs were all right around endogenous decay SDNRs for these tests. There also seemed to be a slight inhibitory effect on the methylotrophic denitrification for 3 of the 5 tests (VIP 9/15, NP 10/8, and VIP 3/3). The methanol-only SDNR dropped by 0.09 mg N/g MLVSS/hr on average for these 3 tests when the acetate dose increased. So the increase in internal C SDNR was somewhat offset by this decrease, and the overall SDNR did not improve in these tests. This suggests some sort of interference between internal C denitrification and methylotrophic denitrification. The half-saturation constant of NO_3 for heterotrophs is 0.5 mg N/L and 0.05 mg N/L for methylotrophs (as used in Sumo), but the concentrations never got below 3 mg N/L in the batch tests. Assuming the internal C denitrifiers have a similar half-saturation, NO_3 likely wasn't limiting and there shouldn't have been major competition for substrate between the two types of denitrifiers. Methanol-acclimated biomass has been shown to be capable of using other carbon sources, such as ethanol or acetate (Cherchi et al., 2009; Dold et al., 2008; Nyberg et al., 1996). Others have implied that methanol adaptation reduces this capability of using other carbon sources, such as the wastewater COD or acetate (Ginige et al., 2009; Hallin & Pell, 1998). This perhaps could be the case for the ability to use internal carbon as well. However, methanol-acclimated biomass was also shown to yield higher denitrification rates than non-acclimatized biomass even when no methanol was added (Louzeiro et al., 2003). This was attributed to more denitrifiers/enzymes available to denitrify with whatever carbon could be scavenged, or even some sort of carbon storage. Regardless, it seems unlikely that the same organisms are responsible for both types of denitrification to explain the trade-off, as methylotrophs are typically not known to be capable of carbon storage. Furthermore, this interference was not observed for the AB test, as the methanol-only SDNR remained relatively constant, and the increase in the internal C SDNR (of 0.28 mg N/g MLVSS/hr) was similar to the increase in the overall SDNR (of 0.31 mg N/g MLVSS/hr).

The test was repeated at VIP in March when internal C SDNRs from the standard ANA/AER/ANX batch tests were generally higher than when the initial test was done the previous summer, to see if more of a difference would be observed between the reactors with high vs. low acetate at this time. The internal C SDNR increased from 0.57 to 0.74 mg N/g MLVSS/hr when acetate was increased. As with the initial test, the methanol-only SDNR dropped slightly when acetate was increased, again suggesting some sort of interference between the internal C and methylotrophic denitrification. However, the overall SDNR still increased slightly from 1.55 to 1.63 mg N/g MLVSS/hr.

Beyond the internal C SDNRs just being low (at least for the initial tests), it could be possible that the minor changes in internal C SDNRs when acetate was drastically increased was because whatever internal carbon storage there was, was actually more reflective of residual storage from the full-scale process instead of what was done during the batch test procedure during the anaerobic stage. The mixed liquor was collected from the reaeration zone at each WRRF, where internal carbon should be at a minimum, especially considering it could be used for denitrification and therefore get depleted post-anoxically. It is likely that it would not be fully depleted though, even at this point in the process. If so, the denitrification rates above endogenous indicates that all WRRFs have internal carbon available full-scale. Something about the VIP full-scale process, and perhaps specifically the post-anoxic zone, facilitates the use of that internal carbon. Or, something about AB and NP inhibits that use full-scale. The nature of the batch test, which is representative of ideal plug flow conditions, suggests that the plug-flow nature of the post-anoxic tanks at VIP could be a major factor for encouraging use of internal carbon for denitrification, as mentioned previously. If that is the case, it apparently doesn't require an adaptation period for the biomass to be able to use internal carbon, as the biomass showed these capabilities immediately on the first and only iteration of the batch tests (vs. running multiple cycles of an SBR to select for this type of denitrifier).

To mitigate the potential effect of residual stored carbon from full-scale, the second test at NP on 1/25/2021 was altered by aerating the reactor overnight prior to the test to deplete any residual internal carbon. In addition, instead of adding 20 mg COD/L of acetate to the low acetate reactor, no acetate was added at all. Somehow there was still internal C denitrification observed in this reactor, at a rate of 0.54 mg N/g MLVSS/hr. Any sbCOD that could have possibly contributed to denitrification during the anoxic phase would have been included in the endogenous decay SDNR which was measured after the overnight aerobic period, and thus was already adjusted for when determining the internal C SDNR. There must have been some other carbon source besides acetate that was available during the anaerobic phase that facilitated storage for use in the post-anoxic phase. There was also OP release observed to support this, as concentrations reached 13.6 mg P/L at the end of the anaerobic phase. Methanol was used to deplete residual NO_x from the endogenous decay SDNR measurement phase in order to obtain anaerobic conditions before starting the test, and may have still been present in the reactor during the anaerobic stage. Again, methylotrophs are not known to be capable of carbon storage, but the results from this test suggests otherwise. Any residual methanol also would have been oxidized in the aerobic phase, and thus not be available in the post-anoxic phase when internal C denitrification was measured. This test should

be repeated to verify results and try to identify the source of carbon being stored in the anaerobic phase when there was no acetate addition.

Batch test results were compared to data obtained from nutrient profiles conducted at VIP over the course of June 2017 to May 2021. ***Figure 23*** shows the amount of COD uptake estimated in the anaerobic zone, based on grab samples of the influent and effluent of the zone, compared to the amount of internal C denitrification for both post-anoxic train 1 and 2. The comparison is on a mass basis rather than by concentration due to different flows in each zone, as the anaerobic zone receives PCE and anoxic recycle, and the post-anoxic zone receive aeration effluent and RAS. The internal C denitrification is estimated from the total NO_x removed minus the amount of NO_x removed due to endogenous decay and methanol. Train 1 almost always yields higher NO_x removal, but with comparable methanol use, so the internal C denitrification contribution is higher than train 2. The reasons for this are yet unexplainable. There are also some days for which no internal C denitrification was apparent in train 2 at all.

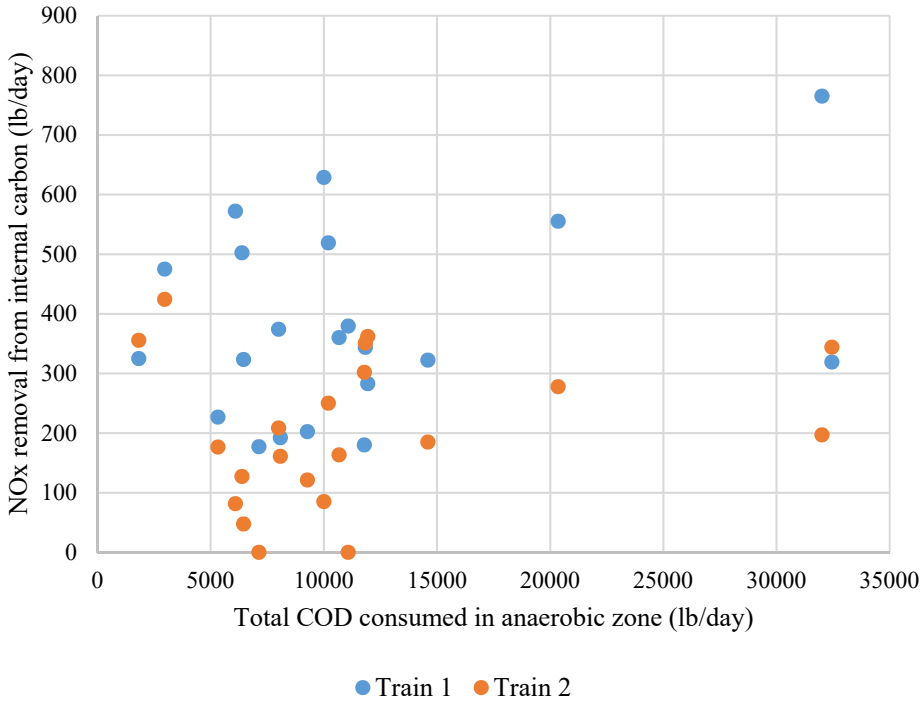

Figure 23. Relationship of carbon stored in the anaerobic zone to the amount of NO_x removal attributed to internal carbon. From VIP full-scale profile data.

For each train in ***Figure 23*** there is not a clear relationship between anaerobic COD consumption and internal C denitrification. As with the high vs. low batch tests, where it was hypothesized that more anaerobic VFA would lead to better carbon storage and higher post-anoxic SDNRs, the higher COD consumption from the profiles was anticipated to be associated with the most internal C denitrification in the post-anoxic zone. There are a couple points in ***Figure 23*** with relatively high COD consumption that show high internal C denitrification in train 1, but these could potentially be outliers and more data at these high COD consumption levels is needed to validate

these points. One potential factor that could skew some of the points from the profile data is that NO_x may start out at very low concentrations from the aerobic zone effluent, or occasionally run out (or at least very low) in the post-anoxic zone. So regardless of how much carbon was stored, there was only so much NO_x that could even be removed. This could result from various WRRF operation factors, such as low DO in the aerobic reactors that encourages some simultaneous nitrification/denitrification, which would reduce the NO_x concentrations entering the post-anoxic zone.

Appendix B contains the results from VFA sampling in the raw water influent (RWI) and PCE over the course of a year at VIP and NP, and the relevant concentrations of COD types for each WRRF. The average PCE VFA concentration was actually very similar between VIP and NP, at 46 mg/L and 49 mg/L, respectively. The average PCE tCOD was 297 mg/L and 467 mg/L for VIP and NP (400 mg/L and 624 mg/L for each RWI tCOD), and VIP appears to have detectable HPr slightly more often than NP. Based on the results from Yun et al. (2013) where higher VFA:tCOD rates and HPr concentrations correlated to longer sewer lengths, this suggests slightly more anaerobic degradation in VIP's collection system, but no major advantage as far as more VFA available for bio-P or other carbon storage (Lopez-Vazquez et al., 2009). The slightly higher frequency of HPr detection at VIP could be favorable for PAOs over GAOs, but may not be enough to be significant here. Due to the comparable VFA (and rbCOD) concentrations at NP and VIP, the reason for the low rbCOD:TKN and rbCOD:TP ratios at NP is thus due to higher TKN and TP in the WRRF influent. Indeed, the TKN and OP concentrations in the RWI and PCE for each WRRF are noticeably higher at NP than at VIP and AB (see **Appendix B**). NP receives flow from industrial dischargers that is likely responsible for the elevated influent nutrient concentrations. For the case of AB, the influent nutrient concentrations are comparable to VIP, and while no VFA sampling was done there, it could be deduced that there may be lower VFA coming into the WRRF than at VIP because of the lower rbCOD:TKN and rbCOD:TP ratios. In either case, the amount of carbon per nutrients that need to be removed is higher at VIP, and this excess of available substrate was expected to play a role in facilitating the hypothesized carbon storage that is used for post-anoxic denitrification.

Yet, while the higher relative amount of rbCOD in the influent at VIP would indicate more opportunity for carbon storage that could be used for denitrification, the batch tests with more acetate added in the anaerobic phase did not lead to much higher SDNRs. The anaerobic carbon storage vs. internal C denitrification from VIP profile data also lacks a strong correlation. Anaerobic conditions and VFA availability is likely only one of many factors relevant to encouraging internal C denitrification. As demonstrated with the long vs. short aeration test, the aeration time has an effect on the SDNR, likely by changing the amount/form of internal carbon available for use post-anoxically. Therefore, a longer aerobic time than the 60 min used in the high vs. low acetate tests might be necessary to show more of a difference between the SDNRs for the reactors with high or low acetate. The low acetate reactors may still have some residual stored carbon from the full-scale process, or enough stored carbon from the minimal acetate that was added, so that enough is left even after 60 minutes of aeration. The rate of internal C denitrification may take on a Monod-shaped relationship to the amount of stored carbon; if well above the half-

saturation, the rate would not change by much for a change in stored carbon concentration. If the aerobic time was extended to a few hours to be closer to actual HRTs, then this internal carbon may be depleted in the low acetate reactor, but not yet in the high acetate reactor. The SDNR in the high acetate reactor would be reduced given the longer aerobic time, but the difference between the high and low acetate reactors may be much more noticeable. Too much aerobic time could deplete even the carbon stored in the high acetate reactor, though. The true impact of the quantity of VFA available in the anaerobic zone for storage on the post-anoxic SDNR needs further examination, particularly in conjunction with the length of the aerobic phase. Analysis of PHA and glycogen (or whatever internal carbon source is actually being used for denitrification) concentrations throughout the tests already done as well as those suggested for the future would help to illuminate the true impact of these conditions.

3.4.6 Relation of Internal C Denitrification to Bio-P Performance

Anaerobic OP release and COD uptake as well as aerobic OP uptake were used to monitor bio-P during the batch tests and compare to denitrification performance. OP release rates, COD uptake rates, OP release:COD uptake ratios, and OP uptake rates were all compared to post-anoxic internal C SDNRs measured during the standard ANA/AER/ANX and the high vs. low acetate batch tests. The correlation with OP uptake is shown in ***Figure 24***. **Appendix A** contains the COD uptake vs. SDNR and OP release:COD uptake vs. SDNR graphs for these tests.

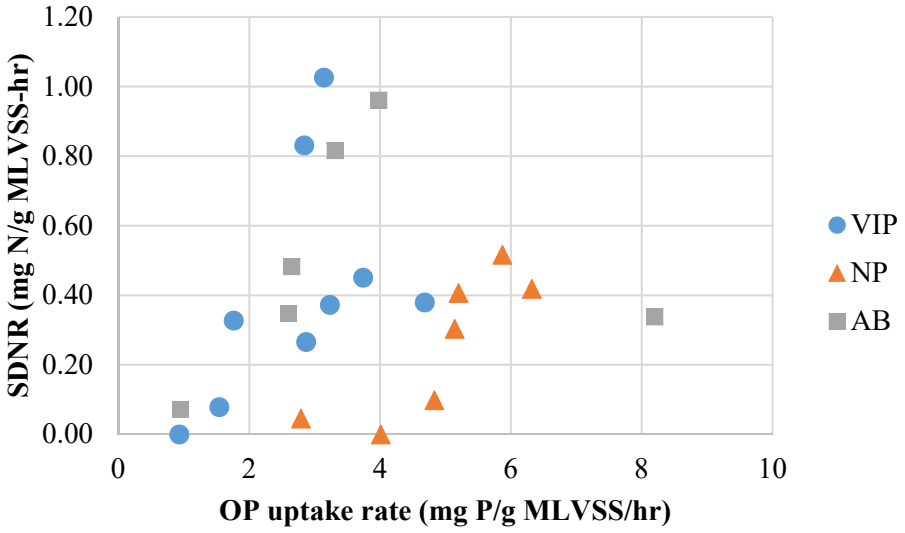

Figure 24. Relationship between OP uptake and internal C denitrification for the standard ANA/AER/ANX and high vs. low acetate batch tests.

On a WRRF-by-WRRF basis, as the specific OP uptake rate increases, the internal C SDNR also increases. There appears to be a distinct upper and lower branch in the trend for VIP, where perhaps a shift in biomass population occurred that caused the SDNRs to increase less drastically with OP uptake (lower branch). A similar phenomenon could have started to occur with AB, to explain the high OP-uptake and low SDNR outlier point in ***Figure 24***. This biomass shift may not

have fully been captured at AB and would require more tests to determine whether this was indeed what was happening or if it was some other issue that caused the outlier.

More OP uptake in the aerobic phase would tend to either consume more PHA that could otherwise be used for denitrification, or consume more PHA that could otherwise be used for glycogen replenishment. Either way, it would initially suggest lower internal carbon left for denitrification in the post-anoxic phase. However, literature suggests that the amount of PHA required for OP uptake and formation of poly-P is actually relatively low compared to that for biomass growth/maintenance or glycogen replenishment (Smolders et al., 1995). In fact, the amount of glycogen replenished was not significantly changed when there was no OP or extra OP added to the medium during aerobic batch tests by Smolders et al. (1994). Therefore, the amount of OP uptake does not seem to be a significant factor for PHA consumption or glycogen replenishment, and would not significantly inhibit the post-anoxic SDNR. This conclusion was supported by a lack of a relationship between the completeness of OP uptake (ratio of OP consumed aerobically to OP released anaerobically) and measured SDNR from the batch tests (**Appendix A**). In fact, for VIP sludge, the SDNRs tend to actually increase as the completeness of OP uptake increases. This likely is just a reflection of the higher OP uptake rates for the seemingly more active PAO population, which therefore appears to be more important to the post-anoxic SDNR rather than losing a minimal amount of extra internal carbon to OP uptake instead of denitrification. Aerobic time in general may be more important, as well as the overall quantity of PHA storage. For instance, biomass growth would be prioritized when PHA storage is low, so PHA storage would ideally be increased to maximize glycogen replenishment (or PHA leftover for denitrification) and still meet growth requirements (Mino et al., 1995).

Even though OP uptake tends to correlate to better internal C denitrification, OP concentrations do not tend to drop during the post-anoxic phase in batch testing with sludge from any of HRSD's 5-stage WRRFs. It is therefore unlikely that dPAOs are responsible for the internal C denitrification. There is usually not much OP left in the post-anoxic zone full-scale, as confirmed by nutrient profiles at VIP, so the presence of dPAOs in the biomass again seems unlikely. At least, not in the sense that they are using NO_x as an electron acceptor specifically for OP uptake; rather, it could be that these organisms are denitrifying merely for maintenance purposes. In fact, Winkler et al. (2011) suggested glycolysis was the supposed source of maintenance energy rather than poly-P hydrolysis after NO_x depletion in a post-anoxic phase of a bio-P process, as glycogen depletion was observed without OP release.

The correlation of SDNR to OP uptake may just result from a more dominant PAO population that is also partaking in the internal C denitrification. However, the quality/quantity of the PAO population would not be the only requirement for internal C denitrification, as AB and NP are both capable of good bio-P performance, but don't necessarily show this type of denitrification full-scale. In addition, with a dominant PAO population, the OP release rates would be expected to increase as well. However, there is no clear trend of the SDNRs with the OP release rates, as shown in ***Figure 25***. There could be several factors during the anaerobic storage stage that might

skew OP release and causes this lack of correlation with the internal C SDNR, such as GAO competition or more efficient storage that requires less energy derived from OP release.

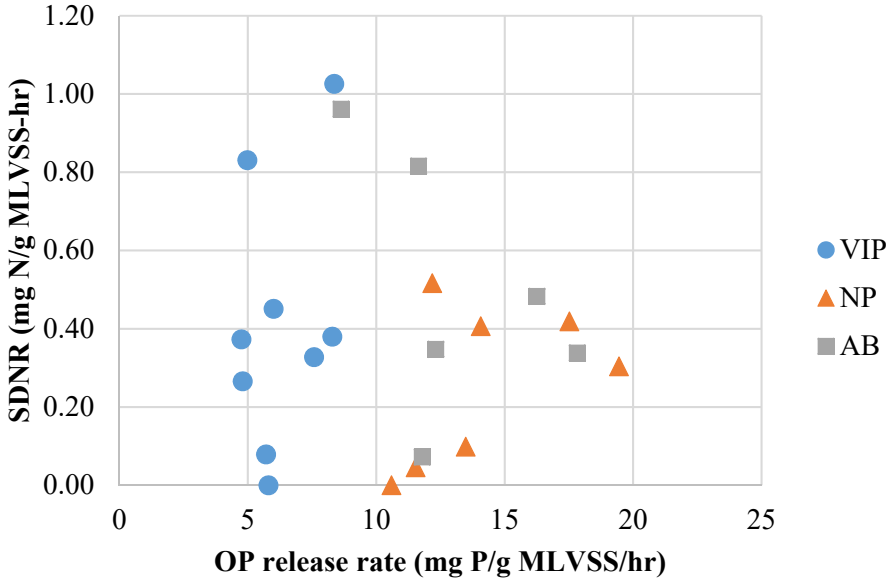

Figure 25. (Lack of) relationship between OP release and internal C denitrification for the standard ANA/AER/ANX and high vs. low acetate batch tests.

From ***Figure 25*** it can also be observed that VIP has relatively low OP release rates compared to NP or AB; they are all well below 10 mg P/g MLVSS/hr at VIP, while at NP and AB are almost always above this rate. There does not seem to be a deficiency in carbon storage, though, as the internal C SDNRs are comparable between all WRRFs. The PAO population at VIP might somehow be more efficient at storing carbon, not needing to generate as much energy from poly-P hydrolysis to do so, thus leading to lower OP release. It would be expected that this efficiency of carbon storage would probably lead to higher SDNRs than with the sludge from other WRRFs, but this is not the case from the batch tests done. On the other hand, the significantly higher F/M ratio in the anaerobic zone at VIP might encourage other types of carbon-storing organisms besides PAOs, such as GAOs or something else entirely, which might result in a smaller proportion of PAOs in the biomass overall, and thus smaller *specific* OP release rates. This is not reflected by lower specific OP uptake rates at VIP, though, which are generally larger than the rates for NP but still similar to AB.

The anaerobic COD uptake associated with bio-P was estimated assuming 7.5 mg of COD per mg of OP removed (Grady et al., 2011). The difference between total COD consumed and that associated with bio-P was compared to the amount of internal C denitrification, shown in ***Figure 26***. Again this data was obtained from VIP nutrient profiles conducted periodically from June 2017 to May 2021. The initial assumption was that with more COD consumed that was NOT used for bio-P, the more the carbon-storing heterotrophs would have available for denitrification. However, the internal C denitrification in each post-anoxic train did not necessarily increase with more non-bio-P carbon storage. It could be possible that the higher COD not associated with bio-

P is just due to GAO competition. So, if it is primarily PAOs performing the internal C denitrification as suspected, then this extra carbon storage by GAOs would not be beneficial for post-anoxic denitrification. If both PAOs and GAOs were capable of internal C denitrification, then a relationship between carbon storage and NO_x removal, as was shown in **Figure *23***, would likely be more distinguishable.

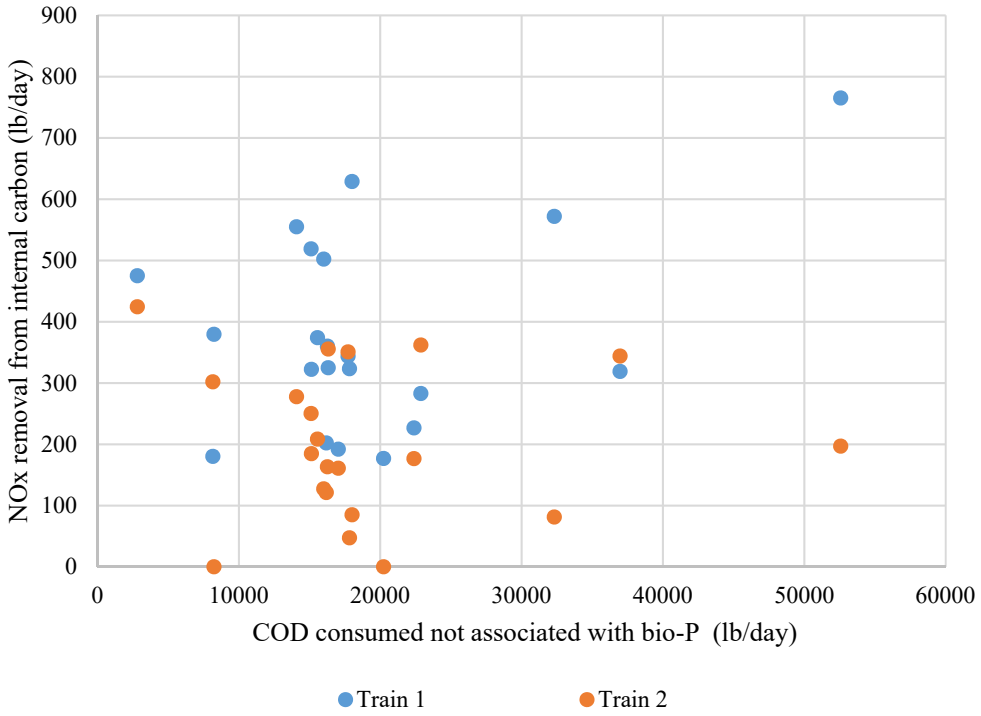

Figure 26. Relationship of carbon stored in the anaerobic zone **NOT associated with bio-P** to the amount of NO_x removal attributed to internal C. From VIP full-scale profile data.

During summer there is more VFA in the WRRF influent (as shown by the VFA data in **Appendix B**), supposedly from high temperatures driving more fermentation within the collection system. So if both PAOs and GAOs were capable of internal C denitrification at VIP, then more internal C denitrification in summer would be expected instead of less, but as indicated in the seasonal graphs in Section 3.2, there are actually higher methanol doses required in summer at VIP. The higher methanol doses seem to be required to make up for suffering internal C denitrification during this time. So while more VFA could be better for carbon storage, it also might encourage more competition from GAOs, and that competition could potentially be detrimental to post-anoxic internal C denitrification if PAOs are really the key organisms.

3.4.7 Internal C Denitrification and Methanol

The relationship of methanol addition at the full-scale WRRFs to the batch test-measured denitrification rates were distinct for each WRRF. Overall SDNRs from the standard ANA/AER/ANX batch tests where methanol and internal carbon were both available for denitrification are shown relative to the full-scale methanol addition to the WRRF at the time the

batch test sludge was collected in ***Figure 27***. The proportion of the overall batch test denitrification due to internal carbon relative to full-scale methanol addition is shown in ***Figure 28***. Methanol addition was averaged over a number of days (equal to the SRT at the time of the test) leading up to the batch test. The higher the methanol addition, the higher the overall SDNR at NP. This indicates that methanol was the dominant contributor to denitrification with this WRRF biomass. The proportion of denitrification due to internal carbon was consistent around 20% across the range of methanol addition rates. Since the overall SDNR increases when methanol addition increases, the internal C SDNR also increases to keep the same proportion. This may be a seasonal dependence, considering that more methanol is typically added during the colder months because the methylotrophs are slower-growing and so denitrify at slower rates. However, bio-P is better at low temperatures, so this could explain why the internal C denitrification rates also increase in winter. If that is the case, it again suggests that PAOs, rather than GAOs, play a more significant role in internal C denitrification. All tests were conducted at 20°C, so it is also possible that the biomass acclimated to lower temperatures would likely yield higher methylotrophic denitrification rates when warmed up to this temperature. This would skew the measured rates high, even if the methylotrophic population is more or less the same year round.

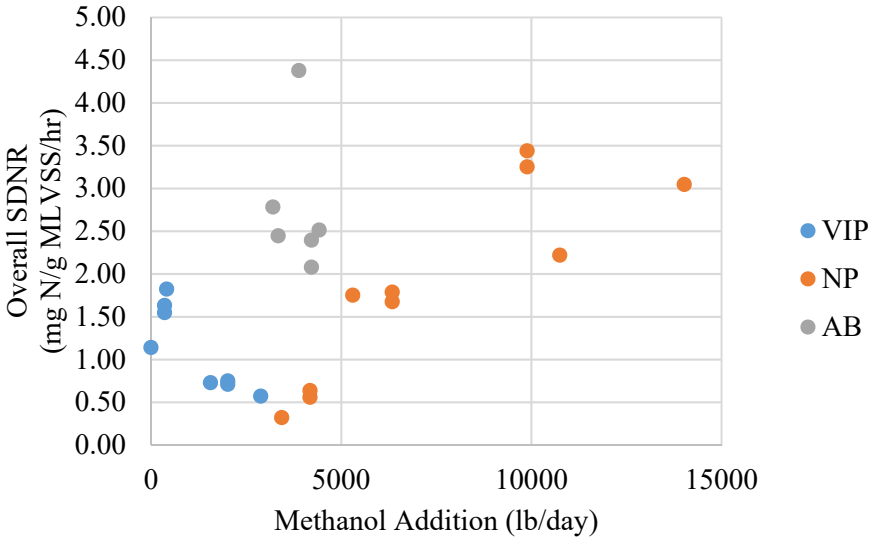

Figure 27. Variation of overall denitrification rate from standard ANA/AER/ANX batch tests (including methanol) with changing full-scale methanol addition.

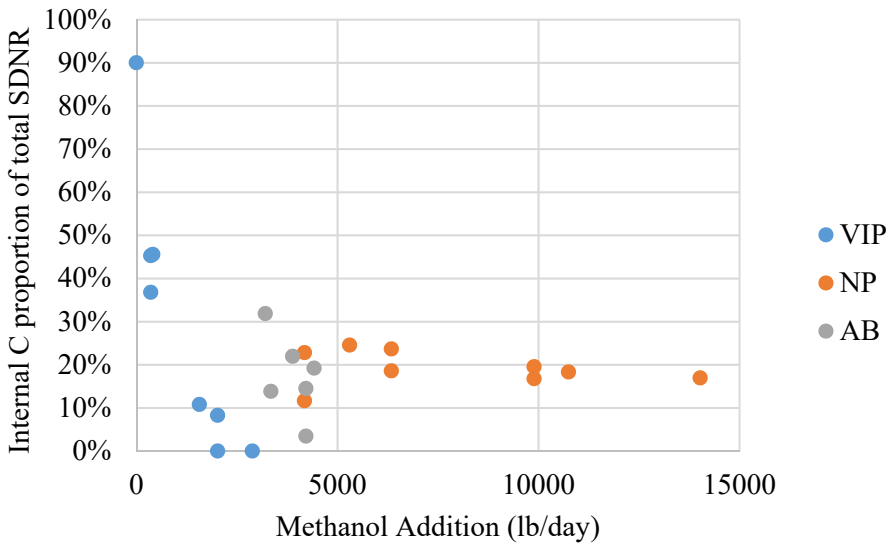

Figure 28. Variation of internal carbon proportion of overall denitrification rate from standard ANA/AER/ANX batch tests (including methanol) with changing full-scale methanol addition.

On the other hand, the higher the methanol addition at VIP, the lower the overall SDNR, and the lower the proportion of internal C denitrification. This indicates that internal carbon was the dominant contributor to denitrification with this WRRF biomass. Generally more methanol is actually added at VIP during the summer months when bio-P performance lags, as shown by the data in **Table *7*** containing 2018-2020 average methanol doses for the summer vs. rest of the year (although the difference is not as significant in 2020). Again this indicates the key role of PAOs rather than GAOs for denitrification. If PAOs are responsible for the internal C denitrification occurring full-scale, but are unable to perform as well at higher temperatures, more methanol must be added to achieve the desired effluent TN concentrations at the WRRF. When external carbon is supplied in the post-anoxic phase, this might disrupt the competitive advantage that carbon-storing biomass would otherwise have, since substrate would be more available. When less biomass is capable of carbon storage, this just feeds back into increasing the methanol demand even more. Yet even the high end of methanol addition at VIP is still quite a bit less methanol than at AB and NP, and especially on a flow-normalized basis (the average flow at VIP is 10 MGD higher than NP and 17 MGD higher than AB on average). Thus, the methylotrophic population is likely a much smaller proportion even at the high end of the methanol addition range for VIP, and so the overall rates at these times are still relatively low (as shown in ***Figure 27***). The internal C denitrifying population seems dominant at VIP.

Table 7. Average methanol doses at each WRRF for the year vs. summer months only at each WRRF. **Bold** indicates a significant difference between the averages.

		SUMMER Average Methanol Dosage (lb COD/lb N removed)	Non-SUMMER Average Methanol Dosage (lb COD/lb N removed)
AB	2018	2.20 (±0.14)	1.95 (± 0.16)
	2019	**2.30 (±0.31)**	**1.69 (± 0.09)**
	2020	3.01 (±0.67)	2.80 (± 0.68)
VIP	2018	**0.89 (±0.10)**	**0.40 (± 0.04)**
	2019	**0.78 (±0.09)**	**0.53 (± 0.04)**
	2020	0.44 (±0.08)	0.34 (± 0.06)
NP	2018	1.52 (±0.26)	1.62 (± 0.12)
	2019	**1.01 (±0.15)**	**1.48 (± 0.13)**
	2020	1.21 (±0.24)	1.35 (± 0.14)

(± 95% confidence interval for the average)

Methanol addition at AB was much more consistent during the period in which the batch tests were conducted. The overall SDNRs and proportion of internal carbon still varied despite the consistent methanol dose, indicating that there must be other factors besides methanol addition, that determines the amount of internal C denitrification and overall denitrification. There was also no evidence of the supposed "interference" between methylotrophs and internal C denitrifiers in the high vs. low acetate batch test with AB sludge, unlike for VIP and NP, as discussed in Section 3.4.5. As with VIP, there seems to be slightly more methanol demand in summer at AB as shown in ***Table 7***, despite the assumed lack of internal C denitrifiers contributing full-scale. There seems to be an aspect of the methylotrophic-internal C denitrifier interaction at this WRRF that is different from VIP or NP that should be investigated further. No clear relationship to methanol addition can be discerned from these tests.

Understanding the dominant denitrifier population at each WRRF can provide insight into how seasonal changes will affect methanol demand. In addition, the effect of changes in methanol dose on overall denitrification, as well as the contribution from internal carbon if applicable, would be better anticipated. For instance, changing factors such as aeration time or DO in the aeration zone in order to facilitate internal C denitrification may not do so if the dominant population is methylotrophs (which appears to be the case at NP) and methanol feed is not reduced.

3.5 Conclusion

From the standard ANA/AER/ANX batch tests, it is evident that all WRRFs have the capacity for internal C denitrification, at least in the batch test setting. The measured internal C SDNRs also changed over time, generally increasing during the winter months; for instance, the internal C SDNR at VIP increased from none in August 2020 up to 1.03 mg N/g MLVSS/hr in December 2020. It is assumed that this is at least partially due to more stable bio-P at the full-scale WRRFs at this time of the year due to GAO out-competition at colder temperatures. From this observation, the capacity for internal C denitrification seems to be linked to PAOs.

One factor that appeared to influence the internal C SDNR was the aeration time prior to the post-anoxic phase. The shorter aeration time of 30 minutes led to higher SDNRs than the long aeration time of 2.5 to 4.5 hours. No methanol was added during these tests, and endogenous decay denitrification was assumed to be consistent between reactors, so the change in SDNR was attributable to different quantities or forms of internal carbon being used for denitrification in the post-anoxic phase. PHA is consumed aerobically for OP uptake, glycogen replenishment, or growth. So at longer aeration times, either more PHA has been consumed and there is less for denitrification, or it is depleted and the less preferable form of glycogen is used for post-anoxic denitrification instead. On the other hand, if glycogen is used in both the short and long aeration reactors, then glycogen seemingly starts to get depleted in the extended aerobic phase, which also leads to lower post-anoxic SDNRs.

Another critical factor for post-anoxic denitrification with internal carbon is that it must be nitrifying/denitrifying biomass. Even with bio-P biomass from AT and CE, there was no denitrification observed beyond that attributable to endogenous decay. While OHOs appear to have no problem denitrifying with endogenous decay products when there has been no exposure to NO_3/NO_2, the group of organisms that use internal carbon for denitrification seem to require this exposure, perhaps to produce the enzymes necessary for this activity. Merely having an anaerobic carbon-storage phase is not sufficient. This factor does not really affect any operation at VIP, NP, or AB, unless perhaps stronger nitrification leads to higher SDNRs due to more exposure to NO_3/NO_2. So maybe operating strategies such as ammonia-based aeration control (ABAC) would somewhat inhibit this type of denitrification as there is generally higher concentrations of NH_4 and less conversion to NO_2/NO_3 aerobically, so less exposure of the internal C denitrifiers to these species.

The amount of carbon available in the anaerobic storage phase was also explored in the high vs. low acetate batch tests. This idea was based on the high rbCOD:TKN and rbCOD:TP ratios in the PCE at VIP relative to NP or AB. The increase in acetate from 20 to 100 mg COD/L did increase the internal C SDNR, but sometimes seemed to somewhat inhibit the methanol-attributed SDNR. The increase in internal C SDNR was less than expected given the drastic difference between the high and low acetate concentrations. The results from the full-scale VIP profile data of carbon storage vs. internal C denitrification in the post-anoxic zone also suggests that the relationship is not as significant as initially hypothesized. The supposed interference between the internal C and methylotrophic denitrifiers is something that needs further investigation.

The link between bio-P and internal C denitrification was first indicated by the seasonal variation in methanol dose and effluent OP at VIP; during the summer, despite higher temperatures and faster methylotrophic denitrification rates, more methanol was generally required than at other parts of the year. This corresponded with generally higher effluent OP concentrations when bio-P performance was less reliable. Therefore, the apparent struggling bio-P population seemed to also cause less efficient internal C denitrification, requiring more methanol to compensate. As previously mentioned, the increase in internal C SDNRs in the standard ANA/AER/ANX batch tests during the winter months was hypothesized to result from the more stable bio-P population full-scale. The tie of internal C denitrification to bio-P was also directly shown from comparison to the OP uptake rates in the batch tests themselves. There seemed to be a direct relationship

between internal C SDNR and the OP uptake rate for each VIP, NP, and AB. Suprisingly, there was not a similar correlation between internal C SDNR and OP release rate.

Also apparent from the standard ANA/AER/ANX batch test SDNRs and the methanol dose to the full-scale WRRF (and thus methylotrophic population) at the time of the batch tests indicate that there are distinct populations of internal C denitrifiers vs. methylotrophs at VIP, NP, and AB. Overall denitrification rates at VIP are lower when methanol addition is highest and bio-P least stable, pointing to an internal C denitrifier-dominant population. Meanwhile at NP, higher SDNRs generally occur when methanol is highest, indicating a greater fraction of methylotrophs. On the other hand, a relatively consistent methanol addition rate at AB corresponding to a range of SDNRs suggests that other factors are controlling the population or denitrification efficiency at that WRRF. Identification of relevant populations will enable prediction of how methanol dose or other factors will change denitrification performance, particularly as seasons change.

It should be considered whether anaerobic storage of carbon for later use in the post-anoxic zone rather than just being used for denitrification in the pre-anoxic zone is any more beneficial. It probably wouldn't matter if the carbon was used pre-anoxically, as long as all of the rbCOD is being utilized by the end of the first anoxic zone and doesn't enter the aerobic zone where it is oxidized and serves no purpose. Being used for denitrification in the first anoxic zone would still likely save on methanol because there would be more upfront NO_x removal and less that would need to be removed in the post-anoxic zone. However, especially for VIP, there may be a limit to the amount of internal recycle that is feasible at a given WRRF, and so only so much NO_x removal can be accomplished in the first anoxic zone. Therefore, it is desirable that carbon is stored and used in the post-anoxic zone instead of potentially passing through the first anoxic zone and into the aerobic zone unused. Use of internal carbon that was stored in the anaerobic phase would likely not occur in the pre-anoxic zone when there is already external carbon available for denitrification. In addition, less N removal pre-anoxically would be desired if simultaneous nitrification-denitrification is targeted in the aerobic zone, where the post-anoxic zone is utilized as a polishing step. Post-anoxic N removal via internal carbon is more favorable in that case as well.

An important future step would be detailed characterization of the organisms responsible for internal C denitrification and the type of internal carbon being used. Explicit measurement of these levels of internal carbon changing during the storage and denitrification phases within distinct organisms would directly verify this theory of internally stored carbon-driven denitrification. Bulk measurements could be used, or coupled with metagenomic analysis to pair carbon stores within specific organisms. If it is some type of PAO responsible as suspected, then the internal carbon may be PHA and glycogen as commonly cited in literature. However, maybe there is some other form of carbon or organism entirely that could be responsible, and the link of internal C denitrification to bio-P performance is explained some other way. Either way, identification of the carbon source and organisms responsible would be useful for developing strategies for selecting this mechanism.

Other future research could involve a series of testing across a range of aeration times instead of just two at a time, as in the long vs. short aeration test. In this case, maybe the amount of time

when the carbon source changes can be pinpointed, like when the shift from post-anoxic PHA to glycogen use occurs. Alternatively, there may be a steady change in SDNR across aeration times if this difference between long vs. short aeration was merely due to lower levels of internal carbon as aeration time increases, rather than a switch in carbon source. Related to the aerobic phase duration, it would be worth repeating the high vs. low acetate tests with aerobic times that more closely matched full-scale HRTs, instead of 60 min that was used in this study. The 60 min might have been too short to see a distinct difference between the high and low acetate reactor SDNRs if there was still plenty of stored carbon in each.

Changing the DO concentration instead of the aeration time is another approach that could be taken to investigate if the same effect is observed on SDNR as merely long or short aeration time. The DO setpoint is a more directly controllable operational parameter than aerobic residence time.

Further investigation into the apparent interference between internal C and methylotrophic denitrification is needed to try to explain some of the results observed in the high vs. low acetate batch tests. Perhaps molecular methods would be useful, such as metatranscriptomics to measure gene expression, to determine whether higher activities of one type of denitrification is observed simultaneous to a decrease in activity of the other type of denitrification. Much more information about the organisms involved, or enrichment strategies in order to even detect these organisms from the rest of the biomass, would be needed before this kind of analysis could be done, though. If these two types of denitrification really do interfere with each other, then understanding this relationship will most definitely have an impact on methanol addition; if internal C denitrification is targeted in order to try to reduce methanol use, it could potentially reduce efficiency of methylotrophic denitrification, and thus the benefits of internal C denitrification for methanol savings would not be as significant.

Based on the batch test results discussed, various factors seem to affect the occurrence of internal C denitrification as well as its rate, despite the remaining uncertainties about the exact nature of the carbon source and the identity of the organisms responsible. While a single factor may not necessarily affect internal C denitrification to great degree, it is likely that a combination of these conditions, such as an active PAO population, plug flow conditions, and high rbCOD:TP in the influent, will facilitate significant contributions from internal carbon in the post-anoxic zone. Maintaining stable bio-P and encouraging internal carbon use for denitrification would maximize use of influent carbon to the WRRF. This reduces the need for external carbon such as methanol.

4. Manuscript 2 – Evaluation of Operational Factors Influencing Post-Anoxic Methylotrophic and Endogenous Decay Denitrification

4.1 Abstract

There are many factors that affect post-anoxic denitrification, whether the carbon source is methanol, internal carbon, or endogenous decay products. For instance, a comparative tracer test between two treatment trains at NP indicated that back-mixing of methanol and its subsequent oxidation in the aerobic zone can be reduced by moving the dose point further into the anoxic zone. Tank performance is another component; the tracer test-determined post-anoxic residence time at VIP may promote over 1 mg N/L more NO_x removal than at AB from endogenous decay denitrification alone. Also considering the plug flow-like post-anoxic zone at VIP, Sumo was used to model the effect of plug flow conditions. It was not shown to significantly benefit endogenous decay or methylotrophic denitrification, but could be favorable for internal C denitrification. Overestimation of endogenous decay denitrification by the model became apparent from comparison to full-scale results. Waste rate is also influential, as specific endogenous decay denitrification rates from batch tests tended to decrease as the SRT of the WRRF's sludge increased. It was assumed that the anoxic conditions prior to methanol dosing might "prime" the methylotrophs to use NO_2/NO_3 at a faster rate. A series of these priming batch tests showed mixed results as to the benefit of more anoxic exposure prior to methanol dosing. Lastly, the apparent contribution from sbCOD to denitrification was minimal, as there was only a 0.08 mg N/g MLVSS/hr difference between reactors with 0.45 μm-filtered vs. non-filtered primary clarifier influent (PCI) as a carbon source.

4.2 Introduction and Background

VIP, AB, and NP are the HRSD WRRFs that add methanol in the post-anoxic zone to facilitate denitrification. Each has a similar treatment process, but vastly different methanol addition rates: per lb of N removed between the PCE and final effluent, VIP averaged 0.49 ± 0.03 lb COD of methanol from 2017-2020, while NP averaged 1.48 ± 0.06 lb COD/lb N removed and AB averaged 2.11 ± 0.15 lb COD/lb N removed. Methanol (MeOH) is a common external carbon source used in post-anoxic denitrification, as it is relatively inexpensive and leads to lower biomass production than other substrates (Onnis-Hayden & Gu, 2008). When biomass growth is included in the demand, the theoretical carbon dose required is 3.2 g MeOH/g NO_3-N removed (4.8 g COD/g NO_3-N). Typical doses in the field range from 3.3-3.8 g MeOH/g NO_3-N, which may incorporate other factors such as DO entering the anoxic zone that might consume methanol, as well as endogenous decay contributions to denitrification (Tchobanoglous et al., 2014). The methanol dose may be adjusted up or down to achieve the necessary concentration in the tank for the desired denitrification rate. For instance, it may be dosed in excess of stoichiometric requirements if the anoxic volume is limited and requires a faster denitrification rate to achieve the target effluent TN concentration. However, there would then be methanol in the effluent that was "over-dosed". Methanol can also be consumed aerobically, so careful consideration must be given to the dose

location, and whether there is the potential for DO there. If so, methanol may be oxidized aerobically before it can be used for denitrification.

Acetyl Co-A is the main compound in the glycolytic pathway and TCA cycle, which are used for processing organic compounds to obtain carbon and energy (Onnis-Hayden & Gu, 2008). Acetate can be transformed to acetyl Co-A easily, and is commonly found in the WRRF influent already, so typically will lead to higher denitrification rates than methanol (Onnis-Hayden & Gu, 2008). Unlike OHOs that can use a variety of carbon sources, only a specialized group of heterotrophs, called methylotrophs, are able to use methanol for denitrification. Methylotrophs are able to transform single carbon compounds such as methanol to acetyl Co-A via the serine cycle (Onnis-Hayden & Gu, 2008). The population of methylotrophs is relatively small compared to OHOs, and their population size depends on the amount of methanol fed to the system (Tchobanoglous et al., 2014).

Compared to acetate, propionate, or fermented primary solids, methanol led to the lowest sludge production, due to the relatively high amount of energy required for assimilation of the single-carbon compound, but also led to the lowest denitrification rate (Li et al., 2020). Methylotrophs are relatively slow growers; Dold et al. (2008) measured a 1.3 d^{-1} specific growth rate for methylotrophs compared to 4 d^{-1} for heterotrophs using acetate. Thus, sufficient SRT must be provided in the system to avoid washout, particularly during winter.

A commonly used and accepted model for decay is the lysis-regrowth model. When biomass decays, part of it becomes "debris", or material that is not biodegradable, at least within the relevant time scale at a WRRF. The other portion becomes particulate biodegradable substrate, which can be hydrolyzed to soluble biodegradable substrate. This substrate can then be used for growth of new biomass, hence the "regrowth" part of the model. As with any other type of rbCOD that is oxidized, this substrate from biomass can also be oxidized with the use of a terminal electron acceptor such as DO or NO_3/NO_2. Thus, the term "endogenous decay denitrification" is the result of NO_3/NO_2 reduction via the use of substrate generated from decay. The amount of new biomass created is less than the amount initially subjected to decay, so there is always a net loss of cell material. The accumulation of debris causes a reduction in viability of the population over time. Thus, as the solids residence time (SRT) increases, the biomass activity is lower. Activated Sludge Models use the lysis-regrowth model. Reduction factors are used to adjust decay rates under varying conditions: decay occurs slower under anoxic and anaerobic conditions than under aerobic conditions.

Cells are subject to decay from predation and cell lysis, which can be called "external decay", and leads to the subsequent hydrolysis and regrowth steps as discussed above (Van Loosdrecht & Henze, 1999). On the other hand, under famine conditions, cells may also undergo "internal decay", which does not reduce the number of cells, but rather their size and activity as internal storage compounds are consumed and the cells become dormant (Kaprelyants & Kell, 1996). When endogenous decay is discussed in this paper in relation to denitrification, it is the external decay, where hydrolysis and regrowth of biomass uses NO_x as an electron acceptor, that is being

referenced. The use of internal carbon for denitrification is a separate mechanism. This could be considered a form of internal decay, but is considered a distinct process from the external endogenous decay because it is suspected to occur via a select (yet unidentified) group of microorganisms that are likely similar to carbon-storing heterotrophs such as polyphosphate accumulating organisms (PAOs) and glycogen accumulating organisms (GAOs), and only under specific (yet unknown) conditions. Denitrification using endogenous decay products as a carbon source will occur regardless of whether an external carbon source, such as methanol, is present or not. An operational parameter that can be manipulated in existing WRRFs is the SRT. Operating at a lower SRT can contribute to higher specific endogenous denitrification rates, presumably due to a younger and more active biomass population (Vocks et al., 2005).

Apart from using NO_3 or NO_2 as the terminal electron acceptor instead of oxygen, denitrifying OHOs use the same biochemical pathway as aerobic respiration on organic carbon; these organisms are actually often facultative, or capable of both aerobic and anoxic respiration (Halling-Sorensen & Jorgensen, 2008). This involves the combination of electron transport (oxidative) phosphorylation and the PMF to generate ATP for a cell. The key for denitrification is the use of the four reductase enzymes that transfer the electron to the final electron acceptor: nitrate reductase (nar), nitrite reductase (nir), nitric oxide reductase (nor), and nitrous oxide reductase (nos).

Under aerobic conditions, the reductase enzyme activities are not inhibited directly, but rather outcompeted by oxygen, the more favorable electron acceptor (Ferguson, 1994). The expression of reductase genes, on the other hand, is directly inhibited by the presence of oxygen (Korner & Zumft, 1989). Rather than acting as a cohesive unit, each reductase is affected to a different extent by varying concentrations of oxygen, as well as by different concentrations of electron acceptors (Korner & Zumft, 1989). A simple lack of oxygen was not enough for expression of these reductases, though, as a nitrogenous oxide compound had to be present (Korner & Zumft, 1989). So, while reductase *activities* are not completely inhibited under aerobic conditions, ensuring *expression* of these enzymes long-term requires minimization of DO concentrations as well as nitrogenous oxide species present to act as electron acceptors.

At facilities with primary clarifiers and nutrient removal, an operating strategy is to overload the clarifiers in warm summer conditions to send more organic material downstream to the treatment process. The intent is that this material would contain and be converted to a usable form of carbon to enhance storage for bio-P or consumption for denitrification. The biodegradable particulate and colloidal material, considered sbCOD gets hydrolyzed to soluble rbCOD that is more accessible to the biomass. Zhang et al. (2016) showed that the sbCOD dropped throughout each stage of the treatment process at a full-scale anaerobic/anoxic/aerobic WRRF, by 20%, 12%, and 30%, respectively. Batch testing confirmed that sbCOD was reduced by 65% under 8 hours of anaerobic or aerobic conditions. An 8 hour anoxic test also showed that after an initial hour-long lag period for hydrolysis, particulate COD served as a feasible carbon source for NO_x removal, although to a lesser extent than acetate or rbCOD as used in other reactors (Zhang et al., 2016). Further support of sbCOD contributions was from a study by Krasnits et al. (2013), where in biofilm reactors operated with either synthetic acetate feed or real wastewater, a greater portion of the COD

required for denitrification was credited to stored PHA for the acetate reactor than the real wastewater reactor (Krasnits et al., 2013). This was because some of the particulate COD from the real wastewater was adsorbed/entrapped during the feed stage, and therefore could have served as an external carbon source during the subsequent anoxic phase.

However, while many papers support the role of sbCOD in denitrification, Winkler et al. (2011) showed that switching from a 90:10 mixture of wastewater:fermenter liquor (with some potential sbCOD) to synthetic acetate feed (no sbCOD) did not change the denitrification rate in the post-anoxic zone. The sbCOD was therefore assumed not to be a significant contributor to post-anoxic denitrification.

In another study by Li et al. (2020), chemically enhanced primary treatment (CEPT) was shown to remove 70% of influent organics, and these solids were subsequently fermented through the hydrolysis and acidogenesis steps to produce soluble COD, including VFAs that could be used for denitrification. Therefore, given that only 10-20% of influent carbon is rbCOD, simply overloading the primaries (without fermentation of primary solids) may not necessarily provide much usable carbon downstream (Peng et al., 2007). That is, unless the carbon is converted to rbCOD during the treatment process, but not completely utilized before it gets to the anoxic zone. The role of sbCOD in post-anoxic denitrification, at least for HRSD's WRRFs, is not known and will be reviewed.

Elements considered include the methanol dose point, tank performance and related residence times, relationship of SRT to endogenous decay denitrification, priming of the methylotrophs to use NO_2/ NO_3 at faster rates, and the role of sbCOD as a post-anoxic carbon source. The degree of plug flow was also considered, which involved the use of Sumo software to model the post-anoxic zone at VIP, as well as subsequent consideration of its potential use to model internal C denitrification.

4.3 Materials and Methods

4.3.1 Tracer Tests

4.3.1.1 Hydraulic Characterization

Tracer tests were conducted on the post-anoxic zones of NP and AB. Results from a previous tracer test conducted on the post-anoxic tanks at VIP from 2017 were used to represent VIP. For the tests conducted during this study, Rhodamine dye was added directly into the first cell in the post-anoxic zone of NP and into the flow stream at the end of the aerobic zone traveling to the post-anoxic tanks at AB. A target concentration of 200 ppb in the first zone of each of the post-anoxic trains was used, and the required dye for this was based on flow rate and expected masking of dye by the mixed liquor. Samples were taken at the end of the post-anoxic zone for each WRRF, starting at a frequency of every 10 minutes until the dye detected started to increase, upon which the frequency was increased to every 5 minutes. After the dye concentrations returned to near

initial levels, sample collection stopped. Samples were collected from 5 feet below the liquid surface in the tank and filtered through 0.45 μm filters. A fluorometer was used to measure the dye absorbance within the filtered sample. The fluorometer calibration curve had been developed across a dye concentration range from 0 to 1000 ppb. The calibration was used to convert absorbance readings to dye concentrations.

Analysis of the dye concentrations measured over the duration of the test was done to characterize the tank flow performance and characteristics following the method outlined in Crittenden et al. (2012). The theoretical hydraulic residence time, τ (min), is calculated as:

$$\tau = \frac{V}{Q} \tag{2}$$

where V is the volume of the reactor (gal) and Q is the flow rate (gal/min). The mean detention time, $\bar{t}$ (min), was determined using the following:

$$\bar{t} = \frac{\int_0^\infty Ct*dt}{\int_0^\infty C*dt} \approx \frac{\sum \overline{Ct}\Delta t}{\sum \bar{C}\Delta t} = \frac{(\frac{C_{i-1}t_{i-1}+C_i t_i}{2})\Delta t}{(\frac{C_{i-1}+C_i}{2})\Delta t} \tag{3}$$

where C_{i-1} and C_i were two successive concentrations (mg/L) at time t_{i-1} and t_i, respectively. The normalized time, θ (dimensionless), was calculated using:

$$\theta = \frac{t_i}{\bar{t}} \tag{4}$$

for each sample point at time t_i. The normalization concentration, C_N (mg/L), is found as:

$$C_N = \int_0^\infty C * d\left(\frac{t}{\bar{t}}\right) = \frac{\int_0^\infty C*dt}{\bar{t}} \approx \frac{\sum \bar{C}\Delta t}{\bar{t}} = \frac{(\frac{C_{i-1}+C_i}{2})\Delta t}{\bar{t}} \tag{5}$$

and the normalized concentration, E(θ) (dimensionless), for each sample is:

$$E(\theta) = \frac{C}{C_N} \tag{6}$$

The exit age distribution curve was generated using normalized time, as $\bar{t}$ is always less than the theoretical HRT, and using normalized concentration, as the recovered tracer is always less than what was injected. Normalization also allows comparison of reactor performance between different tanks and tests.

The degree of plug flow was also estimated from the tracer tests, using the variance and mean detention time of the sample data collected. The spread of the tracer curve is measured by the variance, σ_t^2 (min^2), which is calculated as follows:

$$\sigma_t^2 = \frac{\int_0^\infty (t-\bar{t})^2 C * dt}{\int_0^\infty C * dt} \approx \frac{\sum \overline{(t-\bar{t})^2 C} \Delta t}{\sum \bar{C} \Delta t} = \frac{\frac{1}{2}[(t_{i-1}-\bar{t})^2 C_{i-1} + (t_i-\bar{t})^2 C_i]\Delta t}{(\frac{C_{i-1}+C_i}{2})\Delta t} \quad (7)$$

The variance with respect to the normalized time, σ_θ^2, is (Tchobanoglous et al., 2014):

$$\sigma_\theta^2 = \frac{\sigma_t^2}{\bar{t}^2} \quad (8)$$

The dispersion number, d (dimensionless), for a plug flow reactor with significant amounts of axial dispersion can then be estimated from the variance, using:

$$\sigma_\theta^2 = 2d + 8d^2 \quad (9)$$

The dispersion number is an indication of the amount of axial dispersion in a reactor. When it is low, advection is dominant. Values for the dispersion number range from 0 for ideal plug flow to infinity for completely mixed reactors. The dispersion number is the inverse of the Peclet number, Pe. When divided by two, Pe can give an approximation for the number of ideal CSTRs in series that the given reactor performs like. The higher the number of CSTRs, the closer to plug flow conditions.

The estimation of the number of CSTRs in series using the tracer study results were compared to an empirical estimation based on the tank dimensions, using the same flow conditions and trains in service from when the tracer test was conducted. The Reynolds number, N_R (dimensionless), was calculated as:

$$N_R = \frac{4vR}{\nu} \quad (10)$$

where v is the velocity (m/s), R is the hydraulic radius (m), and ν is the kinematic viscosity ($1.003*10^{-6}$ m^2/s for 20°C). The coefficient of dispersion, D (m^2/s), was found using the empirical relationship (Davies, 1972):

$$D = 1.01\nu N_R^{0.875} \quad (11)$$

The dispersion number, d (dimensionless), is found from the coefficient of dispersion as:

$$d = \frac{D}{\nu L} \quad (12)$$

where L is the length of the tank (m). The number of CSTRs in series is again found from Pe.

4.3.1.2 Methanol Dose Point

The tracer test to evaluate mixing characteristics near the methanol dose point was conducted at NP. Dye was dosed through the methanol feed lines into the post-anoxic zone of two parallel treatment trains: Train 6 and Train 7. Train 6 had dose point modifications and Train 7 was unmodified. The unmodified methanol feed point was located at the end of the aeration tank, at the baffle wall between the aerobic and anoxic tanks, as shown in ***Figure 29***. The modified dose point is located on the other side of the baffle wall, well within the post-anoxic zone. A target concentration of 200 ppb of dye in the first cell of the post-anoxic zone was again used for this study.

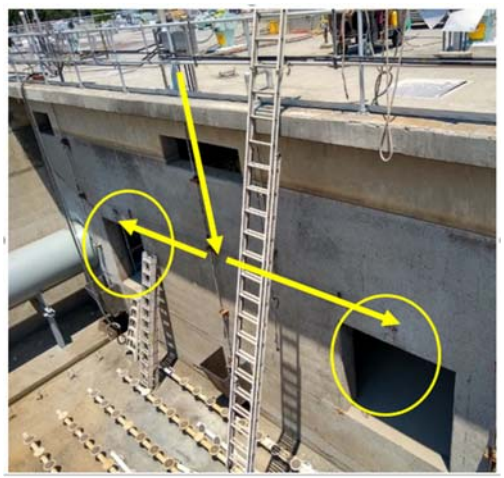

Figure 29. Unmodified methanol dose point at the end of the aeration tank (shown drained) in Train 7.

Samples were taken at the end of the aerobic zone as well as the end of the post-anoxic zone, as noted in ***Figure 30***. The sampling method was the same as described in the previous section, with the exception of sampling frequency for the end of aeration samples. These were collected every 2 minutes, starting immediately when the dye was dosed through the methanol pumps.

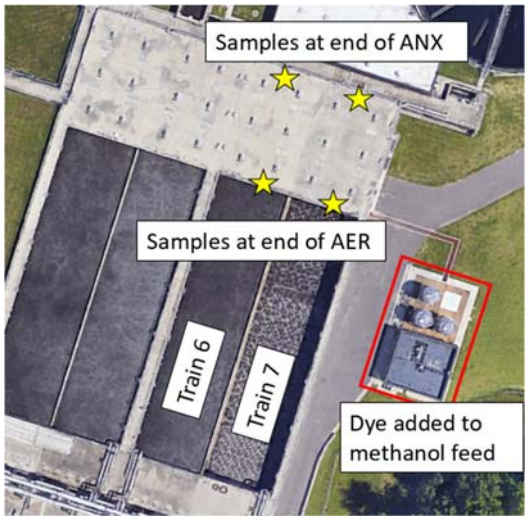

Figure 30. Sample locations for parallel tracer test in Trains 6 and 7 at NP.

The procedure to determine hydraulic characteristics of the tank were also the same as described in the previous section, using the samples collected at the end of the post-anoxic zone. For the samples collected at the end of the aeration zone, the dye concentrations over time were merely compared to determine relatively how much dye was mixing back into the aeration zone between the two trains, and no further analysis was done with those values.

A nutrient profile was conducted on the post-anoxic zone for each Trains 4, 5, 6, and 7. Grab samples were collected with a sludge judge, filtered through 0.45 μm filters, and analyzed for NO_2, NO_3, NH_4, and COD. Analysis for each parameter was done using Hach TNTplus vials (HACH Loveland, CO). Methanol dose was averaged for each train over the 3-hour HRT leading up to the time of sampling and compared to the NO_x removed in that train from the profile. A ratio of the COD added to NO_x removed for each train was used to compare methanol use efficiency of each train to complement the results from the comparative tracer test.

4.3.2 Modeling

Sumo simulation software (Dynamita, France), Version 20, was the process modeling software used to evaluate post-anoxic denitrification at VIP. Sumo2 was the specific model type used, which incorporates two-step nitrification and denitrification. A pre-existing model of VIP calibrated to 2018-2020 operational data was used and modified as necessary. The modeled post-anoxic zone consisted of 4-6 CSTR reactors in series to represent the anoxic cells in each full-scale train. A set of conditions was assembled (including temperature, influent composition, flow rates, volumes based on tanks in service, etc.) for each day that a nutrient profile was done at the full-scale WRRF. A steady state solution was found for each profile day, including NO_x concentrations at the beginning and end of the post-anoxic zone, and could be compared to the actual full-scale profile data from that day.

A steady state solution was also found for a set of assembled conditions for each day that an endogenous decay denitrification batch test was conducted with VIP sludge. The state of the mixed liquor was copied from the VIP model file into a new Sumo file with a single influent and CSTR reactor and run as a batch test. The Sumo batch test followed the same procedure as the actual batch test: fill the reactor, allow to aerate for 1 hour, and then add NO_3 and run anoxic for 24 hours. The predicted denitrification rate at the end of the 24-hour anoxic period in Sumo was compared to the measured endogenous decay denitrification rate from the actual batch test. Given the differences between the model-predicted and the actual MLSS and SRT for the mixed liquor on these days, another set of Sumo batch tests was done. This time, the waste rate in the VIP model was adjusted until the steady state MLSS matched the actual MLSS concentration before the state of the mixed liquor was copied into the Sumo batch test file. Changing the decay rate from the default was done in the model setup after the initial set of model runs for both the full plant and batch test model runs. They hydrolysis rate was similarly changed from default for the batch test runs.

Modifications were done to the base VIP model to evaluate different situations: methanol was turned on and off, and a version of the model was created for which the post-anoxic zone was changed to a single CSTR of the same total volume instead of multiple CSTRs. Since the post-anoxic trains are either run with 4 or 6 of the available 8 cells as anoxic, two new versions of the model file were created for the single CSTR scenarios, one for each equivalent volume.

The contributions to NO_x removal from various carbon sources were quantified using the Gujer matrix output in the model. The reaction rate was multiplied by the stoichiometric coefficient for the state variable (either NO_3 or NO_2) to calculate the change in state variable due to that particular reaction. For instance, the reaction of "OHO growth on SB, NO_2" (where SB is soluble biodegradable substrate) consumes NO_2 at a rate of the stoichiometric coefficient:

$$\frac{-(1 - Y_{OHO,SB,anox})}{(EEQ_{N2,NO2} * Y_{OHO,SB,anox})}$$

multiplied by the reaction rate for "OHO growth on SB, NO_2". $Y_{OHO,SB,anox}$ is the anoxic yield of OHOs on SB and $EEQ_{N2,NO2}$ is the conversion factor for NO_2 reduction to N_2. Thus, the main contributions to denitrification could be quantified directly and compared for different manipulations to the model, such as methanol/no methanol and single/multiple CSTRs. For the original model configuration, where there are multiple CSTRs as part of the post-anoxic zone, a Gujer matrix output and NO_2/NO_3 removal quantities were established for each individual cell and could be summed together for the total across the post-anoxic zone.

4.3.3 Batch Tests Sludge Sources

Mixed liquor from the three HRSD WRRFs with post-anoxic methanol addition as previously described (VIP, NP, AB) was used for the tests conducted. With the exception of the sbCOD test, sample was generally collected as mixed liquor from the end of the biological treatment process, prior to secondary clarification. For the sbCOD tests at NP and VIP, PCI and return activated sludge (RAS) were also collected.

4.3.4 Batch Test Setup

All bench-scale batch tests were conducted in 4 L or 8 L reactors. Top entry paddle mixers were used. Temperature was controlled to 20°C ± 1°C using a water bath. A submersible heater and recirculation of water through copper tubing submersed in a cooler filled with ice water were used to adjust the temperature of the water bath. DO concentration was maintained at less than 0.1 mg/L for anoxic and anaerobic conditions, and greater than 2 mg/L for aerobic conditions via an air pump and aeration stone. DO control was managed via an InsiteIG dual channel controller and DO sensor. N_2 gas was used for sparging DO from the reactor to reach anaerobic/anoxic conditions, and a Styrofoam cover was applied to minimize surface oxygen transfer into the system. Solutions of 22 g/L of $NaHCO_3$ and 0.6% sulfuric acid were used to automatically adjust the pH and maintain it between 6.9 and 7.2.

4.3.5 Batch Test Operation

After mixed liquor collection, the sample was adjusted from the full-scale WRRF temperature to the standard batch test temperature of 20°C. The sample was aerated during this time, which was usually for 1-2 hours prior to starting the test. This would prevent the mixed liquor sample from going anaerobic, which could cause phosphorus release.

4.3.5.1 Endogenous Test

The reactors were kept under anoxic conditions for at least 24 hours prior to measuring the endogenous decay denitrification rate. There was no anaerobic carbon storage phase and no methanol was added, so the only carbon source was endogenous decay products. Additional NO_3 was added as necessary to prevent depletion of NO_x and resulting anaerobic conditions. Samples were collected hourly or so, typically over the course of 4-5 hours, and analyzed for NO_2 and NO_3. COD was also measured at the start and end of the period of sampling from which the rate was calculated to ensure there were no major changes.

4.3.5.2 Priming Tests

These tests explored the effect that the reactor conditions prior to methanol addition had on the denitrification rate when methanol was present.

4.3.5.2.1 Brief 30-min Reaeration

20 mg N/L of NO_3 was added and the reactor was left under anoxic conditions for 3 hours. The mixed liquor was then split into two parallel reactors. In one reactor, 72 mg COD/L of methanol was added and the denitrification rate was measured. In the other reactor, the sample was aerated for 30 minutes, sparged with N_2 gas, and when the DO was back under 0.1 mg/L, 72 mg COD/L of methanol was then added and the denitrification rate was measured. NO_3, NO_2, and COD were measured during this phase to determine the denitrification rates and methanol consumption rate. This test was done with VIP sludge.

4.3.5.2.2 Overnight Anoxic vs. Aerobic Conditions

This test again looked at the effect of either anoxic or aerobic conditions prior to methanol addition. However, these respective conditions were maintained overnight. The test started with anaerobic, aerobic, and anoxic phases at 45 min, 60 min, and 100 min, respectively. ***Figure 31*** shows the test schematic. 60 mg COD/L of acetate was added at the start of the anaerobic phase. The anoxic phase was split into two parallel reactors: one with methanol added (Reactor A), and one without (Reactor B). NO_3 was added to each at the start of the anoxic phase to reach a concentration of approximately 12 mg NO_3-N/L in the reactor. NO_3, NO_2, and COD (when methanol was added) were measured during this phase to determine the denitrification rates and methanol consumption rate. The difference between the denitrification rates in Reactors A and B was assumed to be the

methanol-associated denitrification rate. Reactor A was then aerated for 24 hours while Reactor B was kept under anoxic conditions for that same time. NO_3 was added as needed to keep the reactor from going anaerobic (NO_x concentrations never got below 4 mg N/L in either reactor at any point in the test). Reactor A was then sparged with N_2 gas and once the DO dropped below 0.1 mg/L, 72 mg COD/L of methanol was added to each reactor and the subsequent denitrification rates were again measured. It was assumed that any residual internal carbon that could have been present within the biomass would be depleted during the extended 24-hour phase, so the denitrification measured after the methanol addition was due to methanol and endogenous decay only. The final rates in Reactors A and B were corrected for endogenous decay denitrification to get the methanol-only denitrification rate, but the initial methanol-only rate was not (as this was already a difference between two reactors which were assumed to have the same endogenous decay denitrification in each). This test was conducted with sludge from NP. There was no methanol addition at VIP at the time, so methylotrophic populations would be insufficient there.

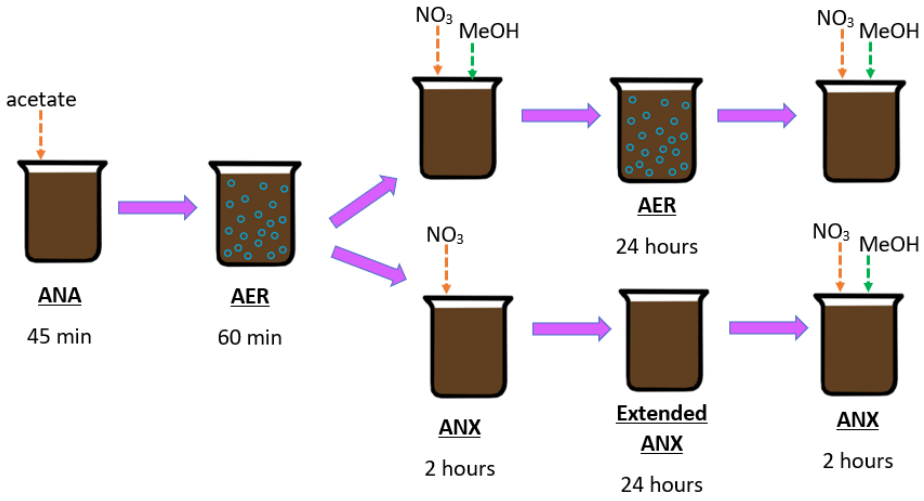

Figure 31. Schematic for the priming batch test with overnight aerobic vs. anoxic periods prior to anoxic methanol addition.

4.3.5.2.3 Varying Pre-anoxic Period Test

This batch test consisted of an initial extended aerobic phase of 4 hours, which was increased to 24 hours for the second set of tests. The intent was to deplete any residual internal carbon that could be in the biomass and eliminate any potential for interference with the methylotrophic denitrification. After the aerobic depletion phase, the mixed liquor was then split into four parallel reactors, and 20 mg N/L of NO_3 was spiked in each reactor at the start of the "pre-anoxic" phase. Approximately 5 mg/L of NO_2-N was also spiked in this phase for the second set of tests, based on observations from the initial set of tests about differences in NO_2 denitrification rates. Each reactor had a different pre-anoxic time: 0, 20, 60, or 120 min. 72 mg COD/L of methanol was then added at the end of the pre-anoxic phase. ***Figure 32*** shows the test schematic. This test was conducted with sludge from NP and AB, where more methanol was added full-scale (than at VIP) and so sufficient methylotrophic populations were assumed to be present.

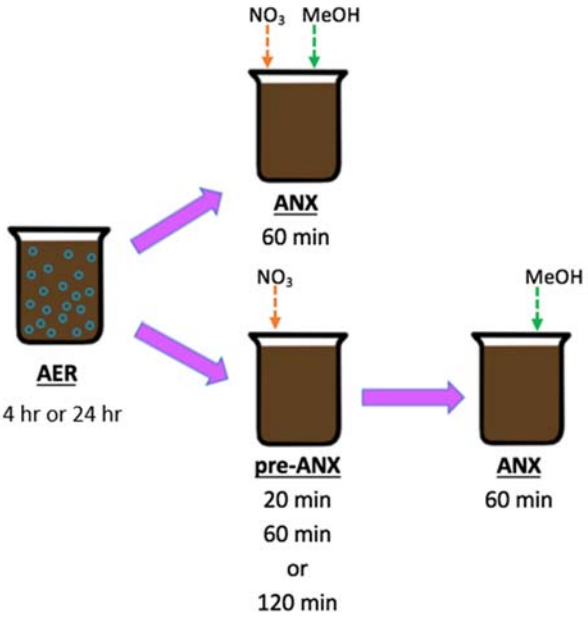

Figure 32. Schematic for the priming batch test with pre-anoxic periods of 0, 20, 60, or 120 min prior to anoxic methanol addition.

4.3.5.3 Overloading clarifiers/sbCOD Test

A combination of PCI, reaeration mixed liquor, and RAS was used to achieve a target MLSS concentration around 2000-3000 mg/L in the reactor for this batch test. Two parallel tests were conducted: one with filtered PCI and one with non-filtered PCI. The filtered PCI was passed through a 0.45 µm filter. The visual difference between the filtered and non-filtered PCI is shown in ***Figure 33***. The test started when the PCI, which served as the carbon source, was added to the mixture of reaeration mixed liquor and RAS, and after the DO fell below 0.1 mg/L. The batch test consisted of 25 min anaerobic, 150 min aerobic, and 130 min anoxic phases. NO_3 was added to each at the start of the anoxic phase to reach an initial anoxic concentration of approximately 15-20 mg NO_3-N/L in the reactor. This test was conducted with sludge from NP, where overloading the primary clarifiers is a common practice, as well as with sludge from VIP.

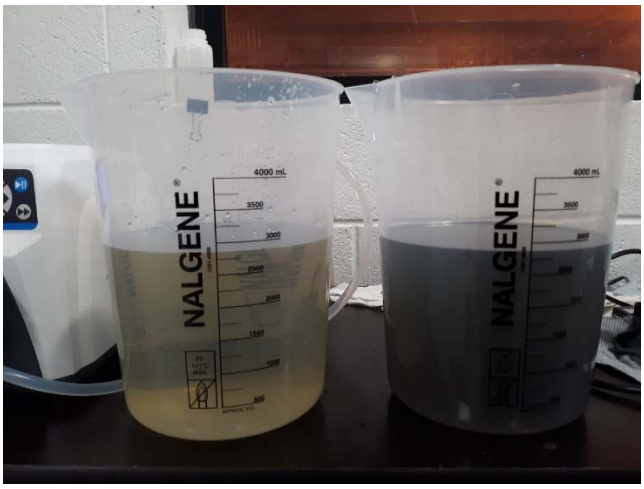

Figure 33. Comparison of filtered (left) and unfiltered (right) PCI used as the carbon source for the overloading clarifiers/sbCOD test.

4.3.6 Batch Test Sample Analysis and Rate Determination

Bio-P and denitrification were monitored by taking samples in each phase of the batch tests. Mixed liquor samples were collected with a 20 mL syringe from the 4 or 8 L reactor and passed through 0.45 μm filters. Filtered samples were analyzed for OP and COD in the anaerobic phase to determine the OP release and COD uptake rates. Initial samples were also analyzed for NO_3 and NO_2 until these concentrations were below 1 mg N/L. The COD consumption attributed to bio-P was determined by taking the total COD consumption measured and subtracting the COD required to denitrify the intial NO_x concentration that was measured in the reactor, which was primarily NO_3. This was done by calculating the consumptive ratio (C_R) of 6.62 g COD/g NO_3-N, as follows (Tchobanoglous et al., 2014):

$$C_R = \frac{2.86}{1 - 1.42Y_H}$$

where 2.86 g COD/g NO_3-N is the stoichiometric requirement for NO_3 reduction, 1.42 g COD/g VSS is the COD value of biomass, and Y_H is the anoxic synthesis yield, which was assumed to be 0.40 g VSS/g COD removed. Samples were analyzed for OP in the aerobic phase to determine the OP uptake rates. In the anoxic phase, samples were analyzed for NO_3-N and NO_2-N to determine denitrification rates, COD to determine methanol consumption rates or monitor COD changes when no methanol was present, OP to monitor any potential additional OP uptake (due to dPAOs), and NH_4 to monitor accumulation from decay. The analytical methods for each parameter are listed in ***Table 8***.

Table 8. Methods used for the batch test sample analysis.

Parameter	Method	Method Name	Product Name, range
PO_4-P	Hach 10209	Ascorbic Acid, EPA 365.1	• Reactive Phosphorus TNTplus LR, 0.05-1.5 mg/L PO_4-P • Reactive Phosphorus TNTplus HR, 0.5-5.0 mg/L PO_4-P
	Hach 10214	Molybdovanadate	• Reactive Phosphorus TNTplus 1.6-30 PO_4-P
COD	Hach 8000	Reactor Digestion	• COD TNTplus LR, 3-150 mg/L COD • COD TNTplus HR, 20-1500 mg/L COD
NO_3-N	Hach 10206	Dimethylphenol	• Nitrate TNTplus LR, 0.23-13.50 mg/L NO_3-N • Nitrate TNTplus HR, 5-35 mg/L NO_3-N
NO_2-N	Hach 10207 Hach 10237	Diazotization	• Nitrite TNTplus LR, 0.015-0.600 mg/L NO_2-N • Nitrite TNTplus HR, 0.6-6.0 mg/L NO_2-N
NH_4-N	Hach 10205	EPA 350.1, 351.1, 351.2 Salicylate	• Ammonia TNTplus ULR, 0.015-2.00 mg/L NH_3-N • Ammonia TNTplus LR, 1-12 mg/L NH_3-N

MLSS was measured using a handheld InsiteIG Model 3150 suspended solids sensor at the beginning of each test. MLVSS was estimated by assuming an 80% volatile fraction of the MLSS, based on the average volatile fraction reported for the full-scale WRRFs. Specific rates, such as the SDNR, were determined by dividing the measured rates by the MLVSS concentration. These normalized rates allow a better comparison between tests from different times and for different WRRFs as the MLVSS concentration, which is representative of the biomass concentration, varies from test to test.

For the overnight aerobic vs. anoxic conditions priming test, on the first day of the test, the "methanol-only" SDNR was determined by taking the difference between the SDNR in the reactor where methanol was added (Reactor A) and subtracting the SDNR in the reactor without methanol (Reactor B). Internal C denitrification would occur in each reactor for this first part of the test, so the difference between the two would be the denitrification attributable to methanol, or the methanol-only SDNR. After the overnight depletion periods, internal carbon should be depleted and the methanol-only SDNR was simply the difference between the overall SDNR and endogenous decay SDNR in each reactor.

4.4 Results and Discussion

4.4.1 Effect of Carbon Dose Location

Dye was detected above background absorbance readings in samples grabbed at the end of the aeration tank in both Trains 6 (modified) and 7 (unmodified). This indicates that at least some back-mixing was occurring in both treatment trains, and that moving the dose point does not entirely mitigate this. However, as shown in ***Figure 34***, the dye detected at the end of the aeration tank in Train 7, where the dose point was unmodified, was significantly higher than the amount of dye detected at the same location in Train 6.

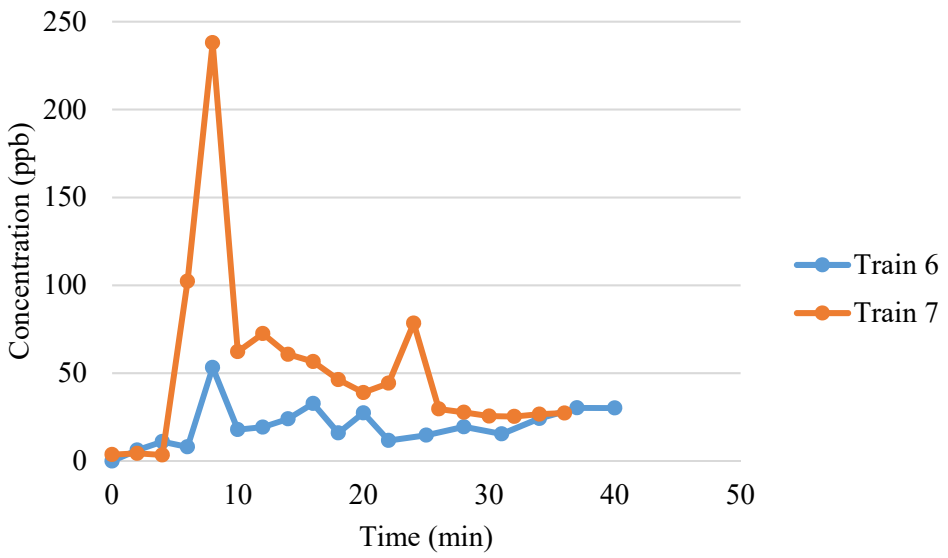

Figure 34. Concentration of dye at the end of the aeration tank in Trains 6 and 7.

There was an approximate travel time of 5 minutes from the methanol pumps, where the dye was introduced, to the entry point in the tanks, after which the concentration of dye detected in the tanks started to increase. Dye was added over the course of 4 minutes, so a drop in concentration in the tanks was seen 9 minutes after initial pumping of the dye. The concentrations then tended to settle to a residual concentration level of around 30 ppb in both tanks, which was above the initial background reading. This indicates a sort of steady state, in which all dye has entered and been thoroughly mixed into the anoxic tanks, and was showing up at the end of the aeration tanks at a consistent concentration due to back-mixing. Sampling at this location stopped after the dye levels steadied out. In order to quantify how much dye was actually present at the end of the aeration tank, or the extent of back-mixing, more samples than from just one location at the end of the aeration tank would be required. A future study where a continuous dye input was used and multiple sample points extending back into the aeration tank would be necessary to establish a dye profile in that tank and estimate the mass present there compared to the amount dosed. This would indicate the proportion of dosed methanol that is actually being oxidized aerobically, and is essentially "wasted". Again, while back-mixing is unavoidable even with the modified dose point, this type of future study could better quantify just how much methanol the dose point relocation actually saves.

The exit age distribution curves for both trains are shown in ***Figure 35***. ***Table 9*** summarizes the results for the comparison of Trains 6 and 7. The theoretical HRT of 2.8 hours was based on an even split of the flow into all active trains, so 7.1 MGD of flow entering each 0.82 MG anoxic zone. The resulting mean detention time for Train 7 from the test was actually slightly shorter than Train 6 despite the suspected higher degree of back-mixing with the unmodified methanol feed point in Train 7 (it had been assumed that the higher degree of back-mixing would delay the dye more and thus it would appear to spend longer in the anoxic tank). It seems that Train 7 is slightly more plug flow than Train 6, as shown by the shape of the distribution curve as well as the

calculated number of CSTRs in series being 6.5 compared to 5.7 in Train 6. These factors, along with the low dye recovery in Train 7, indicate that Train 7 likely receives more flow than Train 6. The dye recovery was calculated based on the amount detected in the samples at the end of the post-anoxic zone and the amount estimated to still be in the tank at the end of the test, compared to the known mass of dye added (adjusted for masking by the mixed liquor). By assuming an even flow distribution, the flow rate used was likely lower than the actual flow rate in Train 7, and so the calculated dye exiting the tank would've been too low, which is reflected by the low dye recovery percentage. In addition, as flow increases in a tank, the degree of plug flow increases, which could explain the slightly higher number of CSTRs in series calculated for Train 7.

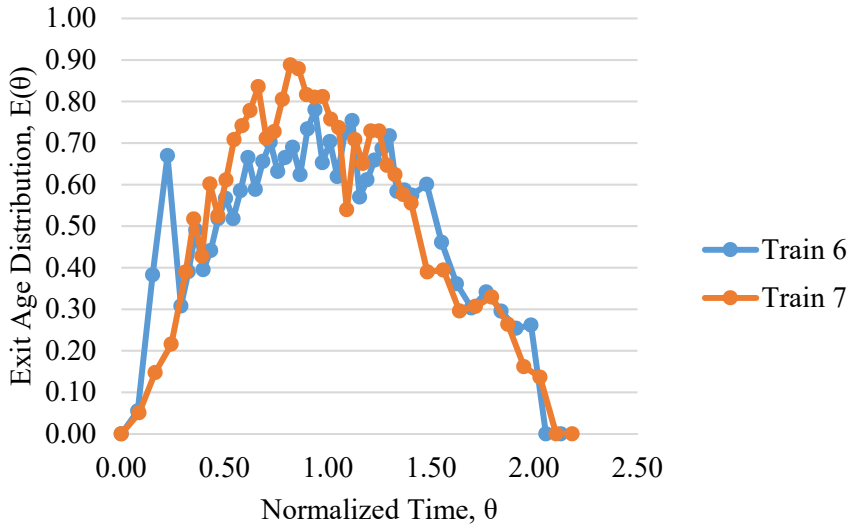

Figure 35. Exit age distribution curve for the Train 6 and 7 post-anoxic zones.

Table 9. Parameters used and derived from the tracer test for Train 6 and 7 post-anoxic zones.

	Theoretical HRT (hr)	Mean detention time (hr)	# CSTRs in series	Dye Recovery (%)
Train 6	2.8	2.3	5.7	90%
Train 7	2.8	2.1	6.5	74%

The results from the NO_x profile in Trains 4 through 7 are shown in ***Table 10***, as well as the methanol dose rates to each train. The amount of denitrification attributed to methanol was estimated assuming a ratio of 4.8 mg methanol as COD per mg of NO_3-N removed, and the non-methanol denitrification was the difference between the total NO_x-N removed and that which was attributed to methanol. The overall efficiency of methanol usage is best in Train 6, as indicated by the lowest ratio of methanol added to NO_x-N removed of 1.8 mg COD/mg NO_x-N. This seems to support the benefit of relocating the methanol feed point further into the anoxic zone to reduce the amount that unintentionally gets oxidized aerobically from back-mixing. However, the unmodified Train 7 is very close in efficiency to Train 6, and seems much better than the other unmodified Trains (4 and 5). This could have something to do with the slightly more plug flow nature of Train 7 as indicated in the tracer test. The degree of plug flow could be beneficial for methanol use, but more likely for other forms of denitrification, such as internal C denitrification.

This would indirectly lead to lower required methanol doses to achieve the same NO_x removal if other types of denitrification are improved. The reason for such efficiency in Train 7 should be investigated further.

Table 10. Profile of Train 4-7 post-anoxic zones and associated methanol dose and utilization efficiency.

Train	NO_x removed (mg N/L)	Methanol added (gph)	Denitrification from methanol (mg N/L)	Non-methanol denitrification (mg N/L)	Methanol added:NO_x removed (mg COD/mg N)
4	4.52	3.71	3.59	0.92	3.8
5	5.03	4.46	4.32	0.71	4.1
6	6.56	2.54	2.46	4.10	1.8
7	6.33	2.70	2.61	3.71	2.0

Although modifying the methanol dose point did not totally eliminate back-mixing of dye into the aeration tank, the amount of dye detected in modified Train 6 was much lower than unmodified Train 7. This indicates that less methanol would be entering the aeration tank, and so less would be wasted aerobically. This was supported by the overall highest efficiency of methanol use in the modified Train 6 based on the profile results. It is expected that the methanol dose requirements to achieve the same NO_x removal will continue to decrease as the dose point modifications are completed in each of the other trains. The oxidation and waste of methanol aerobically can at least partially explain the higher methanol dose rates at NP compared to VIP where the dose point proximity to aerobic conditions is not an issue.

The flow split may also factor into methanol efficiency determination. If Train 7 is getting a higher proportion of flow as suspected, then the amount of methanol used per NO_x removed is actually lower than calculated in ***Table 10***, where equal flow distribution was assumed when calculating the methanol concentration from the dose rate. The reasons for such efficient methanol use could be due to less short-circuiting that somehow facilitates more efficient methanol use (like with better mixing) or facilitates non-methanol denitrification. Further tracer studies on the other trains should be done to compare to the results obtained from this study for Train 6 and 7 as well as to the profile results for all trains.

4.4.2 Hydraulic Characterization of All Post-Anoxic Zones

The hydraulic characterization of the post-anoxic zone at NP and AB was completed by adding dye directly to the post-anoxic zone influent. Including the results from the 2017 tracer study conducted on the post-anoxic tanks at VIP, ***Figure 36*** shows the exit age distribution curve for each WRRF, and ***Table 11*** has the hydraulic parameters determined. As expected from the tank dimensions, the post-anoxic configuration at VIP is much more representative of plug flow compared to NP and AB, as indicated by the shape of the exit age distribution curve and the calculated number of CSTRs in series around 20. The mean residence time for VIP was also much closer to the theoretical HRT when the tracer test was conducted, indicating low potential for short-circuiting.

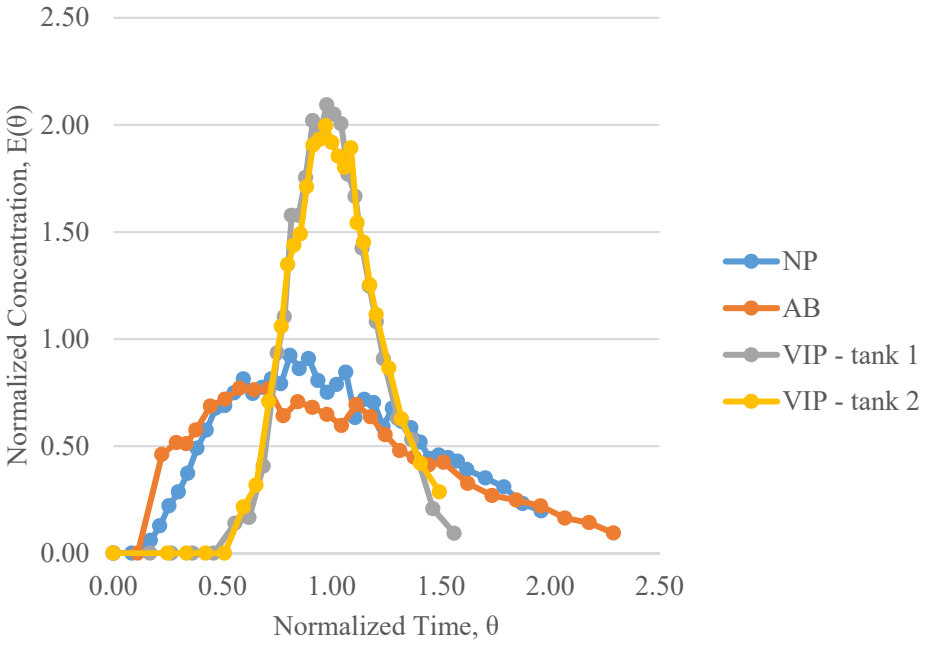

Figure 36. Exit age distribution curves for the post-anoxic zones at each WRRF.

Table 11. Relevant tracer test parameters for the post-anoxic zone at each WRRF, and estimated contributions from endogenous decay denitrification based on residence times.

	Tracer test				Batch test	
WRRF	**Theoretical HRT (hr)**	**Mean residence time (hr)**	**Actual / theoretical HRT ratio**	**# CSTRs in series**	**SDNR (mg N/g MLVSS/hr)**	**Endogenous denitrification (mg N/L)**
AB	0.91	0.75	0.82	5.3	0.50	1.10
NP	2.47	1.96	0.79	7.1	0.45	1.90
VIP – train 1	2.75	2.57	0.94	22	0.49	2.02
VIP – train 2	2.75	2.88	1.05	18	0.49	2.26

The contribution of endogenous decay to denitrification in each of the post-anoxic zones (see ***Table 11***) was calculated based on the endogenous decay denitrification rates determined from batch testing for each WRRF. The maximum batch test rate was used to determine the maximum contribution that could likely be obtained from endogenous carbon sources, but may be an overestimation due to the ideal batch test conditions compared to the actual full-scale tanks. The maximum endogenous decay batch test SDNRs were very similar for each WRRF, ranging from 0.45 to 0.50 mg N/g MLVSS/hr. The batch test SDNRs were adjusted to full-scale conditions using the MLSS, temperature, and HRT conditions for that day. The average endogenous decay NO_x removal for 2020 was 1.10, 1.90, and 2.14 mg N/g MLVSS/hr for AB, NP, and VIP (average train 1 and 2), respectively. So, simply due to the tank size and hydraulic performance (lack of short-circuiting), the endogenous decay NO_x removal at VIP is almost twice as high as AB. Tank configuration is not a factor that can readily be manipulated, but could be one of several reasons that VIP achieves the methanol savings they do.

The degree of plug flow for each post-anoxic zone was also estimated from tank dimensions using an empirical method. This was calculated using the same flow conditions as when the tracer test was conducted, so the results were directly compared in ***Table 12***. Most notably, the empirical method significantly overestimates the number of CSTRs in series for the post-anoxic zone at VIP. It is also overestimated at AB, but not by much. According to the results from the tracer test, NP actually outperforms what is predicted based on its tank geometry. This could partially be due to back-mixing occurring between the anoxic zone and end of the aeration zone where dye was dosed (this was discussed in Section 4.4.1) which possibly prolonged the time that the dye spent in the system. Regardless, the tracer test results were taken to be more reflective of actual tank performance, and so were used for the endogenous decay denitrification estimation. The discrepancies indicate that tracer studies may be very informative of actual tank conditions that can be very different from what is predicted theoretically.

Table 12. Degree of plug flow estimations of each post-anoxic zone using the tracer test vs. empirical method.

	# CSTRs in series	
WRRF	**Tracer test**	**Empirical Method**
AB	5.3	6.2
NP	7.1	3.0
VIP – train 1	22	40
VIP – train 2	18	30

4.4.3 Modeling Post-Anoxic Denitrification at VIP with Sumo

The Sumo steady state solution for each day that a full-scale nutrient profile was done at VIP was compared to the actual profile results, specifically the amount of post-anoxic NO_x removal. The comparison of Sumo to profile results in ***Figure 37*** indicates that Sumo overestimates the amount of denitrification achievable with the given WRRF setup and operation. Since Sumo does not explicitly model the use of internal carbon for post-anoxic denitrification as is thought to be occurring, it would be expected that the model-predicted denitrification would be *lower* than the actual observed denitrification. Sumo does incorporate dGAO and dPAO activity, but based on lack of anoxic OP uptake in batch tests and from full-scale profile data in the post-anoxic zone at VIP, dPAOs are not thought to be present. At least, no dPAOs that are specifically using NO_3/NO_2 as electron acceptors for simultaneous OP uptake. Given the relationship of internal C denitrification to bio-P, the role of dGAOs is also not expected to be central to what is occurring at VIP, since GAOs and PAOs compete with each other.

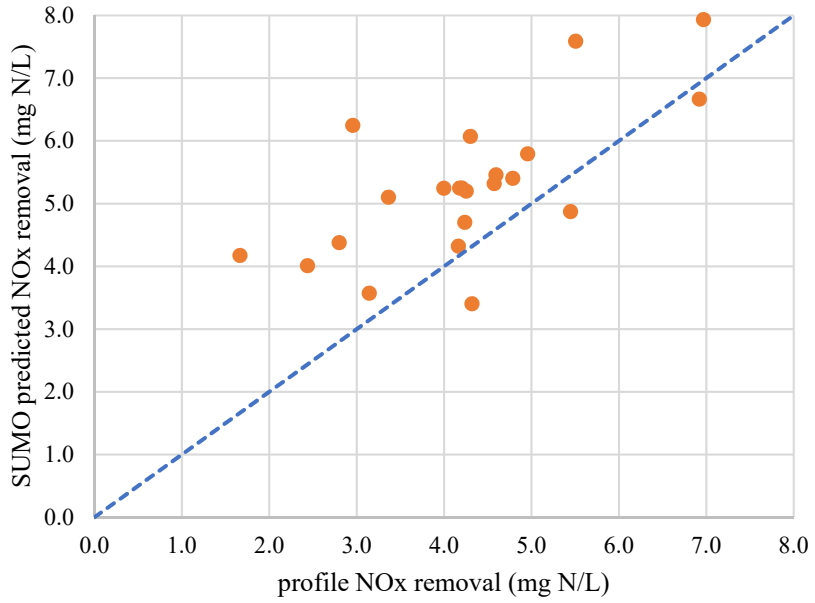

Figure 37. Sumo vs. profile estimation of post-anoxic denitrification. Points indicate Sumo predicted NO_x removal for profile day (dashed line indicates 1:1 for profile values).

Considering the relatively low methanol addition rate at VIP, it was assumed the overestimation by Sumo was mainly due to endogenous decay denitrification. The lysis-regrowth model is used in Sumo, so it was hypothesized that the decay or hydrolysis rates might be too high, leading to over-production of biodegradable substrate that could be used for denitrification. The default parameters used in Sumo2 are listed in ***Table 13***, as well as the default values used in BioWin for the same parameters to provide some context. There are notably lower values for anoxic decay, hydrolysis, and OHO growth under anoxic conditions in BioWin, which again suggests Sumo overestimation of these rates.

Table 13. Default modeling parameters used in Sumo2 and BioWin for lysis-regrowth reactions.

Parameter	Value in Sumo2	Value in BioWin
Decay (AER)	0.62	0.62
Decay (ANX)	0.31	0.23
Hydrolysis (AER)	2.0	2.1
Hydrolysis (ANX)	1.0	0.6
OHO growth (AER)	4.0	3.2
OHO growth (ANX)	2.4	1.6

The decay rate was reduced from the default value of 0.62 d^{-1} to 0.45 d^{-1} and 0.29 d^{-1}. The model calibration does not appear to be much different despite the parameter change. For instance, ***Figure 38*** shows that changing the decay rate from 0.62 d^{-1} to 0.45 d^{-1} did not cause the model-predicted anaerobic and aerobic MLSS to deviate much more from the actual MLSS concentrations over the course of 2018 to 2020 than for when the decay rate was left at default.

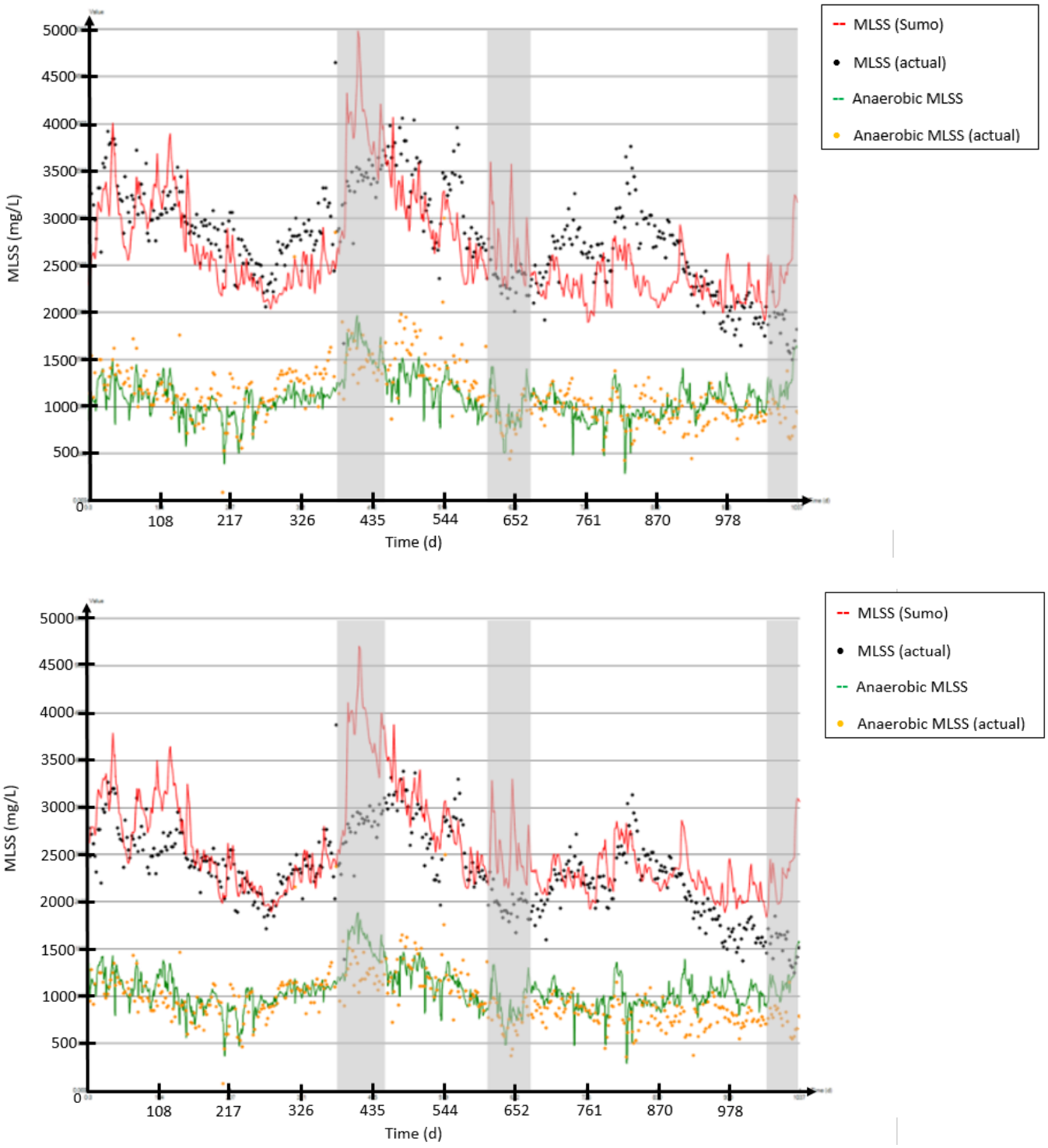

Figure 38. Calibration of Sumo for the default decay rate of 0.62 d^{-1} (top) vs. 0.45 d^{-1} (bottom) using MLSS (mg/L) concentrations at VIP from 2018-2020.

The profile data was then adjusted to include only the denitrification using methanol (estimated directly from the quantity of methanol added) as well as the denitrification from endogenous decay (calculated using the batch test endogenous denitrification rate adjusted for the WRRF conditions

including temperature, MLSS concentration, and post-anoxic HRT). This excludes the denitrification attributed to internally stored carbon, which as discussed is not completely modeled in Sumo. The average discrepancy between the model-predicted and actual denitrification was lowest for the 0.45 d^{-1} decay, but as ***Figure 39*** shows, as a whole the NO_x removal does not seem to increase as the profile NO_x removal increases. Therefore, it is uncertain whether the default decay rate really is higher than the actual rate, or whether the particular Sumo model configuration used is realistic for representing VIP.

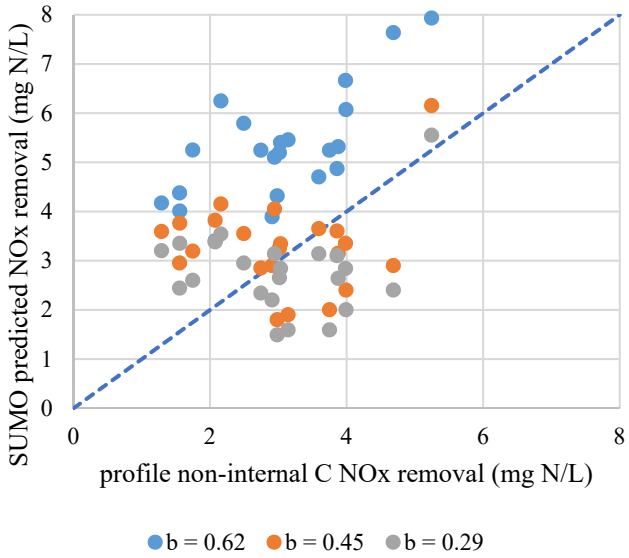

Figure 39. Sumo vs. profile estimation of non-internal C post-anoxic denitrification for varying decay rates (b). Points indicate Sumo predicted NO_x removal for each profile day (dashed line indicates 1:1 for profile values).

While the dynamic run over several years showed the model was fairly calibrated, the MLSS and SRT predicted by the model at steady state did not necessarily match the actual MLSS and SRT values for the respective profile days. Therefore, the comparison between the modeled and actual denitrification across the post-anoxic zone was just a rough indication of the overestimation of denitrification by Sumo. The modeling of the endogenous decay denitrification batch tests in Sumo and comparison to actual measured batch test rates reaffirmed the suspected overestimation by the model. **Table 14** shows the model-predicted endogenous decay SDNRs for both the original conditions and waste-rate-adjusted conditions (when trying to match the MLSS concentrations between the model and reality). The model over-predicts the endogenous decay SDNR by an average of 0.53 mg N/g MLVSS/hr even after the waste rate adjustments. Despite aligning the MLSS concentrations, the waste rate adjustments notably make the discrepancies between the model and actual SRT even more distinct (**Table 14**). The hydrolysis rates matched the decay rates in the reactor for each batch test, so it seems that decay is the controlling factor in the lysis-regrowth cycle that leads to endogenous denitrification. When the hydrolysis rate was either increased or decreased from the default value of 2.0 d^{-1}, the modeled batch test denitrification rates did not change from the original value. This verified that decay is the limiting factor. OHOs were

the dominant organisms present in the mixed liquor, and the equation for the OHO decay rate (mg COD/L/d) is:

$$\text{decay} = b_{OHO,T} * X_{OHO} * (Msat_{SO2,KO2,OHO} + \eta_{b,anox} * Msat_{SNO2,KNO2,OHO} * Minh_{SO2,KO2,OHO} + \eta_{b,anox} * Msat_{SNO3,KNO3,OHO} * Minh_{SNO2,KNO2,OHO} * Minh_{SO2,KO2,OHO}) \quad (13)$$

The concentrations of NO_2, NO_3, and DO present in the batch tests are all similar as to make the Monod saturation (Msat) and inhibition (Minh) expressions consistent for each test. The OHO decay rate constant ($b_{OHO,T}$) and reduction factor ($\eta_{b,anox}$) are also unchanging, so the differences in decay result from the different OHO biomass concentrations (X_{OHO}) present. As shown in **Figure 40**, as the SDNR increases, so does the specific decay rate. Considering that VSS is composed of biomass plus additional components such as decay products that aren't necessarily degradable, this increase is likely due to the larger fraction of VSS that is OHOs (also shown in **Figure 40**). More OHOs/biomass would mean more decay and potential substrate, but also more organisms that are denitrifying as well. The reason for the changing OHO fraction in the full WRRF model from which the mixed liquor for the batch test was obtained was not explicitly identified, but is likely primarily due to waste rate/SRT among other factors. **Table 15** shows the required decay rates in order to reach a similar SDNR in the model as was obtained in the actual batch tests. This requires reduction from the default 0.62 d^{-1} to somewhere between 0.10 to 0.32 d^{-1}. Reported decay values vary greatly, but have been reported as 0.24-0.72 d^{-1} (Grady et al., 2011). The recommended values from the Sumo batch tests are on the low end of this range, but may not be unreasonable. The model overestimation of endogenous decay denitrification could therefore be that there is too much biomass present, or that the decay rate is too high, or both.

Table 14. Endogenous decay SDNRs and mixed liquor characteristics from actual batch tests compared to Sumo batch tests – both initial and waste rate-adjusted.

	Actual				Sumo			Sumo – adjusted WAS			
	NO_x SDNR (mg N/g MLVSS/hr)	**SRT (d)**	**MLSS (mg/L)**	**WAS (MGD)**	**NO_x SDNR (mg N/g MLVSS/hr)**	**SRT (d)**	**MLSS (mg/L)**	**NO_x SDNR (mg N/g MLVSS/hr)**	**SRT (d)**	**MLSS (mg/L)**	**WAS (MGD)**
9/30/2020	0.25	20.5	2050	0.13	0.69	17.5	2504	0.82	13.3	2007	0.17
10/13/2020	0.33	15.6	1696	0.20	0.79	11.1	2600	1.01	6.3	1718	0.36
10/20/2020	0.20	24.1	2050	0.15	0.71	15.3	2143	0.75	14.0	1934	0.16
2/4/2021	0.49	11.3	2540	0.20	1.01	14.1	1909	0.85	21.0	2523	0.13
3/23/2021	0.32	14.2	2860	0.13	0.81	22.6	2845	0.81	22.6	2845	0.13*

*no need to adjust from original

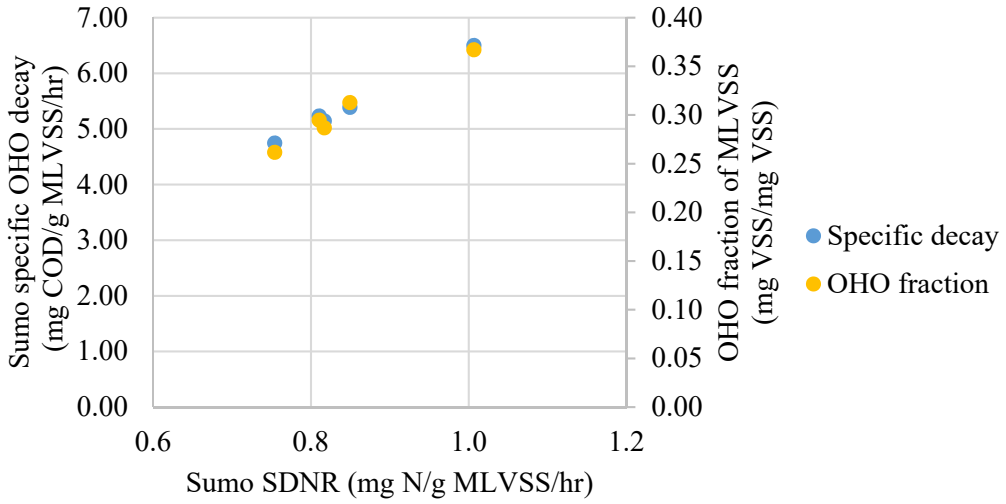

Figure 40. Changes in specific OHO decay rate and OHO fraction of MLVSS with endogenous decay SDNR in Sumo batch tests.

Table 15. Adjusted decay rates and resulting SDNRs in Sumo batch tests to match actual batch test rates.

	Actual	Sumo – adjusted decay	
	NO_x SDNR (mg N/g MLVSS/hr)	**NO_x SDNR (mg N/g MLVSS/hr)**	**Adjusted decay rate (d^{-1})**
9/30/2020	0.25	0.27	0.15
10/13/2020	0.33	0.32	0.15
10/20/2020	0.20	0.19	0.10
2/4/2021	0.49	0.49	0.32
3/23/2021	0.32	0.32	0.20

The effect of the plug-flow nature on denitrification performance was also examined by comparing the post-anoxic trains as they are (8 total available cells, 4 to 6 of which are anoxic) to a single CSTR of the same total anoxic volume. When no methanol is added, the only major denitrification source in Sumo is endogenous decay. As shown in ***Figure 41***, Sumo results show only a slight increase in NO_x removal, averaging only about 0.1 mg N/L more with multiple CSTRs rather than a single CSTR. This suggests that plug flow does not facilitate much higher endogenous decay denitrification, which likely behaves as a zero-order reaction, and so is not dependent on substrate or electron acceptor concentrations. When methanol was added, there was only an average difference of about 0.2 mg N/L between the multiple and single CSTR configurations (see ***Figure 42***). The half-saturation value for methanol in methylotrophs is 0.5 mg COD/L. By the time the methanol concentration gets this low, most of the methanol has already been used. While utilizing that remaining methanol would be facilitated better in a plug flow-like reactor rather than a large well-mixed reactor, the additional NO_x removal is minimal. If the half-saturation value was higher, the plug-flow nature of the post-anoxic zone would likely be more significant in facilitating better methanol utilization. The half-saturation value in methylotrophs for NO_3 is 0.05 mg N/L, so would also not be a limiting factor to removal given the typical effluent concentrations and wouldn't change removal efficiency in CSTR vs. plug flow conditions.

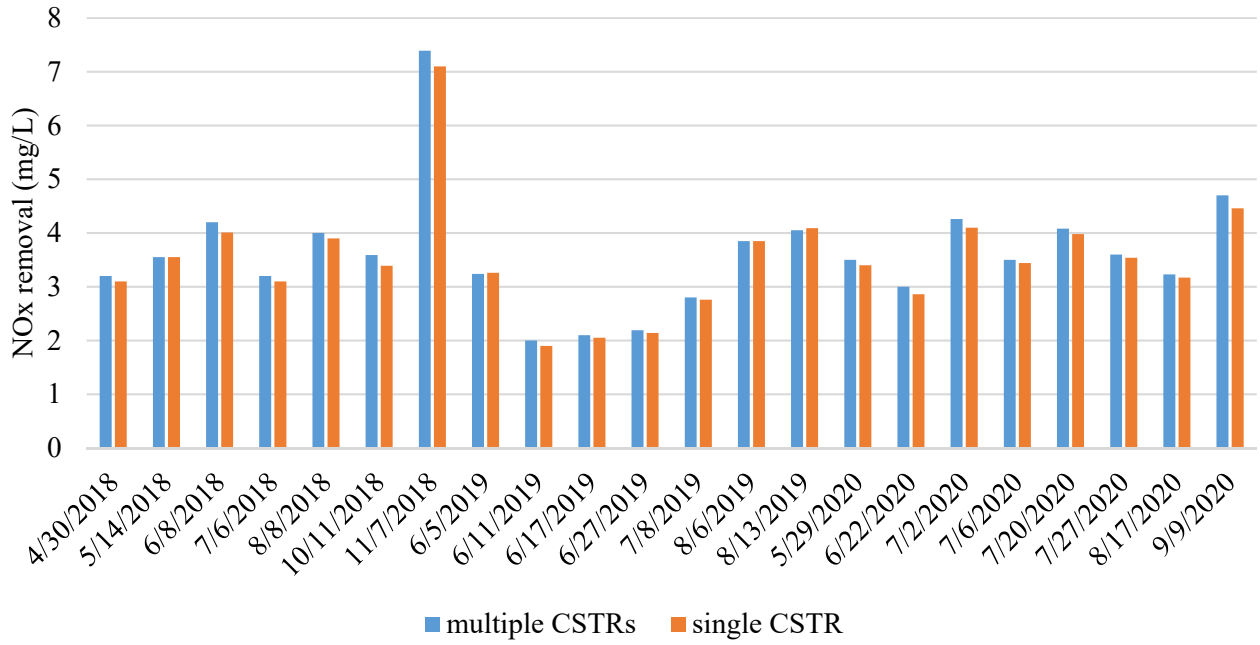

Figure 41. Multiple vs. single CSTR configurations and the effect on Sumo-predicted endogenous post-anoxic denitrification.

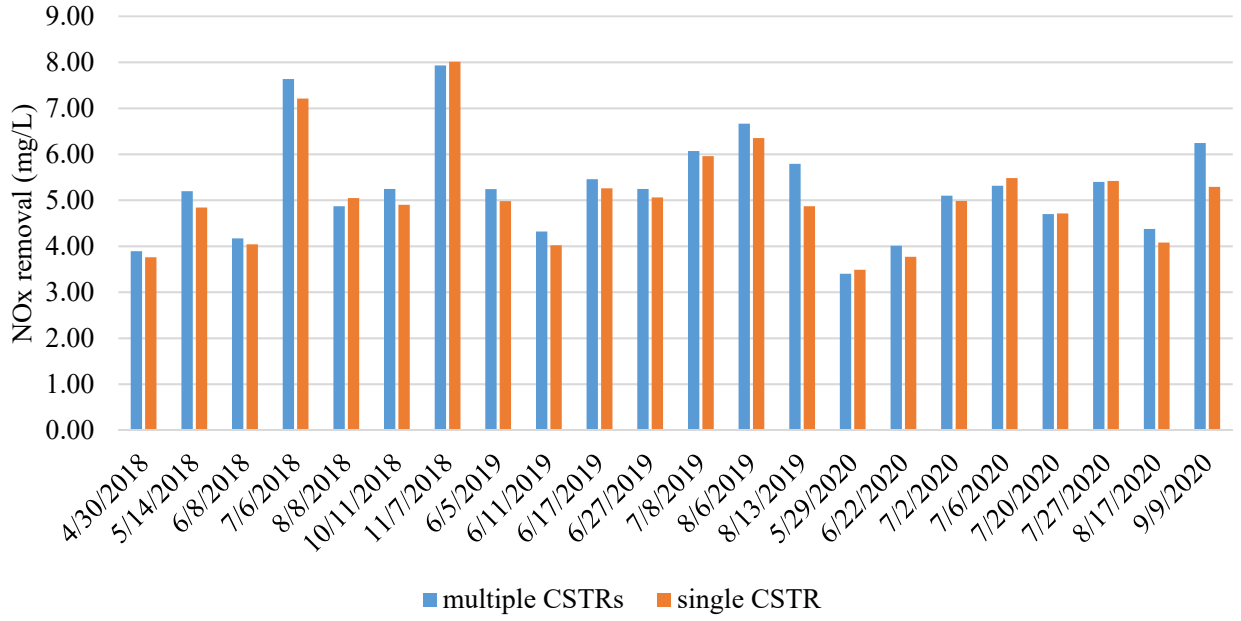

Figure 42. Multiple vs. single CSTR configurations and the effect on Sumo-predicted post-anoxic denitrification **with methanol**.

Since plug flow does not seem to show much benefit for either endogenous or methanol-driven denitrification, it might be more important for internal C denitrification. Again, Sumo does not explicitly model internal carbon as a major source for denitrification.

A more in-depth analysis of the post-anoxic denitrification was done to examine the contributions of various carbon sources and how these change with tank configuration. This was done using the Gujer matrix outputs from the Sumo steady state solution for each profile day. The results for each profile day operated under each of the following four scenarios:

- single CSTR, with methanol
- multiple CSTRs, with methanol
- single CSTR, no methanol
- multiple CSTR, no methanol

are shown in ***Figure 43*** and ***Figure 44***, for when the anoxic zone starts in Cell 3 and 5 of the post-anoxic trains, respectively. Endogenous decay, or OHO growth on readily biodegradable substrate (which comes from decay/hydrolysis), is generally the highest contributor to denitrification, followed by methanol. GAO growth on glycogen with NO_2/NO_3 was the next largest contributor. So, Sumo does incorporate some aspect of carbon storage use for denitrification, but this is attributable specifically to the dGAO population. It is also minor compared to the other sources of denitrification, and well below the expected amount based on full-scale VIP profile data, where on average around 33% of denitrification in the post-anoxic zone is suspected to result from internal carbon. For accurate representation, not only would the quantity of internal carbon denitrification need to be met, but the type of internal carbon used would need to be developed more thoroughly in the model. Glycogen is only associated with GAOs as their sole form of internal carbon in the model, and the same with PHA for PAOs, even though both types of carbon are associated with both types of organisms in reality. Both PHA and glycogen have been shown to be used for post-anoxic carbon sources for denitrification, and PHA typically yields higher SDNRs (Carvalho et al., 2007; Coats et al., 2011; Qin et al., 2005; Vocks et al., 2005). The quantity, type, and accessibility of internal carbon for denitrification are all factors that would need to be incorporated into the model for representation of the full-scale process.

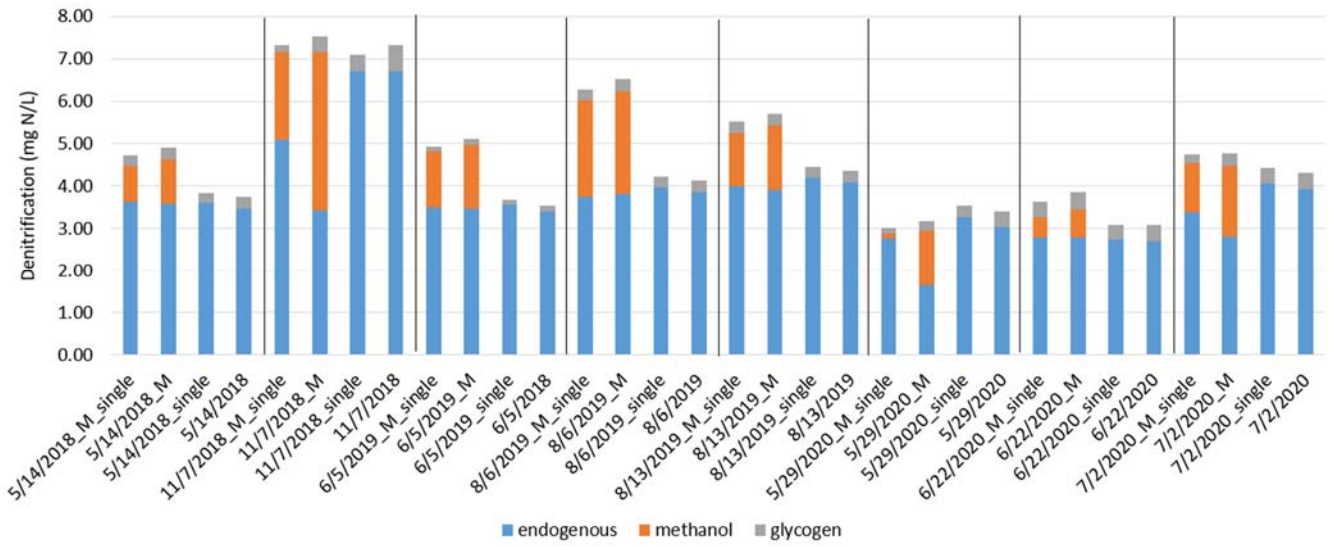

Figure 43. Contributions of carbon sources to Sumo-predicted denitrification when the post-anoxic zone starts in **Cell 3**. Four scenarios for each set of WRRF conditions were modeled (shown in order of: single CSTR, with methanol; multiple CSTRs, with methanol; single CSTR, no methanol; multiple CSTRs, no methanol).

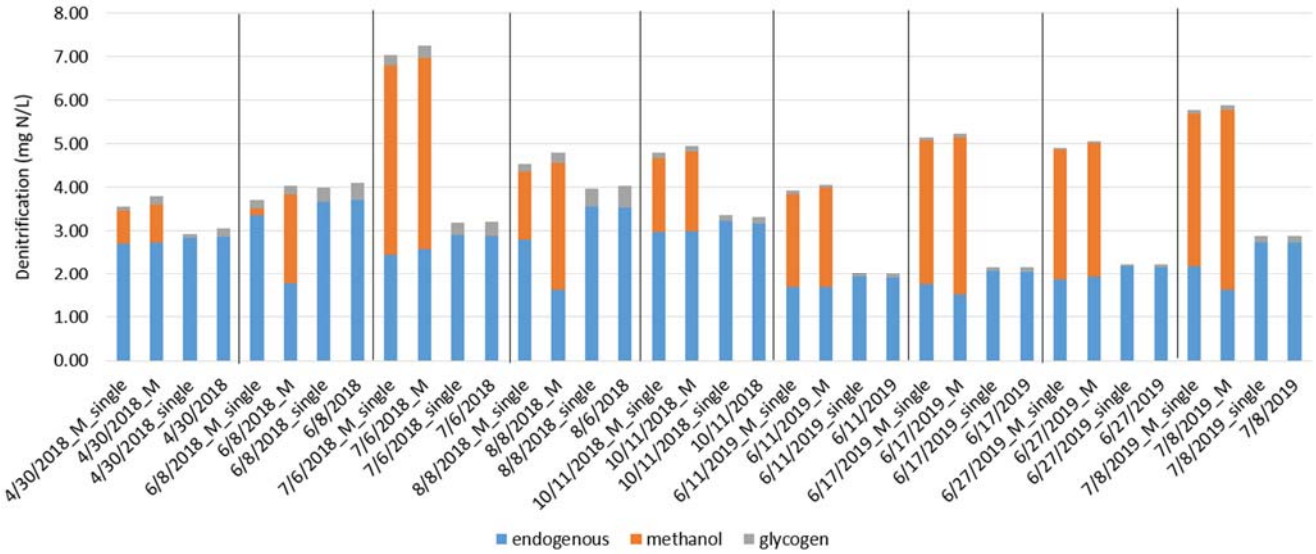

Figure 44. Contributions of carbon sources to Sumo-predicted denitrification when the post-anoxic zone starts in **Cell 5**. Four scenarios for each set of WRRF conditions were modeled (shown in order of: single CSTR, with methanol; multiple CSTRs, with methanol; single CSTR, no methanol; multiple CSTRs, no methanol).

Despite being a low contributor in the model, the average denitrification from glycogen does increase from 0.23 to 0.29 mg N/L on average when methanol is added and 0.28 to 0.32 mg N/L when methanol is not added, when the anoxic zone starts in Cell 3 of the post-anoxic zone. The average denitrification from glycogen increases from 0.12 to 0.15 mg N/L when methanol is added and 0.18 to 0.22 mg N/L when methanol is not added, when the anoxic zone starts in Cell 5 of the post-anoxic zone. This suggests that plug flow does have at least a minimal benefit to internal

carbon denitrification, even within the limited extent that it occurs in the model. The amount of denitrification via glycogen was generally higher when the initial concentration of glycogen was higher at the start of the post-anoxic zone, as shown in ***Figure 45***. This is consistent with previous work that demonstrated highest internal C denitrification rates were obtained when the amount of glycogen present initially was highest (Coats et al., 2011; Winkler et al., 2011). An example of when the plug flow nature did seem to impact glycogen-driven denitrification is shown in ***Figure 46*** for the profile day 11/7/2018 when no methanol is added. The glycogen-driven denitrification rate is always higher in each cell of the multiple CSTR configuration than in the single CSTR, so the total contributions to NO_x removal for each configuration is 0.61 and 0.40 mg N/L, respectively. This is also a day when there are relatively high initial glycogen concentrations (starting at just under 8 mg COD/L, this is on the high end as shown in ***Figure 45***). Plug-flow conditions specifically facilitating the use of internal carbon for denitrification could explain why the potential for this type of denitrification was observed for all WRRFs in batch testing, but is not necessarily used full-scale, except at VIP where the tanks are much more representative of plug flow conditions. Yet, due to the relatively low contribution of internal carbon to denitrification as modeled in Sumo as of now, the true nature of this plug-flow benefit in the post-anoxic zone is unclear.

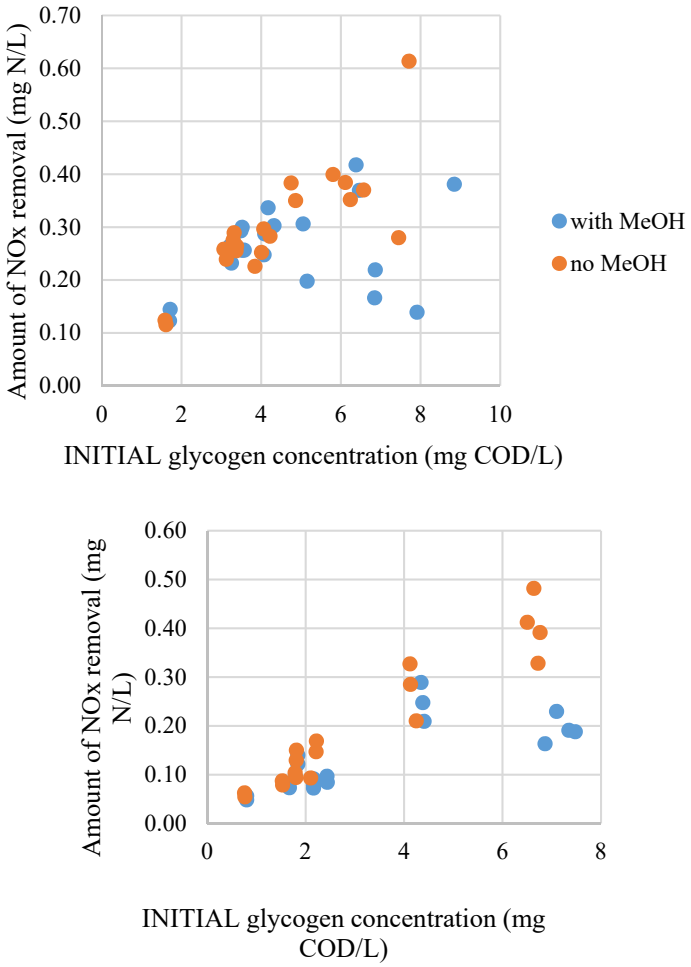

Figure 45. Correlation of modeled glycogen-attributed denitrification to initial glycogen concentrations at the start of the post-anoxic zone, either starting in Cell 3 (top) or Cell 5 (bottom).

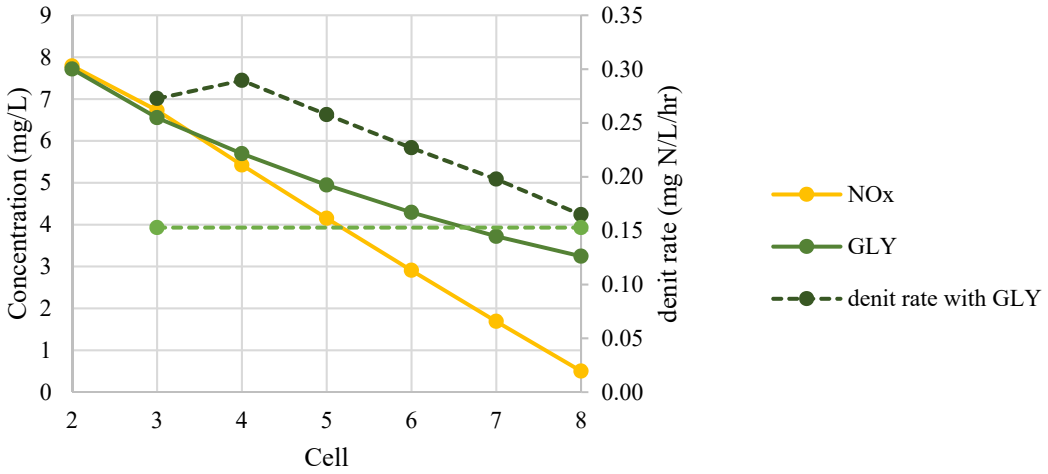

Figure 46. Sumo-predicted NO_x removal and contributions from glycogen for the profile day 11/7/2018 when no methanol was added. The rate for the single CSTR configuration is shown in addition to those for each cell for comparison.

Generally the contribution of endogenous decay and methanol to denitrification as modeled in Sumo are consistent between single and multiple CSTRs. However, on days when NO_x runs out and the zone goes anaerobic, the contribution from methanol increases significantly in the multiple CSTR configuration. As evidenced in ***Figure 43*** and ***Figure 44***, this is the case for the following profile days: 6/8/2018, 8/8/2018, 11/7/2018, 6/7/2019, 7/8/2019, and 5/29/2020. This likely occurs because the methanol-driven denitrification rate is much higher in the initial cells when methanol concentrations are very high, compared to the relatively low methanol concentration and denitrification rate in the single CSTR, as shown in ***Figure 47*** for day 8/8/2018. The high methanol-driven denitrification rates consume NO_x quickly in the initial cells; the initial methanol-driven denitrification rate is over four times higher in Cell 5 for the multiple CSTR configuration than for the single. When there is a low concentration of NO_x, it gets depleted before the end of the anoxic zone, so even if there still is endogenous decay products available for denitrification, there is no NO_x left to denitrify. Therefore, the proportion of denitrification attributable to methanol in the 8/8/2018 case (2.93 mg N/L) is much higher than that for the single CSTR configuration (1.58 mg N/L). There was also excess methanol left after all NOx was removed, so some savings could have been incurred by dosing less.

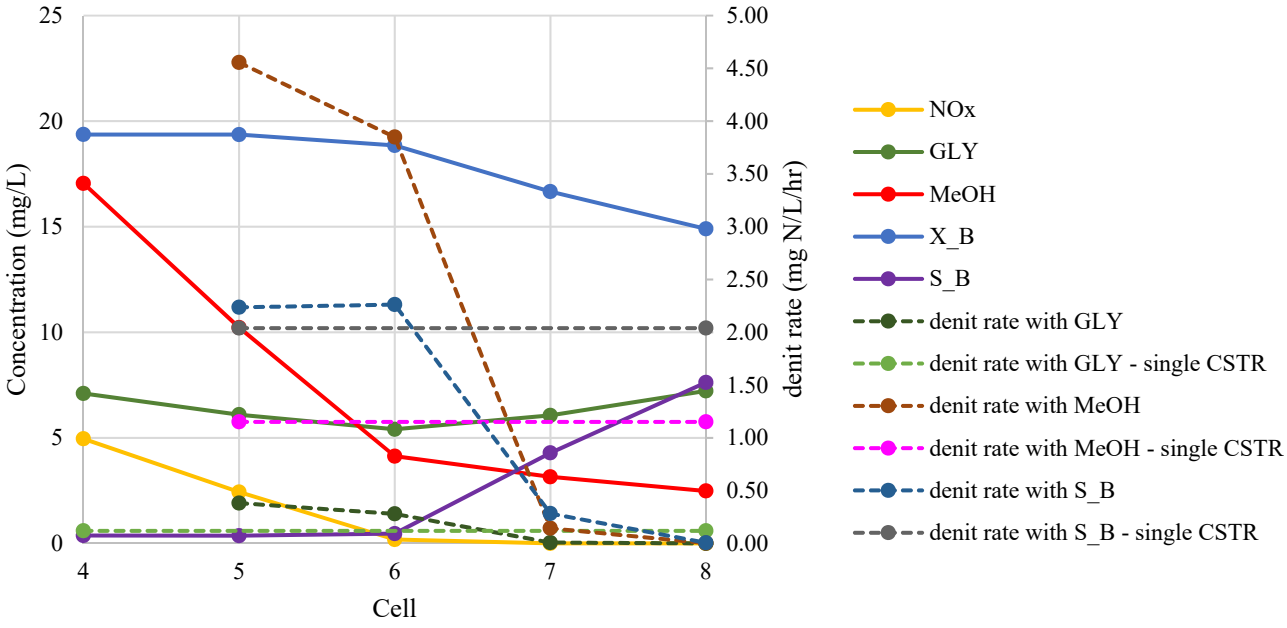

Figure 47. Sumo-predicted NO_x removal and contributions from all carbon sources for the profile day 8/8/2018. Rates for the single CSTR configuration are shown in addition to those for each cell for comparison. X_B = particulate biodegradable COD; S_B = soluble biodegradable COD.

A day with limiting NO_x concentrations like 8/8/2018 can be compared to a day when NO_x is not limiting, such as 4/30/2018. ***Figure 48*** shows the substrate concentrations in each cell, as well as the denitrification rates in each cell compared to the rates in the single CSTR configuration from the same day. NO_x does not run out and the methanol rates are very similar, so the methanol

contributions to denitrification are more consistent between the multiple CSTR (0.85 mg N/L) vs. single CSTR configurations (0.75 mg N/L).

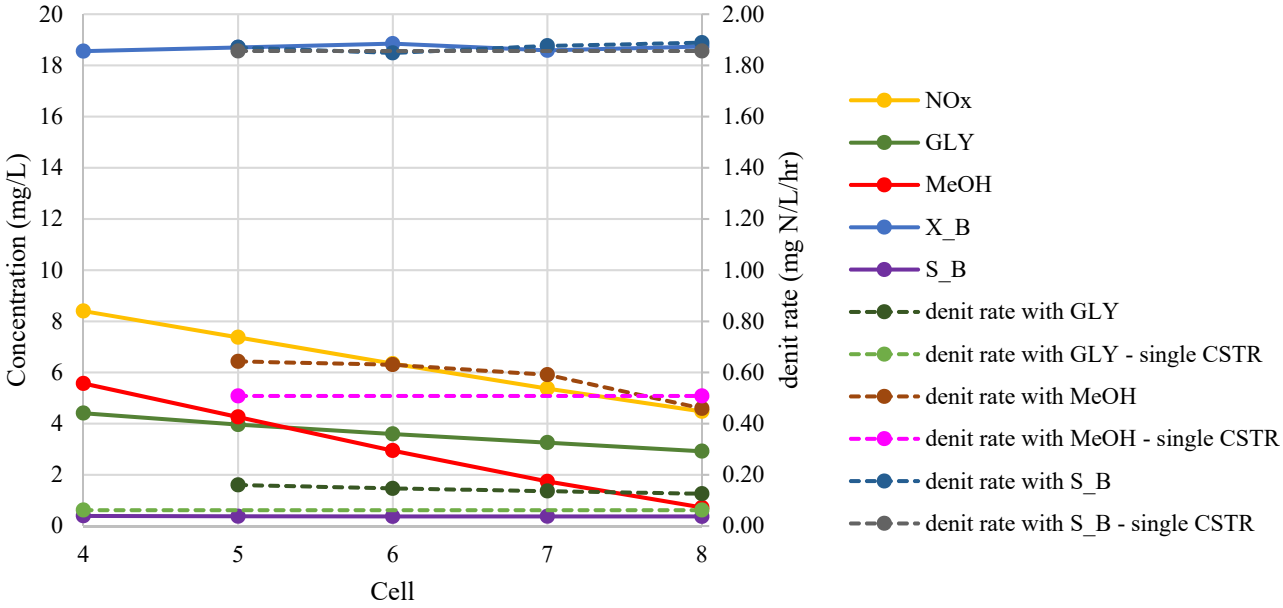

Figure 48. Sumo-predicted NO_x removal and contributions from all carbon sources for the profile day 4/30/2018. Rates for the single CSTR configuration are shown in addition to those for each cell for comparison. X_B = particulate biodegradable COD; S_B = soluble biodegradable COD.

To conclude, modeling of VIP's post-anoxic zone with Sumo verified that the overall volume/HRT affecting the time available for methanol and endogenous decay denitrification is likely more important than the plug-flow nature of the tank, which only minimally improves denitrification. The concentrations of the substrate and/or electron acceptor for methanol and endogenous denitrification result in pseudo-zero-order reactions because they are well above the half-saturation levels (where they start to become rate-limiting); therefore, almost the same amount of denitrification can be achieved regardless of the tank configuration. The impact of tank configuration on internal carbon denitrification when it is a larger contributor to denitrification is uncertain. As it is, Sumo does not explicitly model PHA- and glycogen-driven denitrification to the extent that internal C denitrification is observed full-scale, and so needs further development to be used as a predictive tool for this mechanism.

4.4.4 Effect of SRT on Endogenous Decay Denitrification

The endogenous decay denitrification rate determination tests were done at least once if not multiple times with sludge from the three methanol-utilizing WRRFs (AB, VIP, NP) as well as two of HRSD's high-rate bio-P but non-nitrifying WRRFs (AT, CE), and another plant suspected of using internal carbon for denitrification (JR). The total SRT for the full-scale WRRF at the time the test was done is compared to the endogenous decay SDNR in ***Figure 49***. In general, the longer the SRT, the lower the endogenous decay SDNR. The long SRT sludge has been in the system

longer and had more opportunity to decay, so there is a higher fraction of debris from decay that is not usable within the time frame of the treatment process. Therefore the sludge is "old" and not as feasible for endogenous decay denitrification. For example, the highest endogenous SDNR recorded at VIP was 0.49 mg N/g MLVSS/hr for an 11.3 day SRT, which corresponded to an MLSS concentration of 2540 mg/L (2032 mg VSS/L), for an overall rate of 1.00 mg N/L/hr. The lowest endogenous SDNR recorded at VIP was 0.20 mg N/g MLVSS/hr for a 24.1 day SRT, which corresponded to an MLSS concentration of 2040 mg/L (1632 mg VSS/L), for an overall rate of 0.33 mg N/L/hr. The volatile portion of solids includes debris that does not get hydrolyzed within the time frame of interest at the treatment WRRF, in addition to the active biomass and usable volatile material. This inaccessible portion is not distinguished when measuring VSS. So the actual usable fraction is uncertain, but would likely be lower as the SRT increases and more debris builds up. This could help explain why changes in MLSS or SRT do not necessarily have a proportional impact on the denitrification rate measured, and why normalizing to MLVSS concentrations results in different SDNRs.

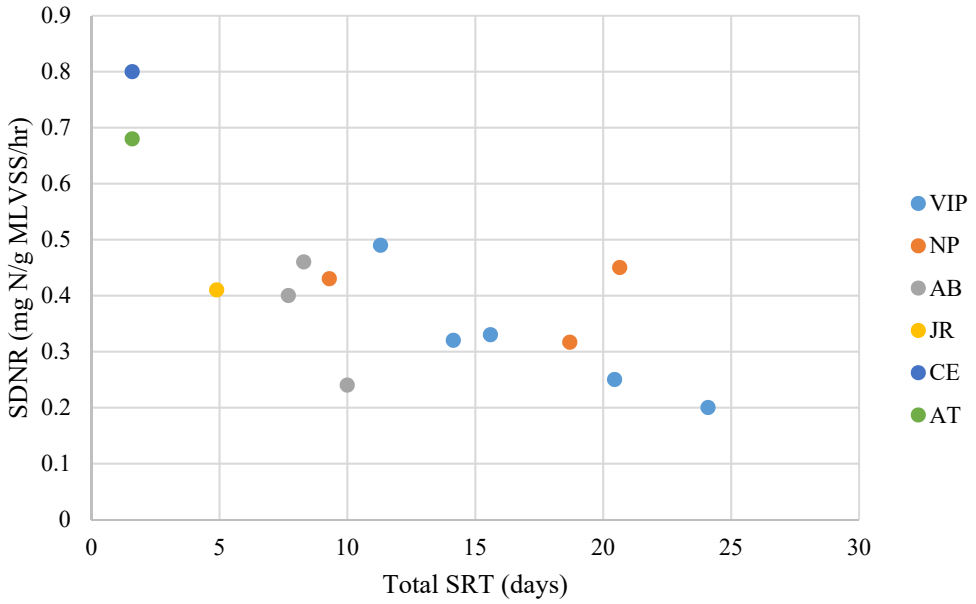

Figure 49. Batch test-determined endogenous SDNRs at varying SRTs for each WRRF.

For the previous example at VIP, assuming average flows of 27 MGD for the influent and 8 MGD for the RAS flowing through the post-anoxic zone, and 6 of the 8 cells operated as anoxic for a total anoxic volume of 3.1 MG, the residence time would be 2.1 hr. The endogenous decay denitrification contribution from the first case (SDNR of 0.49 mg N/g MLVSS/hr) would be 2.09 mg N/L for these conditions, whereas the contribution from the second case (SDNR of 0.20 mg N/g MLVSS/hr) would be 0.68 mg N/L. The difference is 1.40 mg N/L, so assuming 4.8 mg COD/mg NO_3-N, this saves 6.74 mg COD/L. The age of the sludge could therefore factor into the overall denitrification observed within the second anoxic zone and affect methanol costs. Typically increasing the WAS rate will lower the MLSS concentration within the tanks, as more solids are removed from the system. However, other factors are important for consideration, such

as the number of trains in service, because from the previous example, the longer SRT actually corresponded to the lower MLSS concentration.

Despite its affect on endogenous denitrification, the SRT must be kept within reason. For instance, driving the SRT too low could potentially risk washing methylotrophs out of the system, not to mention causing issues with other parts of the treatment process. Assuming the 1.3 d^{-1} specific growth rate for methylotrophs (Dold et al., 2008), the minimum post-anoxic SRT before washout would only be 0.77 days. This is far below the typical operating average of 3.2 days (averaged from 2017-2020), so would likely not be of concern.

Figure 49 shows the inverse relationship between SRT and endogenous decay SDNR across all WRRFs, and this relationship seems to hold for VIP where the most endogenous decay SDNR batch tests have been done. More of these tests would need to be done at each individual WRRF to develop a specific relationship for SRT vs. endogenous decay SDNR for each WRRF, to the point where endogenous decay SDNR could be reasonably estimated at any time just from the SRT without having to measure the rate explicitly.

Regardless of the higher endogenous decay SDNRs at low SRTs, trying to maintain a low SRT with a long post-anoxic HRT to allow more time for the endogenous decay denitrification reaction is operationally not very feasible. For instance, driving the waste rate up could lower SRT, but putting more post-anoxic tanks into service to increase the HRT would also increase the time the solids spent in the system. Low MLSS concentrations would be required in these unrealistic conditions.

4.4.5 Anoxic Priming of Methylotrophs

4.4.5.1 Brief 30-min Reaeration Test

Appendix C has all the results from batch tests discussed in Section 4.4. The denitrification rates for both the reaerated reactor and non-reaerated reactor for the brief 30-min reaeration test are shown in ***Table 16***. The reaerated reactor yielded lower SDNRs. Methylotrophs are capable of using oxygen as an electron acceptor as well as NO_3 and NO_2. The results of this test suggests that even a brief re-introduction of aerobic conditions could cause the methylotrophs to be less willing to use NO_3/NO_2. This could play a role if anoxic conditions are not maintained in the post-anoxic zone, such as reintroduction of oxygen through surface transfer in an uncovered tank. Furthermore, if methanol is added at the start of the post-anoxic zone, or immediately after the aerobic zone, there could still be some residual DO that could consume methanol, or the methylotrophs are less efficient at using NO_3/NO_2 instead of DO as the electron acceptor. For instance, there is great potential for reintroduction of DO in the transition between aerobic and post-anoxic zones at AB, as flow is transferred through a large pipe under a roadway in between separate tanks, instead of directly through a baffle wall between adjacent tanks. The suction and deposition of the flow through the transfer pipe has been shown to yield high DO concentrations (above 5 mg/L) at the inlet channel to the post-anoxic zone right before the first anoxic cell where

methanol is dosed. Again, this could potentially cause the methanol to be oxidized aerobically, or the methylotrophs to be less primed to produce denitrification enzymes when they have been exposed to such high DO conditions. If the reductase enzymes need more anoxic time to maximize their activity level, then perhaps adding methanol further downstream could increase efficiency of methylotrophic denitrification. Methanol is added right away in the post-anoxic zone at all of the WRRFs, but it could be worthwhile to switch the methanol feed point to later on in the post-anoxic zone to determine whether more efficient use of methanol is observed over time. If methanol typically runs out well before the end of the post-anoxic zone anyway, then moving the dose point slightly farther downstream would still be feasible without allowing methanol to leave the WRRF unused. This could also encourage more internal carbon denitrification in that initial part of the post-anoxic zone if no methanol is present, considering the potential interference of methylotrophic and internal carbon denitrifiers. Of the three HRSD WRRFs discussed, moving the dose point could only easily be done at VIP, where methanol can be added in any of the cells within the post-anoxic zone. There is a fixed methanol dose point at the other WRRFs.

Table 16. SDNRs for the non-reaerated and reaerated reactors in the brief reaeration priming batch test.

	NO_2-N SDNR (mg N/g MLVSS/hr)	**NO_3-N SDNR (mg N/g MLVSS/hr)**	**NO_x-N SDNR (mg N/g MLVSS/hr)**
Non-reaerated	-0.14	1.56	1.42
Reaerated	-0.11	1.05	0.94

4.4.5.2 Overnight Pre-Anoxic vs. Pre-Aerobic Conditions Test

This second priming test involved overnight anoxic vs. aerobic depletion periods prior to anoxic methanol addition. If there was any residual internal carbon that was present during the previous priming test, that potential interference would be mitigated with the depletion periods in this next test. The methanol SDNR for the initial anoxic phase as well as the anoxic phases following the 24-hour aerobic or anoxic depletion periods are shown in ***Table 17***. The final SDNR in Reactor B (24 hour anoxic period) was higher than the initial methanol-specific SDNR, and was lower in Reactor A (24 hour aerobic period) than the initial methanol-specific SDNR. There was NO_2 accumulation up to about 4 mg N/L during the overnight anoxic phase in Reactor B, compared to no initial NO_2 present after the overnight aerobic phase in Reactor A. This significant NO_2 removal in Reactor B, instead of accumulation, contributed to the overall NO_x removal rate. However, the NO_3 SDNR for Reactor B was still higher than the initial rate and the Reactor A final rate. The efficiency of methanol use was improved with the extended anoxic conditions, as the COD:N ratio of 3.33 mg COD/mg NO_x-N in Reactor B was much less than the Reactor A ratio of 5.43 mg COD/mg NO_x-N. This reaffirms the results from the previous priming test in that the conditions prior to methanol addition affect the methylotrophic denitrification, and that anoxic conditions prior to methanol addition would tend to increase methylotrophic denitrification rates.

Table 17. Methanol-only SDNRs for each reactor in the overnight pre-aerobic vs. pre-anoxic conditions priming batch test.

	NO_2-N SDNR (mg N/g MLVSS/hr)	NO_3-N SDNR (mg N/g MLVSS/hr)	NO_x-N SDNR (mg N/g MLVSS/hr)	Specific COD Utilization Rate (mg COD/g MLVSS/hr)
A and B (initial)	0.25	1.07	1.32	7.24
A (AER depletion)	0	0.74	0.74	6.19
B (ANX depletion)	0.43	1.32	1.77	7.22

4.4.5.3 Varying Pre-Anoxic Period Test

Considering the post-anoxic zone HRT at these WRRFs is typically less than a few hours, the amount of anoxic exposure prior to methanol addition is limited; i.e., there cannot be 24 hours of anoxic time as was explored in the previous test. Therefore, this next test took a more practical approach in which a pre-anoxic time range of 0-2 hours was analyzed.

Due to differences in NO_2 SDNRs rather than in NO_3 SDNRs, the overall NO_x removal rates for the tests with the 0-120 min pre-anoxic period were converted to electron-specific consumption rates instead of in terms of concentrations as mg N/L. Conversion to electron equivalent rates is common when there is NO_2 accumulation (Ginige et al., 2009). As shown in ***Figure 50***, the reduction of NO_3 to NO_2 and NO_2 to N_2 require 2 and 3 electrons, respectively.

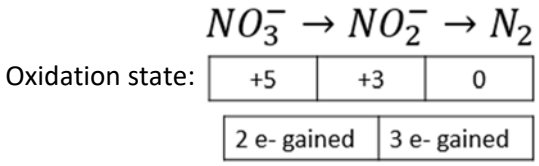

Figure 50. Oxidation states of the denitrification-relevant N species and electrons required for reduction.

These sequential denitrification steps have distinct electron demands and so different methanol demands, which is why this approach was taken (to fully capture the differences in methanol use for each reactor in these batch tests). The following calculations for electron-specific denitrification rates derived from the concentration-based rates were used:

$$NO_3: \frac{\boldsymbol{X}\ mg\ NO_3\text{-}N}{g\ MLVSS\text{-}hr} * \frac{mmol NO_3\text{-}N}{14\ mg NO_3\text{-}N} * \frac{5\ mmol\ e\text{-}}{mmol\ NO_3\text{-}N} = \boldsymbol{X}\ mmol\ e\ {}^{-}/_{g\ MLVSS\ -\ hr}$$

$$NO_2: \frac{\boldsymbol{X}\ mg\ NO_2\text{-}N}{g\ MLVSS\text{-}hr} * \frac{mmol\ NO_2\text{-}N}{14\ mg\ NO_2\text{-}N} * \frac{3\ mmol\ e\text{-}}{mmol\ NO_2\text{-}N} = \boldsymbol{X}\ mmol\ e\ {}^{-}/_{g\ MLVSS\ -\ hr}$$

These were added to get the total denitrification rate in terms of electrons. ***Table 18*** shows the resulting rates from each varying pre-anoxic period batch test. The first tests at NP and AB had the 4-hour aerobic period prior to the anoxic phases, whereas the second tests at these WRRFs had the 24-hour aerobic period. The first test at NP had no NO_2 addition at the start of the methanol phase, the first test at AB had 3 mg N/L of NO_2 addition, and the second tests at each WRRF had

5 mg N/L of NO_2 addition at the start of the methanol phase. All reactors had NO_3 present at the start of the methanol phase, which had already been added at the start of the pre-anoxic phase.

Table 18. Electron-specific denitrification rates for the 0-120 min pre-anoxic priming batch tests.

Test	Reactor	Pre-ANX time (min)	**NO_2** specific e- gain rate (mmol e-/g MLVSS/hr)	**NO_3** specific e- gain rate (mmol e-/g MLVSS/hr)	**NO_x** specific e- gain rate (mmol e-/g MLVSS/hr)
NP 11/30/20	1	0	-0.04	1.17	1.12
	2	20	-0.02	1.15	1.13
	3	60	0.02	0.86	0.88
	4	120	0.12	1.21	1.33
AB 1/20/21	1	0	0.29	1.79	2.09
	2	20	0.63	1.83	2.46
	3	60	0.77	1.71	2.48
	4	120	0.72	1.74	2.46
NP 2/2/21	1	0	0.49	0.86	1.35
	2	20	0.48	0.85	1.33
	3	60	0.54	0.65	1.19
	4	120	0.50	0.85	1.35
AB 4/8/21	1	0	0.63	1.28	1.91
	2	20	0.68	1.22	1.90
	3	60	0.67	1.05	1.72
	4	120	0.65	1.15	1.80

For the initial test with NP on 11/30/2020, the denitrification rate is about 0.2 mmol e-/g MLVSS/hr higher for the 120-min pre-anoxic time than for the lesser pre-anoxic times (except for the 60-min pre-anoxic reactor, which appears to be an outlier). However, this is mostly due to 1.5 mg N/L of NO_2 accumulation during that 120-min pre-anoxic time that resulted in some NO2 reduction when methanol was added, contributing to the overall denitrification rate. There was less than 0.4 mg N/L of NO_2 present initially in the other reactors from the pre-anoxic phase, resulting in continued NO_2 accumulation instead of reduction during the methanol phase. This is why there was NO_2 addition at the start of the methanol phase for all of the following tests.

For the initial test with AB on 1/20/2021, there was a jump in denitrification rate between the 0 and 20 min pre-anoxic reactors, after which it stayed stable at around 2.46 mmol e-/g MLVSS/hr for the remaining reactors as well. The jump is attributable to an increase in the NO_2 specific rate, while the NO_3 rates did not change much between reactors. This suggests that the longer pre-anoxic priming may have more of a benefit for NO_2 reduction rather than NO_3 reduction. The NO_2 concentrations fell below 0.1 mg N/L after 40 min of the methanol phase in each reactor, so the amount of NO_2 spiked at the start of the methanol phase was increased from 3 to 5 mg N/L for the second set of tests at each WRRF.

The second test at NP on 2/2/2021 yielded consistent denitrification rates for each reactor regardless of pre-anoxic time (except for the 60-min pre-anoxic reactor, which again seemed to be

an outlier). Each of the denitrification rates from this second test were similar to the 120-min pre-anoxic reactor in the test from 11/30/2020. It is possible that there was some sort of interference between methylotrophic denitrifiers and internal C denitrifiers. There may still have been some residual internal carbon in the biomass during the initial test at NP on 11/30/2020, but it was more depleted with the 120-min pre-anoxic reactor, and so interfered less with the methylotrophic denitrification there. The second test on 2/2/2021 followed a 24-hour aerobic period instead of 4-hour, so all internal carbon would be depleted, which could explain why the rates were all consistent for this second test. However, the rates in the first test may have been more consistent if the same amount of NO_2 had been available at the start of the methanol phase, as previously mentioned.

The rates for the second test at AB on 4/8/2021 were also very consistent, possibly due to the same explanation as for the NP tests with internal carbon depletion after the 24-hour aerobic period beforehand. However, these rates were lower than those observed during the initial test on 1/20/2021. This may just be due to different methylotrophic populations present in the mixed liquor sample collected from the full-scale WRRF as these tests were conducted over 2 months apart. It may also be possible that the 24-hour aerobic period had a much more significant effect on the reductase enzyme expression that was in a sense irreversible in the comparatively brief pre-anoxic phase of 0-120 min prior to methanol addition. As such, changing the pre-anoxic phase duration did not result in any major differences in denitrification rates because the damage was already done. This could explain the consistency in rates for all four reactors in both 24-hour depletion tests for NP (2/2/2021) and AB (4/8/2021).

The relatively low denitrification rates using internal carbon vs. external carbon have been assumed to lead to more competition between the reductase enzymes for electrons, thus leading to some intermediate accumulations (Krasnits et al., 2013). This could be a factor that led to some NO_2 accumulation during the pre-anoxic phase for the initial set of tests where internal carbon was still suspected to be present.

Even if the effect of priming only makes a difference when internal carbon is present, this would be more relevant to full-scale operation anyway, as the internal carbon would never get as depleted full-scale as it would following the 24-hour aerobic phase in the batch tests. Perhaps adding methanol later on in would allow more internal carbon to be taken advantage of in the first part of the post-anoxic zone, and higher methanol-specific denitrification rates to follow, because the batch tests suggested that rates increase with longer pre-anoxic times (at least when there was not a 24-hour aerobic depletion period before the test). However, this increase of rates pertained more to NO_2 reduction than NO_3 reduction. In any case, greater understanding of the interaction between methylotrophic and internal carbon denitrification would be useful in determining whether priming methylotrophs does have a beneficial effect or not.

4.4.6 Contributions of sbCOD to Post-Anoxic Denitrification

The sbCOD test was performed at VIP as well as at NP, where overloading the primary clarifiers is a common practice. The filtered PCI (passed through a 0.45 µm filter) represents the case of perfect primary clarifier performance, in that all particulate and colloidal material is removed. The non-filtered PCI represents the extreme case of total primary clarifier failure, in that all particulate and colloidal material is passed on to secondary treatment. This material would have the potential to be converted to rbCOD throughout the treatment process, which could be used in the post-anoxic phase as a carbon source. As shown in ***Table 19***, the difference in NO_x removal for the non-filtered and filtered PCI reactor denitrification rates is minimal, at only about 0.08 mg N/g MLVSS/hr. There is higher NO_3 reduction with the non-filtered reactors, but this is mostly offset by higher NO_2 accumulation in these reactors as well, particularly with the NP sludge. It seems that excess sbCOD and its conversion to rbCOD could be favorable for NO_3 reduction to NO_2, but not as favorable for full denitrification to N_2. More tests would be necessary to confirm this.

Table 19. SDNRs for the PCI filtered and non-filtered reactors for the sbCOD batch tests at NP and VIP.

		NO_2 SDNR (mg N/g MLVSS/hr)	**NO_3 SDNR (mg N/ g MLVSS/hr)**	**NO_x SDNR (mg N/g MLVSS/hr)**
NP 11/4/20	Non-filtered	-0.54	1.51	0.99
	filtered	-0.31	1.14	0.90
VIP 11/18/20	Non-filtered	-0.20	0.63	0.50
	filtered	-0.14	0.50	0.42

Using the VIP 2020 averages for MLVSS (2100 mg/L) and post-anoxic HRT (1.81 hr), the difference in rates of 0.08 mg N/g MLVSS/hr attributed to the sbCOD material would only equate to 0.30 mg N/L of extra NO_x removal. Considering that this is based on results from comparing the two *extreme* cases of either no primary clarifier or complete primary clarifier removal of sbCOD, merely overloading the clarifiers under realistic full-scale conditions and pushing more material downstream into the activated sludge process would not result in a significant benefit for post-anoxic denitrification. Extra sbCOD and its conversion to rbCOD is likely not a reason why such efficient post-anoxic denitrification occurs at VIP, and overloading the primaries would probably not result in much methanol savings if this practice was implemented more at NP, AB, or even VIP. On the other hand, it may benefit pre-anoxic denitrification, which could reduce the amount of denitrification required post-anoxically, and save methanol that way. This again depends on recycle efficiency and other factors, and is not guaranteed.

4.5 Conclusion

From the comparative tracer test at NP on the trains with and without the methanol feed point modification, it is evident that the proximity of the carbon dose location to the aerobic zone is an important consideration. Oxidation of methanol aerobically instead of use for denitrification will drive up the apparent methanol demand. Moving the feed point further into the post-anoxic zone in each train is an ongoing project at NP. However, there was evidently still some back-mixing even with the modifications, so this may be unavoidable when the aerobic and post-anoxic zones are directly adjacent on either side of a baffle wall. The NP tracer test results suggested slightly higher loading to Train 7, due to the shorter residence time, higher degree of plug flow, and low

dye recovery compared to Train 6. Flow and load distribution would be important to keep in mind when comparing methanol demand between trains.

The general hydraulic characterization of the post-anoxic zone at each WRRF from the respective tracer tests show the lowest post-anoxic residence time at AB, followed by NP and VIP. The low residence time at AB could minimize the endogenous decay contribution to denitrification, which increases methanol demand.

Using Sumo to model denitrification in the post-anoxic zone at VIP verified that plug flow does not matter much for endogenous or methanol denitrification. However, plug flow could be influential for internal C denitrification. This was modeled in Sumo as GAO growth on NO_2/NO_3, or dGAO activity, but the model needs to be modified to incorporate the much higher suspected levels of internal C denitrification based on full-scale observations. In addition, the representation of endogenous decay denitrification in Sumo was analyzed, and overestimation of the decay rate was apparent. Complete confidence in how Sumo models denitrification as is before adjustments are made is necessary. Sumo could then be used to predict the internal C denitrification capability of different WRRFs under varying conditions. There is a lot of work that needs to be done to understand the characteristics of internal C denitrification before this point is reached, but it is still worth considering Sumo as a potential tool for applying this denitrification strategy. The possible interference of internal C denitrifiers with methylotrophs as discussed for the priming batch tests is another aspect that would need to be clarified and incorporated in the model as well.

Beyond plug flow-like conditions, one other key aspect of the post-anoxic zone at VIP is the big bubble mixing. AB and NP both use surface mixers, which may not be as effective a strategy for distribution of substrate to the biomass. The mixing aspect was not explored via the model or in any other way in this study, and would likely be difficult to capture given the nuances of the specific full-scale mixing systems at each plant. However, superior mixing could be significant to the major methanol savings at VIP.

The compilation of endogenous decay SDNRs obtained from batch test measurements compared to SRT of the sludge at the time of collection indicate the benefit of short SRT for higher SDNRs. This is likely because a longer SRT increases the debris portion of endogenous decay products. This debris is not susceptible to hydrolysis within the relevant time spent at the WRRF, and thus cannot be used as a carbon source for denitrification. However, a short SRT is not feasible to maintain concurrent with a long anoxic HRT to maximize time for denitrification reactions to occur. This would generally require a low MLSS concentration, and so finding a balance could be difficult and unrealistic.

The results from the priming batch tests also suggest careful consideration of methanol dose point. Specifically, what are the conditions prior to the methanol addition point? If anoxic, how long has it been anoxic? The results of the batch testing indicate that aerobic conditions prior to methanol addition could be detrimental to denitrification efficiency. As such, the major reintroduction of DO in the flow stream during the transition at AB could be one of the reasons the methanol demand

is so much higher relative to VIP. Adding methanol farther downstream rather than at the beginning of the anoxic phase could be beneficial. This is perhaps due to greater exposure to anoxic conditions that stimulate denitrification enzymes as hypothesized, or maybe due to less interference from internal C denitrifiers. This interference concept is still unclear.

While overloading the primaries is a potential operating strategy at WRRFs that perform biological nutrient removal, batch testing with filtered vs. non-filtered PCI indicated that sbCOD likely has minimal impact on post-anoxic denitrification. Parallel batch reactors represented the extreme cases of either perfect primary clarification and removal of all sbCOD, or the absence of primary clarification and the maintained presence of these carbon sources to be hydrolyzed throughout the treatment process. The minimal difference in SDNRs of only 0.08 mg N/g MLVSS/hr between these reactors suggested that overloading primary clarifiers will likely not enhance post-anoxic denitrification by much and methanol savings would not be significant. However, overloading the primaries could have more of an impact on pre-anoxic denitrification if the internal recycle is adequate. This would remove more N in the pre-anoxic zone that would lead to lower required N removal in the post-anoxic polishing zone, and indirectly reduce methanol demand. This aspect could be worth investigating further for HRSD's methanol-adding WRRFs.

Of the various operational factors affecting post-anoxic denitrification, there is not one best solution for reducing methanol demand. Moving the dose point and providing a longer anoxic residence time are both clear advantages, but are not feasible for all WRRFs. The relationship of endogenous decay contributions to SRT, and the effect of priming of methylotrophs was hinted at, but how to best take advantage of these aspects needs further consideration. Key insights into how Sumo models each type of post-anoxic denitrification were gained, and will be particularly useful moving forward when using the model to predict contributions from internal C denitrification. It is likely that the combination of multiple factors will result in the most efficient post-anoxic denitrification performance.

5. Engineering Significance

Evaluating the factors that influence internal carbon use for denitrification will help focus implementation strategies at denitrifying bio-P WRRFs with a post-anoxic zone. This and analyzing other factors related to endogenous decay denitrification and methylotrophic denitrification itself are also useful for cutting down on methanol use. The extent of methanol savings is exemplified by direct methanol cost estimates at VIP, AB, and NP. The 2020 HRSD unit cost of MicroC (the specific proprietary methanol chemical used) is $1.28/gallon, and at a concentration of $1.188*10^6$ mg COD/L, this equates to approximately $0.13/lb methanol as COD. ***Table 20*** shows the average daily and total yearly methanol mass added for treatment in 2020 at each of the three HRSD WRRFs, and the associated costs. While handling the highest flow at around 28 MGD at VIP, the average methanol cost is the lowest here by over $100,000 per year. Alternatively, using the methanol dose rate and cost per lb, the cost of N removal at VIP is only $0.05/lb N, which is is seven times lower than the $0.35/lb N required at AB. This results in major savings in chemical costs that can free up funding for other aspects of WRRF operation.

Table 20. Estimated costs of methanol addition at each WRRF for 2020.

	MeOH dose	Cost of N removal	Avg daily MeOH demand		Total MeOH demand 2020	
	lb COD/lb N	$/lb N	lb COD/day	$/day	lb COD/yr	$/yr
VIP	0.37	$0.05	1,655	$210	600,659	$78,000
NP	1.31	$0.17	8,004	$1,030	2,921,410	$377,000
AB	2.87	$0.35	4,354	$560	1,589,093	$205,000

Internal C denitrification was demonstrated at AB, NP, and VIP in the batch test setting, so the capacity is there even if it is not completely utilized at full-scale. Factors that were explored regarding this type of denitrification, as well as other types of denitrification, are listed in ***Table 21***. The results from this set of experiments in regards to whether each factor seems to have an impact on denitrification rate are also summarized in ***Table 21***. One factor that was more uncertain was the effect that the degree of plug flow has on internal C denitrification. The extent of internal C denitrification is not fully modeled in Sumo, so it is not clear from the model whether plug flow is of importance. Still, the fact that each WRRF yields potential for internal C denitrification in the batch test setting, which is ideal plug flow, supports this theory. Another aspect that needs some clarification is the priming of methylotrophs to denitrify at a faster rate. The results of the various batch tests point to the aerobic vs. anoxic conditions having an effect, but there is not a clear indication that increasing the anoxic time up to 2 hours prior to methanol addition is actually beneficial. There is some potential interference of internal carbon with the measured methylotrophic denitrification that is not fully understood.

Table 21. List of factors explored in this study and indication of their impact on denitrification.

Type of Denitrification/ carbon source	Factor	Impact?	
		Yes	No
Internal C	Aeration time	X	
Internal C	Nitrifying/denitrifying biomass	X	
Internal C	Amount of acetate available in ANA phase	X	
Internal C	Bio-P performance (uptake rate)	X	
Methanol	Dose location	X	
Endogenous	Mean cell residence time	X	
Methanol	Plug flow		X
Endogenous	Plug flow		X
Internal C	Plug flow	X	
Endogenous	SRT	X	
Methanol	Priming/anoxic time prior to methanol addition	X	
sbCOD	Overloading clarifiers		X

Once the important denitrification factors are clearly defined, the next step is to facilitate operational changes at each WRRF to increase denitrification efficiency and minimize methanol requirements. For instance, the benefits of short aeration time for internal C denitrification could mean shortening aerobic HRT by taking trains out of service or using a lower DO setpoint in the aerobic tanks. Of course, these changes have to be in coincidence with maintaining aspects of treatment such as adequate nitrification and OP uptake, which both dictate aerobic demand. As another example, facilitating more carbon in the anaerobic zone could be accomplished by using fermentation of primary solids and feeding the VFA-rich fermentate to the anaerobic zone. In addition, ensuring successful bio-P performance would be possible by facilitating GAO out-competition (whether through low DO, high pH, etc.) and avoidance of chemical OP removal when possible. Being mindful of biomass management, through wasting rate and thus SRT, could also play into more efficient endogenous decay denitrification rates in the long run as well.

Physical tank characteristics are generally less feasible to change, but still relevant. For instance, reconfiguring the reactors to be closer to plug flow could be done via installation of more baffle walls, if this was proven important for internal C denitrifcation after further exploration. Furthermore, the methanol dose point relocation is already ongoing at NP, but could be considered at the other WRRFs as well. The capacity for methanol addition is possible in each cell of the post-anoxic zone at VIP, and so the dose point could be shifted to a later cell rather than in the first anoxic cell. There is only two CSTRs per post-anoxic train at AB, so the options for methanol dose are more limited there.

None of the operational changes are straightforward; for instance, shortening the aerobic time or lowering the DO setpoint would likely already be done if possible within the constraints of nitrification/OP uptake to save on energy costs. Therefore, there may not be much more leniency that a particular WRRF has to work with for these parameters. Nonetheless, short aeration time for higher post-anoxic internal C denitrification potential is still valuable to keep in mind for

operational control. Fine-tuning of these operation strategies comes with time and experience seeing how the WRRF performance responds to such changes.

Many different operational factors and types of denitrification were evaluated in this set of experiments. There is not a singular approach that will guarantee methanol savings at every WRRF, whether via internal carbon or some other carbon source. Instead, it might take lowering the aerobic DO setpoint, establishing more plug flow-like conditions, and moving the methanol dose point further downstream in the post-anoxic tank before there starts to be a decrease in methanol addition requirements. There are also more aspects beyond those analyzed in this study that could influence denitrification performance and should be explored, such as the type of mixing. In addition, identifying the organisms responsible and forms of carbon used for internal C denitrification would also give significant insight into how to encourage their activity. The ultimate goal of significant methanol savings to rival those seen at VIP will likely require a combination of various factors.

References

Basset, N., Katsou, E., Frison, N., Malamis, S., Dosta, J., & Fatone, F. (2016). Integrating the selection of PHA storing biomass and nitrogen removal via nitrite in the main wastewater treatment line. *Bioresource Technology*, *200*, 820–829. https://doi.org/10.1016/j.biortech.2015.10.063

Basturk, S. B., Dancer, C. E. J., & McNally, T. (2020). A continuous plug-flow anaerobic/aerobic/anoxic/aerobic (AOAO) process treating low COD/TIN domestic sewage: realization of partial nitrification and extremely advanced nitrogen removal. *Pharmacological Research*, 104743. https://doi.org/10.1016/j.phrs.2020.104743

Brdjanovic, D., Slamet, A., Van Loosdrecht, M. C. M., Hooijmans, C. M., Alaerts, G. J., & Heijnen, J. J. (1998). Impact of excessive aeration on biological phosphorus removal from wastewater. In *Water Research* (Vol. 32, Issue 1, pp. 200–208). https://doi.org/10.1016/S0043-1354(97)00183-8

Carvalho, G., Lemos, P. C., Oehmen, A., & Reis, M. A. M. (2007). Denitrifying phosphorus removal: Linking the process performance with the microbial community structure. *Water Research*, *41*(19), 4383–4396. https://doi.org/10.1016/j.watres.2007.06.065

Chen, H. B., Wang, D. B., Li, X. M., Yang, Q., & Zeng, G. M. (2015). Enhancement of post-anoxic denitrification for biological nutrient removal: effect of different carbon sources. *Environmental Science and Pollution Research*, *22*(8), 5887–5894. https://doi.org/10.1007/s11356-014-3755-1

Cherchi, C., Onnis-Hayden, A., El-Shawabkeh, I., & Gu, A. Z. (2009). Implication of Using Different Carbon Sources for Denitrification in Wastewater Treatments. *Water Environment Research*, *81*(8), 788–799. https://doi.org/10.2175/106143009x12465435982610

Coats, E. R., Mockos, A., & Loge, F. J. (2011). Post-anoxic denitrification driven by PHA and glycogen within enhanced biological phosphorus removal. *Bioresource Technology*, *102*(2), 1019–1027. https://doi.org/10.1016/j.biortech.2010.09.104

Crittenden, J. C., Trussell, R. R., Hand, D. W., Howe, K., & Tchobanoglous, G. (2012). *MWH's water treatment: principles and design*. John Wiley & Sons.

Davies, J. T. (1972). *Turbulence Phenomena*. Academic Press.

Dircks, K., Henze, M., van Loosdrecht, M. C. M., Mosbaek, H., & Aspegren, H. (2001). Storage and degradation of poly-B-hydroxybutyrate in activated sludge under aerobic conditions. *Water Research*, *35*(9), 2277–2285.

Dold, P., Takács, I., Mokhayeri, Y., Nichols, A., Hinojosa, J., Riffat, R., Bott, C., Bailey, W., & Murthy, S. (2008). Denitrification with Carbon Addition-Kinetic Considerations. *Water Environment Research*, *80*(5), 417–427. https://doi.org/10.2175/106143007x221085

Ferguson, S. J. (1994). Denitrification and its control. *Antonie van Leeuwenhoek*, *66*(1–3), 89–110. https://doi.org/10.1007/BF00871634

Foglar, L., & Briški, F. (2003). Wastewater denitrification process - The influence of methanol and kinetic analysis. *Process Biochemistry*, *39*(1), 95–103. https://doi.org/10.1016/S0032-9592(02)00318-7

Ginige, M. P., Bowyer, J. C., Foley, L., Keller, J., & Yuan, Z. (2009). A comparative study of methanol as a supplementary carbon source for enhancing denitrification in primary and secondary anoxic zones. *Biodegradation*, *20*(2), 221–234. https://doi.org/10.1007/s10532-008-9215-1

Grady, C. P. L., Daigger, G. T., Love, N. G., & Filipe, C. D. M. (2011). *Biological Wastewater Treatment* (Third). Taylor & Francis Group.

Hallin, S., & Pell, M. (1998). Metabolic properties of denitrifying bacteria adapting to methanol and ethanol in activated sludge. *Water Research*, *32*(1), 13–18. https://doi.org/10.1016/S0043-1354(97)00199-1

Halling-Sorensen, & Jorgensen. (2008). *Process chemistry and Biochemistry of denitrification*.

Henze, M. (1991). Capabilities of biological nitrogen removal processes from wastewater. *Water Science and Technology*, *23*(4–6), 669–679. https://doi.org/10.2166/wst.1991.0517

Kaprelyants, A. S., & Kell, D. B. (1996). Do bacteria need to communicate with each other for growth? *Trends in Microbiology*, *4*(6), 237–242.

Korner, H., & Zumft, W. G. (1989). Expression of denitrification enzymes in response to the dissolved oxygen levels and respiratory substrate in continuous culture of Pseudomonas stutzeri. *Applied and Environmental Microbiology*, *55*(7), 1670–1676. https://doi.org/10.1128/aem.55.7.1670-1676.1989

Krasnits, E., Beliavsky, M., Tarre, S., & Green, M. (2013). PHA based denitrification: Municipal wastewater vs. acetate. *Bioresource Technology*, *132*, 28–37. https://doi.org/10.1016/j.biortech.2012.11.074

Kujawa, K., & Klapwijk, B. (1999). A method to estimate denitrification potential for predenitrification systems using NUR batch test. *Water Research*, *33*(10), 2291–2300. https://doi.org/10.1016/S0043-1354(98)00459-X

Li, Y. yu, Lin, L., & Li, X. yan. (2020). Chemically enhanced primary sedimentation and acidogenesis of organics in sludge for enhanced nitrogen removal in wastewater treatment. *Journal of Cleaner Production*, *244*. https://doi.org/10.1016/j.jclepro.2019.118705

Liu, G., Xu, X., Zhu, L., Xing, S., & Chen, J. (2013). Biological nutrient removal in a continuous anaerobic-aerobic-anoxic process treating synthetic domestic wastewater. *Chemical Engineering Journal*, *225*, 223–229. https://doi.org/10.1016/j.cej.2013.01.098

Lopez-Vazquez, C. M., Oehmen, A., Hooijmans, C. M., Brdjanovic, D., Gijzen, H. J., Yuan, Z., & van Loosdrecht, M. C. M. (2009). Modeling the PAO-GAO competition: Effects of carbon source, pH and temperature. *Water Research*, *43*(2), 450–462. https://doi.org/10.1016/j.watres.2008.10.032

Louzeiro, N. R., Mavinic, D. S., Oldham, W. K., Meisen, A., & Gardner, I. S. (2003). Process control and design considerations for methanol-induced denitrification in a sequencing batch reactor. *Environmental Technology (United Kingdom)*, *24*(2), 161–169. https://doi.org/10.1080/09593330309385547

Meinhold, J., Filipe, C. D. M., Daigger, G. T., & Isaacs, S. (1999). Characterization of the denitrifying fraction of phosphate accumulating organisms in biological phosphate removal. In *Water Science and Technology* (Vol. 39, Issue 1, pp. 31–42). https://doi.org/10.1016/S0273-1223(98)00773-2

Mino, T., Liu, W. T., Kurisu, F., & Matsuo, T. (1995). Modelling glycogen storage and denitrification capability of microorganisms in enhanced biological phosphate removal processes. In *Water Science and Technology* (Vol. 31, Issue 2, pp. 25–34). https://doi.org/10.1016/0273-1223(95)00177-O

Nyberg, U., Andersson, B., & Aspegren, H. (1996). Long-term experiences with external carbon sources for nitrogen removal. In *Water Science and Technology* (Vol. 33, Issue 12, pp. 109–116). https://doi.org/10.1016/0273-1223(96)00464-7

Oehmen, A., Lemos, P., Carvalho, G., Yuan, Z., Keller, J., Blackall, L., & Reis, M. (2007). Advances in enhanced biological phosphorus removal: From micro to macro scale. *Water Research*, *41*, 2271–2300.

Onnis-Hayden, A., & Gu, A. Z. (2008). Comparisons of organic sources for denitrification: biodegradability, denitrification rates, kinetic constants and practical implication for their application in WWTPs. *Proceedings of the Water Environment Federation*, *17*, 253–273.

Peng, Y., Ma, Y., & Wang, S. (2007). Denitrification potential enhancement by addition of external carbon sources in a pre-denitrification process. *Journal of Environmental Sciences*, *19*(3), 284–289.

Qin, L., Liu, Y., & Tay, J. H. (2005). Denitrification on poly-β-hydroxybutyrate in microbial granular sludge sequencing batch reactor. *Water Research*, *39*(8), 1503–1510. https://doi.org/10.1016/j.watres.2005.01.025

Shi, L., Ma, B., Li, X., Zhang, Q., & Peng, Y. (2019). Advanced nitrogen removal without addition of external carbon source in an anaerobic/aerobic/anoxic sequencing batch reactor. *Bioprocess and Biosystems Engineering*, *42*(9), 1507–1515. https://doi.org/10.1007/s00449-019-02148-z

Smolders, G. J. F., van Loosdrecht, M. C. M., & Heijnen, J. J. (1995). A metabolic model for the biological phosphorus removal process. In *Water Science and Technology* (Vol. 31, Issue 2, pp. 79–93). https://doi.org/10.1016/0273-1223(95)00182-M

Song, K., Harper, W. F., Hori, T., Riya, S., Hosomi, M., & Terada, A. (2015). Impact of carbon sources on nitrous oxide emission and microbial community structure in an anoxic/oxic activated sludge system. *Clean Technologies and Environmental Policy*, *17*(8), 2375–2385. https://doi.org/10.1007/s10098-015-0979-9

Tchobanoglous, G., Stensel, D. H., Tsuchihashi, R., & Burton, F. (2014). *Wastewater Engineering, Treatment and Resource Recovery* (5th ed.). McGraw-Hill.

Van Loosdrecht, M. C. M., & Henze, M. (1999). Maintenance, endogeneous respiration, lysis, decay and predation. *Water Science and Technology*, *39*(1), 107–117.

Vocks, M., Adam, C., Lesjean, B., Gnirss, R., & Kraume, M. (2005). Enhanced post-denitrification without addition of an external carbon source in membrane bioreactors. *Water Research*, *39*(14), 3360–3368. https://doi.org/10.1016/j.watres.2005.05.049

Winkler, M., Coats, E. R., & Brinkman, C. K. (2011). Advancing post-anoxic denitrification for biological nutrient removal. *Water Research*, *45*(18), 6119–6130. https://doi.org/10.1016/j.watres.2011.09.006

Yun, Z., Yun, G. H., Lee, H. S., & Yoo, T. U. (2013). The variation of volatile fatty acid compositions in sewer length, and its effect on the process design of biological nutrient removal. *Water Science and Technology*, *67*(12), 2753–2760. https://doi.org/10.2166/wst.2013.192

Zeng, R. J., Yuan, Z., & Keller, J. (2003). Enrichment of denitrifying glycogen-accumulating organisms in anaerobic/anoxic activated sludge system. *Biotechnology and Bioengineering*, *81*(4), 397–404. https://doi.org/10.1002/bit.10484

Zhang, Q. H., Jin, P. K., Ngo, H. H., Shi, X., Guo, W. S., Yang, S. J., Wang, X. C., Wang, X., Dzakpasu, M., Yang, W. N., & Yang, L. (2016). Transformation and utilization of slowly biodegradable organic matters in biological sewage treatment of anaerobic anoxic oxic systems. *Bioresource Technology*, *218*, 53–61. https://doi.org/10.1016/j.biortech.2016.06.068

Zhou, Y., Pijuan, M., Zeng, R. J., & Yuan, Z. (2009). Involvement of the TCA cycle in the anaerobic metabolism of polyphosphate accumulating organisms (PAOs). *Water Research*, *43*(5), 1330–1340. https://doi.org/10.1016/j.watres.2008.12.008

Appendices

Appendix A - Results from Internal Carbon Batch Tests

Table 22. All SDNRs (both raw and corrected for endogenous decay) and relevant bio-P rates from internal carbon batch tests.

				Raw Value			Endogenous-corrected						
Date	WRRF	Test	Rate type	SDNR – NO_2 (mg N/g MLVSS/hr)	SDNR – NO_3 (mg N/g MLVSS/hr)	SDNR – NO_x (mg N/g MLVSS/hr)	SDNR – NO_3 (mg N/g MLVSS/hr)	SDNR – NO_x (mg N/g MLVSS/hr)	OP release (mg P/g MLVSS/hr)	COD uptake (mg COD/ g MLVSS/hr)	OP release /COD uptake	Adjusted OP release/ COD uptake	OP uptake (mg P/g MLVSS/hr)
8/5/20	VIP	Standard	With methanol	-1.15	2.01	0.86	1.61	0.57	5.80	21.5	0.27	0.5	0.93
			No methanol	-1.23	1.52	0.29	1.12	0					
			Difference	0.09	0.48	0.57	0.49	0.57					
8/11/20	NP	Standard	With methanol	-0.45	1.02	0.57	0.57	0.32	10.6	24.7	0.43	0.58	4.01
			No methanol	-0.2	0.45	0.25	0.03	0					
			Difference	-0.25	0.58	0.32	0.54	0.32					
8/26/20	VIP	Long vs. short	Long	-0.05	0.22	0.18	0	0	5.69	26.5	0.21	-	0.75
			Short	-0.51	1.07	0.56	0.84	0.38					
			Difference	-0.46	0.84	0.38	0.84	0.38					
9/8/20	NP	Long vs. short	Long	-0.14	0.47	0.33	0	0	14.9	33.7	0.44	0.56	2.31
			Short	-0.25	0.75	0.51	0.28	0.17					
			Difference	-0.11	0.28	0.17	0.28	0.17					
9/10/20	VIP	Standard	With methanol	-0.23	1.39	1.16	0.98	0.73	5.71	29.2	0.20	0.32	1.54
			No methanol	-0.28	0.79	0.51	0.38	0.08					
			Difference	0.05	0.59	0.64	0.60	0.65					
9/14/20	AB	Standard	With methanol	0.09	2.71	2.75	2.47	2.51	16.3	43.7	0.37	0.57	2.65
			No methanol	0.05	0.7	0.72	0.46	0.48					
			Difference	0.04	2.01	2.03	2.01	2.03					
9/15/20	VIP	High/low acetate	With methanol	-0.09	1.1	1.01	0.88	0.75	4.0	22.2	0.18	0.20	0.61
			No methanol	-	-	-	-	-					
			Difference	0.09	1.1	1.01	0.88	0.75					
			With methanol	-0.24	1.21	0.97	0.99	0.71	4.91	38.4	0.13	-	1.77
			No methanol	-0.15	0.47	0.32	0.25	0.06					
			Difference	-0.09	0.74	0.65	0.74	0.65					
10/6/20	AB	High/low acetate	With methanol	-0.04	2.34	2.32	2.10	2.08	11.8	28.2	0.42	-	0.95
			No methanol	-0.01	0.31	0.31	0.07	0.07					
			Difference	-0.02	2.03	2.01	2.03	2.01					
			With methanol	0.04	2.63	2.63	2.40	2.39	12.3	46.8	0.26	0.35	2.60

			No methanol	-0.05	0.60	0.58	0.36	0.35					
			Difference	0.08	2.04	2.05	2.04	2.05					
10/8/20	NP	High/low acetate	With methanol	-0.33	1.37	1.03	0.95	0.64	11.5	14.1	0.82	1.82	2.79
			No methanol	-0.18	0.65	0.47	0.23	0.07					
			Difference	-0.16	0.72	0.56	0.72	0.56					
			With methanol	-0.38	1.33	0.95	0.91	0.56	13.5	41.8	0.32	0.46	4.83
			No methanol	-0.27	0.79	0.52	0.37	0.13					
			Difference	-0.11	0.54	0.43	0.54	0.43					
10/20/20	VIP	Standard	No methanol	-0.19	0.72	0.53	0.54	0.33	7.6	42.1	0.18	0.33	1.76
11/10/20	AT	Standard	No methanol	0.35	0.93	1.28	0.25	0.60	25.0	90.2	0.28	0.32	12.81
11/16/20	NP	Standard	With methanol	-0.13	2.28	2.15	1.86	1.75	17.5	29.3	0.60	0.65	6.32
			No methanol	-0.37	1.20	0.83	0.78	0.43					
			Difference	0.25	1.07	1.32	1.07	1.32					
11/23/20	CE	Standard	No methanol	0.06	0.79	0.81	0	0	10.8	39.2	0.28	-	5.49
12/3/20	AT	Standard	No methanol	0.04	0.71	0.70	0	0	18.2	40.5	0.45	-	13.2
12/8/20	VIP	Standard	With methanol	-0.15	1.56	1.46	1.26	1.14	8.4	45.5	0.18	0.34	3.14
			No methanol	-0.23	1.58	1.35	1.29	1.03					
			Difference	0.07	-0.03	0.11	-0.03	0.11					
12/15/20	AT	Standard	No methanol	0.03	0.73	0.72	0.05	0.04	21.6	68.9	0.31	-	13.7
1/6/21	AB	Standard	With methanol	0.01	3.20	3.21	2.77	2.78	11.7	34.3	0.34	0.47	3.31
			No methanol	-0.03	1.35	1.32	0.92	0.89					
			Difference	0.04	1.86	1.90	1.86	1.90					
1/7/21	JR	Standard	No methanol	-0.06	1.00	0.93	0.58	0.52	12.6	59.3	0.21	0.34	9.37
1/13/21	VIP	Long vs. short	Long	-0.14	1.10	0.97	0.65	0.50	4.84	48.3	0.10	-	0.91
			Short	-0.33	1.49	1.16	1.03	0.69					
			Difference	-0.19	0.38	0.19	0.38	0.19					
1/22/21	NP	Long vs. short	Long	-0.38	0.97	0.59	0.66	0.27	17.6	38.7	0.45	0.83	5.50
			Short	-0.54	1.21	0.67	0.90	0.35					
			Difference	-0.16	0.24	0.08	0.24	0.08					
1/25/21	NP	High/NO acetate	With methanol	-0.01	3.71	3.70	3.23	3.25	-	-	-	-	-
			No methanol	-0.25	1.24	0.99	0.76	0.54					
			Difference	0.24	2.47	2.71	2.47	2.71					
			With methanol	-0.01	3.90	3.89	3.42	3.44	9.9	22.8	0.43	-	3.55
			No methanol	-0.26	1.38	1.12	0.90	0.67					
			Difference	0.25	2.52	2.77	2.52	2.77					
2/4/21	VIP	Long vs. short	Long	-0.15	0.80	0.65	0.31	0.16	4.1	27.0	0.15	0.24	1.70
			Short	-0.44	1.45	1.01	0.96	0.52					
			Difference	-0.29	0.65	0.37	0.65	0.37					
2/8/21	NP		Long	-0.19	0.82	0.63	0.51	0.31	14.0	28.1	0.50	0.72	4.88

		Long vs. short	Short	-0.30	1.13	0.83	0.82	0.51					
			Difference	-0.11	0.31	0.20	0.31	0.20					
2/18/21	VIP	Standard	With methanol	0.00	2.25	2.25	1.84	1.82	5.0	25.7	0.19	0.45	2.84
			No methanol	-0.20	1.45	1.25	1.04	0.83					
			Difference	0.19	0.80	0.99	0.80	0.99					
2/22/21	JR	Long vs. short	Long	-0.04	1.54	1.50	1.13	1.09	10.5	12.7	0.82	-	5.68
			Short	-0.51	2.43	1.92	2.02	1.51					
			Difference	-0.48	0.90	0.42	0.90	0.42					
3/3/21	VIP	High/low acetate	With methanol	0.00	1.95	1.95	1.56	1.55	5.4	16.6	0.33	0.60	2.57
			No methanol	-0.07	1.04	0.97	0.65	0.57					
			Difference	0.07	0.91	0.98	0.91	0.98					
			With methanol	0.01	2.02	2.03	1.64	1.63	5.4	23.6	0.23	0.27	3.83
			No methanol	-0.02	1.15	1.14	0.77	0.74					
			Difference	0.03	0.86	0.89	0.86	0.89					
3/8/21	VIP	Standard	No methanol	-0.02	0.87	0.85	0.49	0.45	6.0	22.2	0.27	0.33	3.74
			No methanol	-0.01	0.78	0.77	0.40	0.37	4.8	-	-	-	3.23
3/10/21	AB	Standard	With methanol	0.01	4.80	4.81	4.37	4.38	8.6	13.1	0.66	1.01	3.98
			No methanol	-0.03	1.42	1.39	0.99	0.96					
			Difference	0.04	3.38	3.41	3.38	3.41					
3/15/21	NP	Standard	With methanol	-0.14	3.43	3.36	3.13	3.05	12.2	21.9	0.56	0.72	5.87
			No methanol	-0.18	1.02	0.83	0.71	0.52					
			Difference	0.04	2.42	2.53	2.42	2.53					
3/18/21	VIP	Standard	No methanol	-0.05	0.80	0.75	0.45	0.38	8.3	24.7	0.34	0.51	4.68
			No methanol	-0.02	0.65	0.63	0.30	0.27	4.8	8.8	0.55	-	2.87
3/23/21	VIP	Long vs. short	Long	-0.02	0.54	0.52	0.22	0.20	8.7	34.9	0.25	0.91	4.68
			Short	-0.10	1.04	0.94	0.72	0.62					
			Difference	-0.09	0.51	0.42	0.51	0.42					
3/31/21	JR	Standard	No methanol	-0.44	1.71	1.27	1.30	0.86	9.5	56.7	0.17	0.38	4.11
4/13/21	AB	Standard	With methanol	0.00	2.90	2.90	2.44	2.44	17.8	23.9	0.75	0.79	8.20
			No methanol	-0.02	0.81	0.79	0.35	0.34					
			Difference	0.02	2.09	2.11	2.09	2.11					
4/20/21	NP	Standard	With methanol	0.00	2.54	2.54	2.23	2.22	14.1	27.3	0.52	0.48	5.20
			No methanol	-0.17	0.89	0.72	0.58	0.41					
			Difference	0.17	1.65	1.81	1.65	1.81					

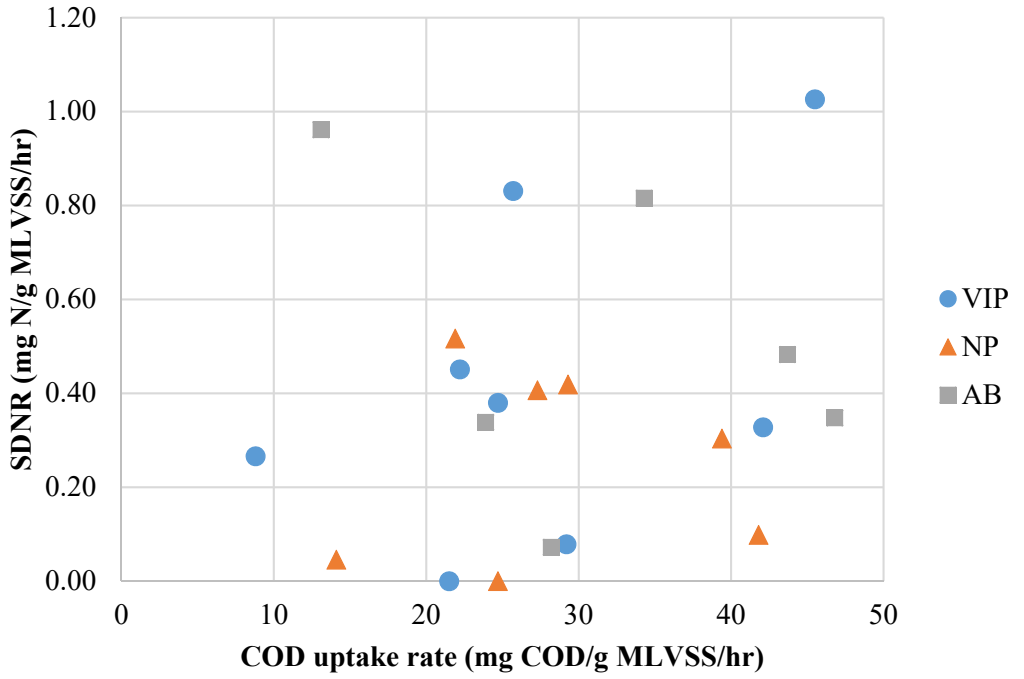

Figure 51. Relationship between COD uptake and internal C denitrification for the standard ANA/AER/ANX and high vs. low acetate batch tests.

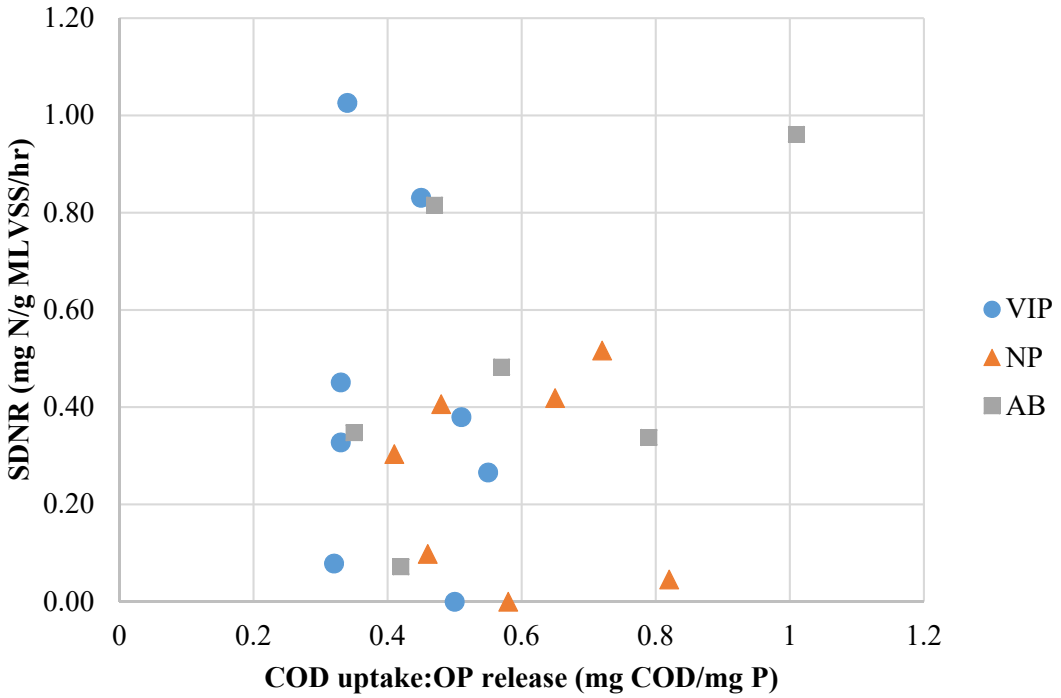

Figure 52. Relationship between the COD uptake:OP release ratio and internal C denitrification for the standard ANA/AER/ANX and high vs. low acetate batch tests.

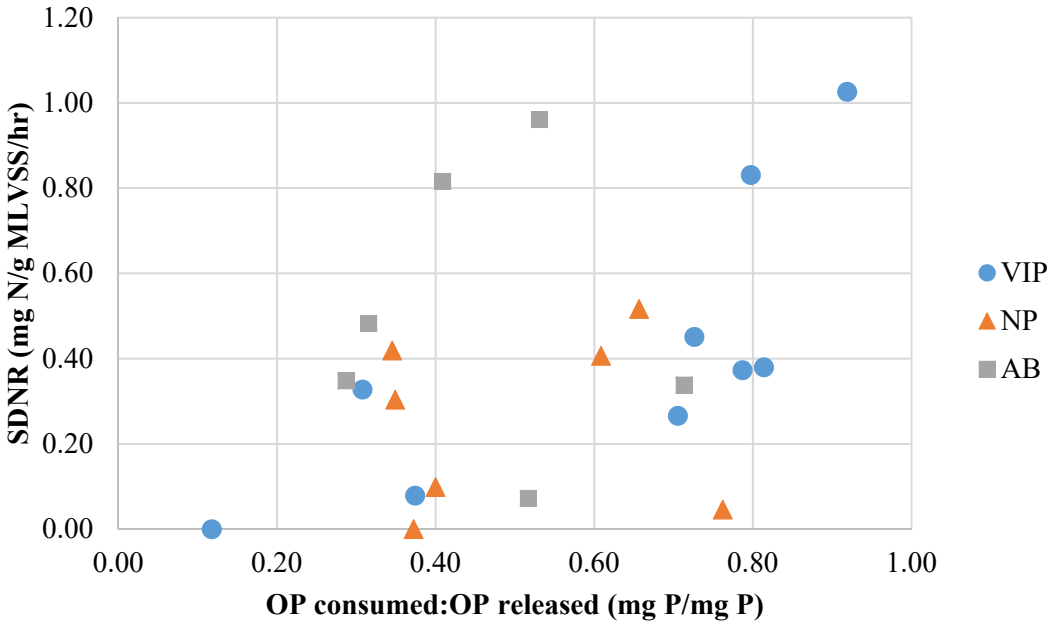

Figure 53. Completeness of OP uptake (ratio of OP consumed aerobically to OP released anaerobically) and measured SDNR.

Appendix B - Results from VFA special sampling

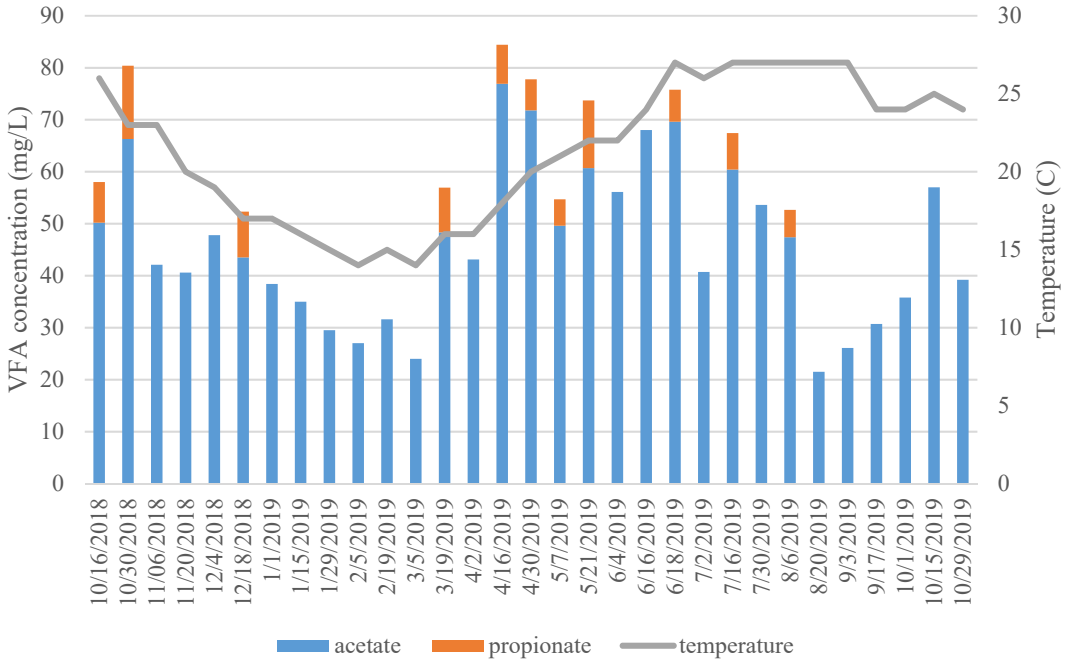

Figure 54. PCE VFA concentrations and wastewater temperature at **NP** over the course of a year.

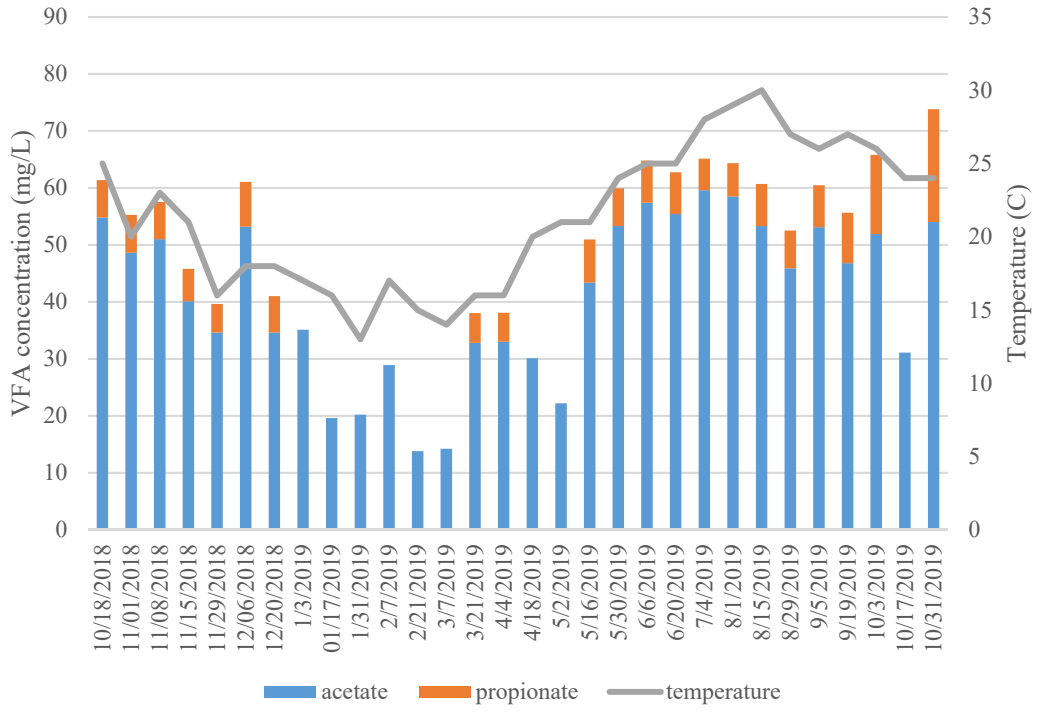

Figure 55. PCE VFA concentrations and wastewater temperature at **VIP** over the course of a year.

Table 23. Comparison of PCE COD concentrations at VIP and NP averaged over the course of a year when VFA sampling was done.

	VIP PCE	NP PCE
VFA (mg/L)	46 (± 6)	49 (± 6)
rbCOD (mg/L)	134 (± 13)	140 (± 14)
sCOD (mg/L)	223 (± 18)	212 (± 18)
tCOD (mg/L)	297 (± 19)	467 (± 77)

(± 95% confidence interval for the average)

Table 24. Raw water influent and PCE concentrations of TKN, TP, and OP at each WRRF. Values are averages for 2017-2020.

	RAW INF SOL TKN (mg/L)	RAW INF TP (mg/L)	RAW INF OP (mg/L)	PRI EFF SOL TKN (mg/L)	PRI EFF TP (mg/L)
AB	29.4 (± 1.2)	4.41 (± 0.06)	2.81 (± 0.05)	22.7 (± 0.9)	4.01 (± 0.09)
VIP	24.0 (± 1.1)	4.44 (± 0.22)	2.88 (± 0.07)	22.5 (± 0.9)	3.67 (± 0.08)
NP	37.7 (± 0.9)	7.72 (± 0.14)	5.38 (± 0.12)	38.0 (± 0.8)	8.80 (± 0.22)

(± 95% confidence interval for the average)

Appendix C – Results from Priming and sbCOD Tests

Table 25. All SDNRs (both raw and corrected for endogenous decay) and relevant bio-P rates from priming and sbCOD batch tests.

				Raw Value			Endogenous-corrected					
Date	WRRF	Test	Rate type	SDNR – NO_2 (mg N/g MLVSS/hr)	SDNR – NO_3 (mg N/g MLVSS/hr)	SDNR – NO_x (mg N/g MLVSS/hr)	SDNR – NO_3 (mg N/g MLVSS/hr)	SDNR – NO_x (mg N/g MLVSS/hr)	OP release (mg P/g MLVSS/hr)	COD uptake (mg COD/ g MLVSS/hr)	OP release/ COD uptake	OP uptake (mg P/g MLVSS/hr)
9/28/20	VIP	Brief 30-min reaeration	Methanol only - no air	-0.14	1.56	1.42	1.10	0.95	-	-	-	-
			Methanol only - air	-0.11	1.05	0.94	0.83	0.68				
11/4/20	NP	sbCOD	Non-filtered	-0.54	1.51	0.99	-	-	18.1	47.7	0.38	4.93
			Filtered	-0.31	1.14	0.90	-	-	19.6	38.6	0.51	5.30
11/16/20	NP	Overnight anoxic vs. aerobic conditions	With methanol	-0.13	2.28	2.15	1.86	1.75	17.5	29.3	0.60	6.32
			No methanol	-0.37	1.20	0.83	0.78	0.43				
			Difference	0.25	1.07	1.32	1.07	1.32				
			Methanol - aerobic priming	-0.02	1.16	1.14	0.74	0.74	-	-	-	-
			Methanol – anoxic priming	0.43	1.74	2.17	1.32	1.77				
11/18/20	VIP	sbCOD	Non-filtered	-0.20	0.63	0.50	-	-	1.2	11.8	0.10	0.89
			Filtered	-0.14	0.50	0.42	-	-	1.9	12.9	0.15	0.69
11/30/20	NP	Varying pre-anoxic period	0 min pre-anoxic	-0.20	3.27	3.07	2.85	2.67	-	-	-	-
			20 min pre-anoxic	-0.11	3.23	3.12	2.81	2.72				
			60 min pre-anoxic	0.10	2.41	2.52	1.99	2.12				
			120 min pre-anoxic	0.57	3.39	3.96	2.97	3.56				
1/20/21	AB	Varying pre-anoxic period	0 min pre-anoxic	1.37	5.02	8.29	4.78	8.05	-	-	-	-
			20 min pre-anoxic	2.94	5.12	9.61	4.88	9.37				
			60 min pre-anoxic	3.58	4.80	8.85	4.56	8.62				
			120 min pre-anoxic	3.34	4.87	7.60	4.63	7.36				
2/2/21	NP	Varying pre-anoxic period	0 min pre-anoxic	2.28	2.40	4.68	2.10	4.36	-	-	-	-
			20 min pre-anoxic	2.24	2.38	4.62	2.07	4.30				
			60 min pre-anoxic	2.53	1.82	4.35	1.51	4.03				
			120 min pre-anoxic	2.34	2.37	4.83	2.06	4.52				
4/8/21	AB	Varying pre-anoxic period	0 min pre-anoxic	2.94	3.58	6.53	3.15	6.10	-	-	-	-
			20 min pre-anoxic	3.19	3.40	6.59	2.97	6.16				
			60 min pre-anoxic	3.13	2.94	6.07	2.51	5.64				
			120 min pre-anoxic	3.04	3.22	6.26	2.79	5.83				